FAP24

Government of the People's Republic of Bangladesh

Water Resources Planning Organization

European Commission

Delft Hydraulics

Danish Hydraulic Institute

Hydroland

Approtech

Osiris

RIVER SURVEY PROJECT

Special Report No.9

Bedform and Bar Dynamics in the Main Rivers of Bangladesh

October 1996

Special Report 9

Bedform and Bar Dynamics in the Main Rivers of Bangladesh

October 1996

Executive summary

- *Study of the evolution, morphology and flow dynamics associated with dunes and bars in the main rivers of Bangladesh shows that these bed features are ubiquitous within all the active channels. Dunes and bars largely control the rates and patterns of bedload transport and significantly influence the location and rate of bank erosion/bed scour. Use of both routine survey data and a series of special surveys between 1994 and 1996 has permitted assembly of an unrivalled database concerning dune and bar dynamics throughout the flood hydrograph. Principal conclusions from the study are:*
- *Dunes are the dominant bedform within all active channels and on bar margins/edges at all flow stages*
- *Dune height and wavelength range from 0.15-6.3 m and 4-350 m respectively*
- *Dune leeside angle ranges from 3-50° with a mean of 9°*
- *Dune superimposition is common although there are no clear morphological relationships between the size of primary and secondary dunes.*
- *Bedform response to flow stage is rapid with little lag effect but the variability in dune height and wavelength increase at higher flow stages*
- *Dunes create individual flow fields which control the local suspension of sediment, both over low and high angle leeside dunes*
- *Dunes are the dominant mode of bedload transport and therefore are of central importance in generating local bed morphology and initiating the formation of bars*
- *Mid-channel bars are the most common bar type in the Jamuna and exert considerable influence on the local flow structure, channel change and bank erosion*
- *Sand bars often form downstream of a zone of flow convergence and are initially deposited as a central symmetrical bar core, aligned sub-parallel to the primary flow direction*
- *The basic planform morphology of a mid-channel bar is rhomboidal with two protruding bartail limbs. This morphology is characteristic of all scales of mid-channel bars*
- *The bartail may be an important storage zone for fine sediment and can form highly cohesive 'plugs' which may be difficult to erode. Downstream migration of the barhead may preserve this plug and temporarily 'remove' the finest fractions from the channel and floodplain transport system*
- *Mid-channel bars grow through (i) flow divergence at the barhead and deposition at the bar margins, (ii) lateral accretion induced by secondary flows in the anabranches, (iii) vertical aggradation by successive stacking of dunes, and (iv) downbar migration of an accretionary dune field front. This front may only form during short-lived (days) fluctuations in discharge at the hydrograph peak*
- *Bar growth and channel change is not always accompanied by downstream migration of the bar nucleus*
- *Channel change and the rate of sediment erosion and deposition is strongly stage dependent with no lag behind the hydrograph peak. The mean erosion and deposition rates are in balance throughout the hydrograph suggesting no net aggradation or degradation of the braidbelt*
- *A six-stage model for mid-channel bar growth and morphological change in the study area is proposed which is consistent with observations in the literature and may be applied more widely in the Jamuna*

Contents

List of Figures

Figure 3.9: Scatterplots of (a) height of primary dunes -vs- height of secondary dunes and (b) wavelength of primary dunes -vs- wavelength of secondary dunes, subdivided according to position on the primary dune (leeside, stoss side or crestal shoulder)

Figure 3.10: Scatterplot of dune migration rate -vs- dune height at Bahadurabad for high flow stage.

Figure 3.11: Histograms of (a) dune height, (b) wavelength, (c) form index and (d) leeside angle through the 1994 and 1995 flood hydrographs. Each year is divided into low flow (< 1.5 m s^{-1}), high flow (> 1.5 m s^{-1}) and rising and falling limbs of the hydrograph (> 1.5 m s^{-1}).

Figure 3.12: Temporal variation in the mean, maximum and minimum values of (a) dune height, (b) wavelength, (c) form index and (d) leeside angle through the 1994 and 1995 flood hydrographs.

Figure 3.13 Plots of leeside angle as a function of a) time and b) mean downstream velocity; (c) dune height as a function of mean downstream velocity.

Figure 3.14: Hysteresis plots for 1994 and 1995 hydrographs at Bahadurabad for (a) dune height, (b) dune wavelength and (c) dune form index plotted as a function of mean flow velocity derived from ADCP records.

Figure 3.15: Plots of downstream and vertical flow velocities and backscatter intensities over a) steep and b) low-angle leeside dunes at Bahadurabad.

Figure 3.16: At-a-point time series records of (a) downstream and (b) vertical velocities at 5 heights above a dune trough (bold figures denote height above bed in metres). These plots illustrate the occurrence of low downstream velocity upwellings associated with the dune leeside. Both velocities are expressed as deviations from the mean at-a-point temporal average velocity; absolute velocities are shown in Figure 3.15(a).

Figure 3.17: Temporal occurrence of 'boils' associated with dunes at Bahadurabad, August 1994 estimated from a) visual records of 'boil' surface upwellings and b) spectral analysis of ADCP downstream and vertical velocity records over a dune crest and trough.

Figure 4.1: Morphology of a 55 km reach of the braided Jamuna River traced from 1:50000 SPOT images G11 and G12 during low flow on (a) 3/3/92, (b) 12/3/93, (c) 3/3/94, and (d) 24/3/95. Coordinates are SPOT. Note the position of the study bar in (d) downstream of a major flow convergence.

Figure 4.2: (a) Channel change and bar migration from 12/3/93-3/3/94. Bar positions are traced from G11 and G12 1:50000 SPOT images.

Figure 4.2: (b) Channel change and bar migration from 3/3/94-24/3/95. Bar positions are traced from G11 and G12 1:50000 SPOT images. The bars labelled A show the

characteristic barhead erosion and bartail deposition, the bars labelled B migrate upstream by accretion of secondary lobes onto the barhead and margin.

Figure 4.3: (a) and (b) Bar morphology and channel change in the study area north of Bahadurabad ghat from March 1991-March 1995. Diagrams are traced from biannual 1:50000 SPOT images approximately coinciding with low and high flow in the monsoon hydrograph (see Figure 2.1c). The mean water level at the time of satellite imagery is shown. Coordinates are SPOT.

Figure 4.4: Spyglass® contour maps of bed topography for (a) 10-18 November 1993, (b) 10-14 August 1994, (c) 1-10 November 1994, (d) 7-8, 13 March 1995, (e) 25-26 June 1995, (f) 31 July/1 August 1995, (g) 12-16 September 1995, (h) 11-25 November 1995, (i) X-X March 1996. The area of bed survey is different for special and bathymetric surveys (see Table 2.2) but all the figures are plotted at the same scale. All heights are reduced to SLW to enable comparison between dates. The position of the water edge for each bathymetric survey period is digitised from the bed contour at the relevant SLW level (emergent bar shown as black). These water edges are also used to defined the approximate water margin for special surveys (emergent bar highlighted with dotted fill). The land survey over the study bar in February 1996 is incomplete so the bartop contours are unrealistically low.

Figure 4.5: Superimposed cross-sections for the five bar transects (BT5X024, 34, 25, 33, and 26) and BT5X030 and 28, 750 and 1250 m downstream of BT5X026 respectively (see Figure 2.1b). The periods of special survey are (a) 10-14 August 1994→7-8, 13 March 1995, (b) 7-8, 13 March 1995→25-26 June 1995, (c) 25-26 June 1995→31 July/1 August 1995, (d) 31 July/1 August 1995→12-16 September 1995, and (e) 12-16 September 1995→24-26 February 1996. The area of each block of erosion and deposition is given in Table 4.2 later. Note that the February 1996 land survey is incomplete.

Figure 4.6: (a) Planform morphology of the emergent study bar as land surveyed in March 1995. The two dunes fields terminate in a 3 m high, steep, accretionary front (see text). Measurements of dune orientation indicate the flow was strongly divergent over the bartop. (b) 100MHz ground penetrating radar trace for transect BT5X026. The trace is west to east (left to right) with the lateral distance from the water edge shown on the top scale (280-400 m). The trace shows steeply dipping (note the vertical exaggeration), bar slip faces, prograding east to west, superimposed by a 1 m layer of low-amplitude dunes. An impermeable layer (strong radar reflectance) at 330 m cross-stream and 5-6 m depth, represents the 'old' bartail area where a substantial quantity of fine-grained sedimentation occurred (see text and Figure 4.6a).

Figure 4.7: Spyglass® contoured ADCP records of the resolved (*U-W*) downstream velocity and direction and backscatter intensity for transects (a) BT5X023, (b) BT5X036, (c) BT5X021, (d) BT5X034 (see text and Figure 2.1b) taken on 11-12 August 1994. Flow directions must be considered relative to the bearing of the bar's long-axis which is 148°.

Figure 4.8: Spyglass® contoured ADCP records of the resolved (*U-W*) downstream velocity and direction and backscatter intensity for transects (a) BT5X035, (b) BT5X024, (c) BT5X034 (d) BT5X025, (e) BT5X033, and (f) BT5X026 (see Figure 2.1b) taken on 31 July

1995. The transects are 250 m apart with BT5X035 furthest upstream. Flow directions must be considered relative to the bearing of the bar's long-axis which is 148°.

Figure 4.9: Downstream bed profile of the newly emergent bar in August 1994 (line BB1Y038). Note the accretionary dune front migrating onto the barhead (labelled DF) and the changing dune size over the bar with large dunes in the deeper flows around the bar flanks and progressively smaller dunes as flow shallows on the stoss side of the bar. The flat bartop area (labelled BT) has few dunes and is not characterised by upper-stage plane beds, thus it must be an area of lower sediment transport rates,

Figure 4.10: View of the accretionary dune fronts as exposed on the emergent study bartop in March 1995. The survey pogo is 1.8 m high and flow is right to left.

Figure 4.11: 100MHz ground penetrating radar trace for transect BT5X033 (250 m upstream of BT5X026 shown in Figure 4.6b). The trace is west to east (left to right) with the lateral distance from the water edge shown on the top scale (280-400 m). The trace shows bar slipface accretion, with several sharp erosion surfaces, superimposed by a 3m layer of stacked, low-amplitude, dunes. The dunes are typically 0.5 and 1 m high, with well defined crests and troughs.

Figure 4.12: 2m trench section taken on GPR line BT5X026 showing the preservation of stacked, low-amplitude dunes with trough cross-stratification (note penknife for scale). Mean D_{50} grain size of the preserved dunes is 0.24 mm.

List of Tables

1. Introduction

1.1 Context of study

The River Survey Project (RSP, or FAP24) was initiated on June 9, 1992, and is scheduled for completion on June 8, 1996. The project has been executed by the Flood Plan Coordination Organisation (FPCO) under the Ministry of Irrigation, Water Development and Flood Protection, presently the Ministry of Water Resources. By the end of 1995, FPCO merged with the Water Resources Planning Organisation (WARPO) under the same Ministry, at which time WARPO took over the project execution. Funding has been granted by the European Commission (formerly the Commission of the European Communities). The Consultant is a joint venture of DELFT HYDRAULICS and the DANISH HYDRAULIC INSTITUTE (DHI), in association with Osiris, Hydroland and Approtech. Project supervision is done by a Project Management Unit with participation by FPCO/WARPO, a Project Advisor, and a Resident Project Advisor.

The objective of the project is to contribute to the basis of the FAP programme, as well as to other national planning, design, and impact assessment activities within the domain of water resources and river engineering.

The project consists of three categories of activities:

- a survey component, comprising a comprehensive field survey programme of river hydrology, sediment transport, and river morphology;
- a study component, comprising investigations of processes and effects within river hydrology, sediment transport, and river morphology;
- a training component.

The proceedings of the River Survey Project are described in several report series that cover the overall progress, surveys, studies, general professional issues, and administrative matters. The final reporting is organised as follows:

- A Main Final Report, which contains a summary of the background, a short overview of the activities within each project component, and overall recommendation
- Annexes to the Final Report, covering

1: Surveys
2: Sustainable survey techniques
3: Hydrology
4: Sediment transport
5: River morphology

A listing of all River Survey Project reports is given in the Main Report.

The University of Leeds team (UoL) comprises Dr. Phil Ashworth (Geography), Dr. Jim Best (Earth Sciences) and a U.K. Natural Environment Research Council funded Ph.D student, Ms. Julie Roden. The UoL have also been assisted in parts of the study by Dr. Charlie Bristow (Geology, Birkbeck College, London). The joint FAP24-UoL study covers the

special study topics 6 (bars) and 7 (bedforms). This report treats each study topic separately although there is a close relationship between the bedform and bar topics (see later). Five periods of fieldwork were completed by the UoL, usually coinciding with the times of special survey. In addition, Ms. Roden spent three, six-week periods at the FAP-24 office collating and reducing data and visited DHI (Copenhagen) to discuss software development.

1.2 Introduction and definitions

A number of terms and definitions exist for the different types and sizes of bedforms (e.g. Allen, 1982; Ashley, 1990; Dalrymple and Rhodes (1995)) and bars (e.g. Lewin, 1978; Smith, 1978) that can exist in sand-bed rivers. In order to be consistent, the following definitions are used here:

1.2.1 Bedforms

An understanding of the nature of bedforms within all of the main rivers of Bangladesh is of critical importance for the estimation of bedload transport, analysis of resistance factors, prediction of local scour depths and in planning well-constrained sampling/measurement programs (Klaassen et al., 1988; Lukanda et al., 1992; Peters, 1993). Additionally, the role of bedforms in the growth of larger scale bar features, and associated bank erosion/channel incision, form key factors in assessing river channel behaviour. Past work on bedforms within the Jamuna has suggested the occurrence of a wide range of bedforms from ripples → dunes → upper-stage plane beds (Coleman, 1969; Klaassen et al., 1988), although there is uncertainty on the relative occurrence of each bedform type and their stability in relation to flow stage. For example, past work has both suggested that upper-stage plane bed conditions may become common at high flow stages and that dunes persist throughout the peak flows (Klaassen et al., 1988). Flattening of the river bed has also been recorded in other large rivers, such as the Zaire (e.g. Peters, 1977; Peters and Goldberg, 1989)

Coleman (1969) documented a range of large bedforms within the Bramahputra and reasoned that some of the largest avalanche faces, up to 15 m high, represented very large 'sand waves'. Coleman also noticed the close association between dunes and the occurrence of strong 'boils' on the water surface that carried high concentrations of suspended sediment. Julien and Klaassen (1995) compiled data from a range of very large alluvial channels, including the Jamuna, and showed that mean dune steepness and van Rijn's (1984) bedform height parameter do not always decrease at high transport stages in large rivers, and that large bedforms may exist even at high transport stages. Julien and Klaassen (1995) also demonstrated the importance of considering the Froude number in addition to the transport stage in large rivers, since the Froude number in such large channels may often be low and allow the stability of dunes at transport stages that are dominated by upper-stage plane beds in shallower flows. It is evident from past work on bedforms in the large alluvial channels that there is a need for high quality morphological data throughout the flood hydrograph (Peters, 1993) and integration of these morphological measurements with details of the flow field, especially in relation to bedload transport estimates and controls on sediment suspension.

Arising from this work, and that of others (see reviews in Allen, 1982; Ashley, 1990; Yalin, 1992; van Rijn, 1993; Dalrymple and Rhodes, 1995; Kostaschuk and Ilersich, 1995), the following definitions are adopted in this study:

Ripple: an asymmetrical profile bedform with height (H) < 0.05 m and wavelength < 0.60 m. These bedforms usually cannot be resolved on echo-sounder traces but maybe identified from some side scan sonar images and are common in bartop sections exposed at low flow.

Dune: an asymmetrical profile bedform whose maximum dimensions may scale with the flow depth such that $H \sim 0.2/0.3h$ and $\lambda \sim 5\text{-}7h$, where H and λ are bedform height and wavelength respectively and h is flow depth. However, bedform superimposition and lag effects through the flood hydrograph may result in many excursions from these relationships. Maximum dune heights of ~6m and wavelengths of 340m have been documented in this study. It should be noted the large (~15 m high) bedforms recorded by Coleman (1969) are not in fact dunes but more likely avalanche/leeside faces associated with bars, possibly at tributary junctions, confirming the earlier suggestions of Klaassen et al. (1988).

Upper-stage plane bed: a flat bed, with minor relief (mm→several cm) associated with intense sediment transport (Allen, 1982; Best and Bridge, 1992).

Bar: a larger scale morphological feature which scales with channel width, whose height is often a significant proportion of the flow depth, and may become emergent at constant or waning flow conditions.

The descriptive classification of dunes outlined by Dalrymple and Rhodes (1995), which is based on a consensus view from many workers (e.g. Ashley, 1990), was also adopted in this study (Table 1.1). The term 'dune' encompasses the bedform previously described as megaripples by several other researchers (e.g. Coleman, 1969; Bristow, 1987; Klaassen et al., 1988) which are dynamically analogous to dunes (Ashley, 1990).

26

First-order descriptors					
Size:	Term	**small**	**medium**	**large**	**very large**
	Wavelength, λ, m	0.6-5	5-10	10-100	>100
	Height, H, m	0.15-0.25	0.25-0.5	0.5-3	>3
Shape:	**2-Dimensional** - relatively straight-crested, lacking scour pits				
	3-Dimensional - sinuous to lunate, with scour pits				
Second-order descriptors					
Superimposition:	**Simple** - lacks superimposed dunes				
	Compound - bears smaller, superimposed dunes (termed secondary and tertiary dunes)				
Sediment Characteristics	grain size, sediment sorting				
Third-order descriptors					
Bedform profile:	bedform shape (λ/H); stoss and lee slope lengths and angles				
Orientation:	transverse, oblique, longitudinal				
Dune behaviour:	migration rate, change in form and hysteresis effects				
Occurrence:	percentage of bed covered by dunes				
Flow history:	mean flow & turbulence fields associated with dunes				

Table 1.1: Descriptive classification of dunes and terms used in this study (after Dalrymple and Rhodes, 1995)

1.2.2 Bars

Braided reaches of the main rivers of Bangladesh contain many different types and size of bar (Coleman, 1969; Bristow, 1987; Klaassen and Masselink, 1992; Klaassen et al., 1993; Peters, 1993; Thorne et al., 1993), one of the most common being the mid-channel bar which is associated with flow divergence immediately downstream of a confluence or node of flow convergence (Klaassen et al., 1993; Thorne et al., 1993; Mosselman et al., 1995). A mid-channel bar may be defined as an accumulation of sediment which is unattached from the cutbanks. Bar width scales with wetted channel width (Parker, 1976; Tubino, 1991; Yalin, 1992) but bar height is independent of local water depth (unlike dunes - see Section 1.2.1) and bars often become emergent via anabranch incision without a change in flow stage or discharge (Leopold and Wolman, 1957; Ashmore, 1982).

Recent work in sand and gravel-bed rivers across a range of scales has shown that mid-channel bars are one of the fundamental building blocks of braided rivers (Church and Jones, 1982; Ferguson, 1993; Ashworth, 1996) because they control local flow structure (M^{c}Lelland et al., 1996; Richardson et al., 1996), sediment transport distributions (Laronne and Duncan, 1992; Lane et al., 1995), channel scour and deposition (Goff and Ashmore, 1994), bank erosion (Mosselman, 1995; Parker, 1996), channel avulsion (Cheetham, 1979; Ashworth and Ferguson, 1986; Leddy et al., 1993) and, ultimately, the evolution of channel pattern (Carson and Griffiths, 1987; Murray and Paola, 1994). These diagnostic features all apply to mid-channel bars in the main Bangladeshi rivers (Peters, 1993) and therefore quantification of the rate, form and flow processes responsible for bar growth and emergence is a prerequisite for successful prediction of bed scour, bank retreat and channel evolution.

1.3 Objectives

The main objective of the two study topics is to understand the dynamics of bedforms and braid bars and their influence on the morphological behaviour of Bangladesh's main rivers. Specific objectives are to:

- Quantify the morphology of bedforms (size, shape, three-dimensionality) and how these vary through the flood hydrograph Examine the occurrence of different bedforms within the active channels and how this changes through the flood hydrograph
- Assess the hydraulic controls on bedform stability (e.g. discharge, flow velocity, shear stress)
- Examine the flow fields associated with dunes and their influence on sediment suspension
- Examine the nature of bedform-bedform and bedform-bar superimposition,
- Examine the morphology and dynamics of bars
- Assess the time and stage dependency of bar growth and its impact on local and downstream channel change
- Quantify the flow structure associated with mid-channel bar growth, and,
- Examine the role of dune bedforms in the process of bar growth

2. Site description and methodology

2.1 Study reach description

2.1.1 Dune surveys

This topic used data acquired during normal routine surveys as well as more detailed special surveys conducted at Bahadurabad.

1) Routine Surveys
Data from most routine gauging surveys from November 1993 - December 1995 were used for analysis of bedform longitudinal profiles. Three longitudinal profiles were normally run during each routine measurement, approximately 1 km long and oriented parallel to the main flow. All lines from both the Phulchari and Bahadurabad (Figure 2.1) main sites have been used in this analysis together with data from Sirajganj and Bhairab Bazar.

2) Special Surveys
Five special surveys over dunes occurring at Bahadurabad were conducted over the period August 1994 - March 1996 (Table 2.1, Figure 2.1). During each survey, repeat lines were run in order to examine dune morphology, migration and flow structure as revealed by ADCP. Side scan sonar surveys were also run on three surveys (Table 2.1) to detail dune planform morphology. Additionally, run lines from Bahadurabad-Aricha during transit between routine surveys permit assessment of bedform occurrence within a large area of the Jamuna. Examination of dunes on exposed bartops during March 1995 and February 1996, conducted in association with the study of bars (Topic 6), also aided study of dune morphology.

Special Survey Date	Equipment employed	Water level*
10-14 August 1994	Standard surveying equipment - DGPS, ADCP, EMF, echo-sounder, MEX-4, suspended sediment sampler and bed grab samples	17.86
19-20 September 1994	Standard surveying equipment	17.56
7-13 March 1995	Standard surveying equipment and side-scan sonar	13.18
11-17 September 1995	Standard surveying equipment and side-scan sonar	17.86
26 February - 4 March 1996	Standard surveying equipment and side-scan sonar	13.31

Table 2.1: Special surveys at Bahadurabad concerning dune dynamics.

*SLW at Bahadurabad is 12.03m + PWD

Bedform morphology was measured using 30 and 210 kHz echo-sounders with a resolution of ± 0.05 m and, when combined with the DGPS location, allowed survey and resurvey of specific lines. All dune survey lines were run upstream and parallel to flow. Dunes were defined as those bedforms greater than 0.15 metres in height and measurements were obtained directly from on-screen analysis of the digital records. Bedform superimposition was

common where smaller secondary dunes are superimposed on both the stoss and lee sides of larger wavelength primary bedforms. Details of echo-sounder and DGPS resolution can be found in SPR-3.

2.1.2 Bar surveys

A special study site was identified in November 1993 for monitoring bar growth and changes in channel morphology. The site is approximately 6 km north-west of Bahadurabad, bounded by BTM co-ordinates N780000→N788000, E467000→E472000 (Figure 2.1). The site was selected because (i) it was a zone of potential mid-channel bar growth since the main channel was downstream of a significant flow convergence, (ii) it possessed a relatively 'simple' channel configuration with a parabolic cross-section and no other actively aggrading bars nearby, (iii) it lies within the zone of the Bahadurabad bathymetric survey, and (iv) it is of strategic importance being adjacent to the navigation cross-channel to Phulchari and immediately upstream of both Bahadurabad ghat and the new FAP21 embankment scheme.

Data on bed morphology were obtained from a combination of bathymetric and special surveys using conventional echo-sounding and DGPS techniques (see SPR-XX). Bathymetric lines run West→East at 100 m spacing and cover a 20 km^2 area (see SPR-XX). For the special surveys, a series of transect lines was established perpendicular to the local flow direction (58°) and spaced 250 m apart (Figures 2.2a-g). These lines were usually supplemented by lines parallel to flow (148°) over the study bar and in the left and right anabranches. The number of special survey transects was progressively increased during the study period to cover the downstream migration of the study bar and associated channel changes (Figures 2.2a-b, Table 2.2). Bed surveys were undertaken at different times of the flood hydrograph (i.e. rising, peak and falling limbs, Figure 2.1c) to quantify the temporal variability in channel change and bar aggradation during the monsoon season (see Sections 4.1 and 4.2). Ship surveys were supplemented by EDM land surveys over emergent parts of the study bar in March 1995 and February 1996. All special surveys were undertaken by the DHA vessel.

Survey period	Survey type	Water Level* m	Number of survey lines
10-18 November 1993	Bathymetric	15.48	90+
10-14 August 1994	Special Survey	17.86	19
19-20 September 1994	Special Survey	17.56	11
1-10 November 1994	Bathymetric	15.18	90
24-27 February 1995	Bathymetric	13.03	90
7-8, 13 March 1995	Special Survey	13.18	21
25-26 June 1995	Special Survey	19.25	19
4-25 July 1995	Bathymetric	19.65	90
31 July, 1 August 1995	Special Survey	18.52	20
12-16 September 1995	Special Survey	17.86	27
11-25 November 1995	Bathymetric	15.52	90
24-26 February 1996	Special Survey	13.22	38
7-13 March 1996	Bathymetric	13.41	90

Table 2.2: Source of data for monitoring bar growth and morphology, Bahadurabad, 1993-1996.

29

* SLW at Bahadurabad is 12.03 m + PWD

+ Only bathymetric lines between N779000 and N788000 are used to produce the bed topographic maps

2.2 Data sources

2.2.1 Dune surveys

Standard techniques were used in this study with data from routine surveys from vessels DHA and DHB (see SPR-XX, Table 2.1). For examination of the mean and fluctuating flow structure associated with dunes, ADCP measurements were conducted using 10 ping ensembles for each profile averaged approximately every six seconds. Side-scan sonar was deployed both at low and high flow - although excellent results were obtained in low flow conditions in the deeper talwegs, less well-defined images were obtained at high flow with high suspended sediment concentrations causing signal attenuation and loss of bottom tracking.

2.2.2 Bar surveys

Flow velocity data were obtained from ADCP (300 kHz) profiles taken along special survey lines (see SPR-XX for a detailed description of these techniques). Velocities from each 0.5 m vertical bin were reduced to produce the resolved primary velocity vector and relative backscatter intensity. Secondary flows were not computed because of the difficulty in defining a common plane of reference in strongly non-uniform flow (though see M^{c}Lelland et al., 1994 and Richardson and Thorne, SPR-16).

Topographic and velocity data were contoured using the Spyglass® visualisation package with a 25 m grid and kriging parameters that used a spherical distribution model, a variance of unity and 150 samples per kriging pass. The interpolation used between 11,672 (September 1995, Special Survey) and 346,000 (July 1995, Bathymetric Survey) individual bed survey points. The mean water level for each survey period was used to define the bank edges for each topographic map. Rates of erosion and deposition were digitised from superimposed cross-sections adjusted to a common 'Start of Line' (SOL) position. The minimum digitisation area was 2.01 m^2.

Likely sources of error in the data collection and analysis are: (i) standard measurement error associated with the survey instruments (see discussion in Annex 1), (ii) underestimation of erosion and deposition rates because of short-term scour and fill events (i.e. between survey periods), and (iii) smoothing of abrupt changes in topography by the contouring package. The consistency of channel change at the special survey site suggests that the frequency of surveys was adequate, but, because the sediment transport rate is so high in the Jamuna, some minor channel scour and fill events will undoubtedly be missed (see discussion in Peters, (1993)). The implication of this for the morphological estimate of sediment transport rates is elaborated in Section 4.3.

3. Dune dynamics

3.1 Factors controlling bedform stability

The stability and morphology of alluvial bedforms is governed by several factors:
1) Applied bed shear stress
2) Flow depth
3) Grain size
4) Froude number
5) Occurrence of suspended sediment
6) Available generation time (*cf.* duration/intensity of sediment transport)
7) Flow unsteadiness and bedform response to changing flow conditions through a flood hydrograph (Wijbenga and Klaassen, 1981)

These topics are reviewed in Allen (1982), Southard and Boguchwal (1990) and Best (1996). In relation to the main rivers in Bangladesh, whose bedload is predominantly fine sand (SPR-14) and whose suspended sediment concentrations are insufficient to affect flow turbulence and bedform generation (see Wan, 1993), bedform stability is largely a function of factors 1, 2, 4, 6 and 7 above. These parameters are discussed below when examining bedform morphology.

3.2 Bedform occurrence and distribution

Dunes are the predominant bedform occurring at varying flow stages and in many parts of the main channels. Figure 3.1a illustrates examples from Bahadurabad, Sirajganj and Bhairab Bazar which demonstrate the percentage of channel talweg covered by dunes during the study period. Over 40% of the bed is always occupied by dunes at any one flow stage, with this figure often being in excess of 70%. Additionally, Figure 3.1b plots the percentage occurrence of dunes on a long profile taken between Sirajganj and Aricha (encompassing both talweg and bar margins) and demonstrates once again that between 40 and 95% of the bed is covered by dunes. Ripples may also be expected to be superimposed on many of these dunes but are smaller than the echo-sounder resolution. Dunes are also very commonly superimposed on bars (see Section 4.6) and confirm that dunes are ubiquitous in both the deep channel talwegs and bar margins. Flat beds can also occur on steep bar margins and bar tops but the bar top plane beds are usually associated with regions of lower flow velocity (Section 4.5) and are probably rippled surfaces where bed shear stresses are too low to generate dunes. Additional evidence concerning the widespread occurrence of dunes within the main channels and superimposed on the larger barforms also comes from ground-penetrating radar studies of the subsurface bar structure (Section 4.6, Figure 4.11) which show that dunes comprise the majority of the preserved sediments both near surface and to depths of ~5 m. Together with the pattern of dune superimposition on bars (Section 4.6, Figure 4.9), this confirms that dunes are the predominant bedform within all the active channels, both in the talwegs and bar margins.

3.3 Bedform geometry - height, wavelength, shape and planform morphology

Dune height and wavelength plotted for all data at Bahadurabad, Sirajganj and Bhairab Bazar (Figure 3.2a,b; Table 3.3) demonstrate that dune height ranges from 0.15 - 6.3 m and wavelength from 4.6 - 342 m. Both distributions have a log-normal form. The form index (wavelength/height) of such dunes (Figure 3.2c) shows a range of values from 3.6 - 132.

Van Rijn (1984, 1993) proposed that dune height and steepness vary as a function of a transport stage parameter, T, where

$$T = (u_*' - u_{cr}) / u_{cr} \qquad \textit{(Eq. 3.1)}$$

in which

$u_*' = \rho g(\overline{U} / C)^{0.5}$ = grain related bed shear stress, where ρ = fluid density, g = acceleration due to gravity, $\overline{U}$ is the depth averaged velocity and C is the grain-related Chézy coefficient ($C = 18\log(12h / 3D_{90})$, where h is flow depth and D_{90} is the 90th percentile of the grain size distribution), and

u_{cr} = critical bed shear stress obtained from a Shields plot.

Van Rijn (1993) presents a table (see Table 3.1) summarising the stability of bedforms dependent on the transport stage parameter, T, and a dimensionless particle diameter, D_*, given by:

$$D_* = (D_{50} \ ((\rho_s / \rho) - 1)g / \nu^2)^{0.33} \qquad \textit{(Eq. 3.2)}$$

where D_{50} is the 50th percentile of the grain size distribution, ρ_s and ρ are the density of the sediment and fluid respectively and ν is the kinematic viscosity of the fluid.

Transport Regime		Particle Size	
		$1 \le D_* \le 10$	$D_* > 10$
Lower	$0 \le T \le 3$	ripples	dunes
	$3 \le T \le 10$	dunes	dunes
	$10 \le T \le 15$	dunes	dunes
Transition	$10 \le T \le 15$	washed-out dunes, sand waves	
Upper	$T \ge 25$, $Fr < 0.8$	(symmetrical) sand-waves	
	$T \ge 25$, $Fr \ge 0.8$	plane bed and/or antidunes	

Table 3.1: Classification of bedforms according to T and D_* parameters. Shaded columns depict the T-D_* flow conditions monitored in the present study (not Fr conditions which are <0.8). (modified after van Rijn, 1993; Fr = Froude number)

Values of T for the dunes documented in this study (D_*~4) span a wide range from 1 to 65, illustrating that dunes may exist at a wide range of T values in large alluvial channels, confirming the work of Julien and Klaassen (1995); in such large alluvial channels upper-flow regime conditions and related bedforms (plane-bed and antidunes) are not produced at a threshold value of T~25 since the Froude number of the flow is nearly always<<1.

Derivation of van Rijn's bedform height and steepness functions allows further comparison of the current results with past work. These parameters are given by:

$$\text{bedform height function} = H / h(d_{50} / h)^{0.3} \quad (Eq.\ 3.3)$$

$$\text{bedform steepness} = \lambda / h(d_{50} / h)^{0.3} \quad (Eq.\ 3.4)$$

and are plotted as a function of T in Figure 3.3. Both of these plots again illustrate that dunes are present at a wide range of T values and that in the main rivers of Bangladesh there is no evidence that plane beds exist at T>25; indeed dune height and steepness seem fairly invariant with increasing T in the flow depths present in the rivers studied. Julien and Klaassen (1995) suggest that the presence of dunes in large alluvial channels at T>25 is principally due to the fact that Froude numbers in these channels are often <0.8. Plots of local Froude number against T for the sites examined in this study (Fig. 3.4) also confirm this contention; even at the largest peak flows, Froude numbers rarely exceed 0.28 and dunes remain the stable bedform. It is clear that values of T>>25 are required to generate a transition to upper-stage plane beds in many of the talwegs and bar margins of the Bangladeshi main rivers, as witnessed by the ubiquitous occurrence of dunes at all flow stages. The trend in the Froude number data shown in Figure 3.4 suggests that conditions may rarely be achieved which produce supercritical flow in these channels.

Besides the form index of dunes, which is important for bedload transport estimates using dune tracking (see Section 3.5), the leeside angle of bedforms is of considerable importance in relation to energy expenditure and flow resistance over bedforms. A composite histogram of leeside angle from the three study sites (Figure 3.2d where leeside angle is defined as the slope between points at the crest and trough of the bedform) shows a range of values from 2 - 58° (greater than the static angle of repose), with a mean dune slipface angle of 8.6° (Table 3.2), providing confirmation of the mean value reported by Klaassen et al. (1988). Flow separation in the leeside of bedforms may be expected to occur when the change in slope exceeds approximately 12°, and hence energy losses associated with the bedform increase (Klaassen et al., 1986, 1988; Ogink, 1988; van Rijn, 1993). The range of leeside angles present on dunes in the Jamuna span this critical leeside angle and suggest that leeside angle, as well as bedform shape, should be quantified when deriving bedform dimensions for use in resistance calculations.

Recent work by Kornman (1995) has suggested that the angle of the leeside is better expressed through local slope changes at the crest and brinkpoint rather than the crest-trough slope ($\alpha 1$, see Fig. 3.5 inset). Many dunes within the main rivers of Bangladesh possess complex downstream profiles, with the highest point on the crestal shoulder often being upstream of the brinkpoint of the main slipface (see Fig. 3.5 inset). Derivation of the leeside angle at the point of slope change at the brinkpoint of the dune ($\alpha 2$, Fig. 3.5) and at the point of flow expansion at the crestal shoulder ($\alpha 2$, Fig. 3.5) allows two alternative measures of

leeside slope to be derived (Fig. 3.5). The mean value of $\alpha 2$ is larger than that of α 1 at 11.7° as compared to 8.6°. However, $\alpha 3$ has a mean value of 4.1°, demonstrating the more gentle break of slope at the crestal shoulder as compared to the brinkpoint. The complexities induced by this compound dune shape are several. First, the influence of flow separation in the leeside of the dune may be expected to be lessened where a gentle crestal shoulder break of slope is present, this producing smaller separation zones with a lower velocity gradient across the shear layer. However, a second point is that this effect may not act in just one way to diminish turbulence generation, since the additional turbulence generated along the shear layer of this first separation zone may feedback to produce enhanced local velocity gradients at the point of separation of the brinkpoint separation zone. It is clear that more detailed laboratory and field work is required to address the issues of hydraulic resistance, turbulence generation and sediment suspension over these complex dune morphologies.

Plots of dune height and wavelength as a function of flow depth (Figure 3.6a, b) show a wide scatter but clearly illustrate that maximum dune height approximates 0.25-0.33 of the flow depth (see Bennett and Best, 1995) and that dune wavelength is generally less than ~ 7h (see Julien and Klaassen, 1995). It is also evident that dune leeside angle shows little relationship with flow depth (Figure 3.6c). Although the modification of dunes to upper-stage plane beds is associated with increasing shear stresses and a larger suspension/partial-suspension load (e.g. Klaassen et al., 1986; Southard and Boguchwal,, 1990; Best and Bridge, 1992), it is evident that the shear stresses/Froude numbers present in many of the channels in the present study are not high enough to generate upper-stage plane beds. Consequently, flow depth (which may act as a surrogate for shear stress if all other factors, such as slope, are constant) shows little influence on the leeside angle over most dunes.

	Mean	Standard Deviation
Height, H, m	1.02	0.97
Wavelength, λ, m	36.7	40.4
Form index, λ/H	39.7	29.3
Leeside angle, degrees	8.6	7.9

Table 3.2: Summary of mean dune morphology for all data at Bahadurabad, Sirajganj and Bhairab Bazar

Side-scan sonar images of dunes collected at low flow (Figure 3.7a) show both two-and three dimensional dunes with heights of 0.6 - 1.75 metres, wavelengths of 5 - 30 metres and crestline sinuosity ranging from 1.12 - 1.54. Composite tracings of these images allows the three-dimensionality of the dune crestlines to be measured (Figure 3.7b). Records of dune planform shape at high flow show that the bedforms are also three-dimensional, with scour troughs and spurs between adjacent crestlines. These morphologies are also present in both small (H ~0.4m) and larger (H~2m) dunes exposed on bar tops at low flow (Figure 3.8). Bedform three-dimensionality has been proposed to reflect the strength of the flow (e.g. Allen, 1982), although recent work has suggested that bedform three-dimensionality more

properly reflects the length of time available for bedform development, or the amount of bedload transport and its spanwise variation (Baas, 1994). Given that bedform migration occurs both throughout high and low flow, it is likely that all bedforms will display some degree of three-dimensionality and few dunes will remain two-dimensional. This is borne out by both side-scan sonar records and examination of exposed dunes in bartop sediments at low flow.

3.4 Bedform superimposition

Bedform superimposition is common within all the rivers of Bangladesh with smaller dunes generated in evolving internal boundary layers upon the stoss sides of the larger bedforms. Ripples will also be developed on the backs of dunes although these cannot be resolved with the echo-sounder. Plots of the relationship between the height and wavelength of the primary and secondary/tertiary dunes (Figures 3.9a,b) demonstrate that the height and wavelength of secondary/tertiary dunes generally becomes larger as the size of the primary dunes increases, although there is much scatter in this relationship. Dalrymple and Rhodes (1995) suggested that secondary/tertiary dunes only form on primary dunes with wavelength of approximately 8-10 m, this length being required in order to develop a new boundary layer in which the secondary/tertiary dunes may grow. Since most of the dunes studied in the rivers of Bangladesh have wavelengths greater than 10m, dune superimposition may be expected to be common and supports the contention of Dalrymple and Rhodes (1995). It should also be noted that secondary dunes may be both superimposed on any part of the primary dune (stoss, shoulder or leeside) and occur on the leeside of low-angle leeside primary dunes, again highlighting the need for consideration of bedform superimposition in resistance calculations (Klaassen et al., 1986).

3.5 Time-dependent behaviour of bedforms

3.5.1 Migration rates and short-term change in form

Estimates of bedform migration rates for dunes documented at high stage at Bahadurabad range from 1.11-16.8 m hr^{-1} whilst at low stage rates vary from 0.04 - 0.41m hr^{-1} (Figure 3.10). Dunes of smaller height superimposed on the stoss sides of larger, primary dunes generally possess greater migration rates, although there is much scatter in this relationship.

Several studies have suggested that the migration and morphology of bedforms may be used to yield estimates of bedload sediment transport rates (e.g. Simons et al., 1995; Williams, 1997; Crickmore, 1970; Engel and Lau, 1980; van Rijn, 1993). Morphological estimates of bedload transport may yield more accurate results than traditional direct sampling, especially when it is difficult to precisely locate the direct sampler or when samplers are used in complex flow fields, for instance in the leeside of dunes. In this study, the method outlined in van Rijn (1993) is used to estimate bedload transport rate. The migration rates and dune form indices recorded at Bahadurabad may be used to calculate estimates of bedload transport rate, Q_b (in kg s^{-1} m^{-1}) from:

26

$$Q_b = \beta (1-p) \rho_s c H \qquad Eq. (3.5)$$

where β is a shape factor (often taken as ~0.55, van Rijn, 1993), p is a porosity factor (~0.4), ρ_s is the density of the sediment (~2650 kg m^{-3}), c is the mean migration rate (m s^{-1}) and H is the average dune height.

However, this relationship should only be applied with two important caveats: 1) this method of bedload transport estimation ignores partially or fully suspended material that may become deposited in the dune leeside and contribute to bedform migration (e.g. van Rijn, 1993; Kostaschuk and Ilersich, 1995). Some past studies in large rivers have suggested that as little as 5% of dune migration may be accounted for by bedload transport (see Kostaschuk and Ilersich, 1995), and, 2) these estimates assume a two-dimensional bedform (see Figure 3.7b)

Use of Equation 3.5 with the migration rates, dune heights and shape given in Figure 3.2 produce a range of bedload transport rates from 0.45-10.0 kg s^{-1} m^{-1} at high flow and from 0.014-0.063 kg s^{-1} m^{-1} at low flow.

3.5.2 Stage dependency of bedforms, lag times and hysteresis

Analysis of dune behaviour at Bahadurabad during the flood hydrograph for 1994 and 1995 shows that the dune height and wavelength respond rapidly to changes in flow velocity. Figures 3.11a-d display histograms of dune height, wavelength, form index and mean leeside angle through the 1994 and 1995 flood hydrographs. Each hydrograph is divided into stages of low flow (< 1.5 m s^{-1}), high flow at the peak of the hydrograph (> 1.5 m s^{-1}) and periods of high flow (>1.5 m s^{-1}) on the rising and falling limbs of the hydrograph. Table 3.3 presents a summary of the mean, standard deviation and skewness figures for dune height, wavelength, form index and mean leeside angle over this period. Additionally, the temporal trends in the mean, maximum and minimum values of dune height, wavelength, form index and leeside angle are displayed in Figure 3.12a-d.

Dune height increases through the flood hydrographs (Figs. 3.11a, 3.12a) with the variability in height also rising with flow stage. It is noticeable that the skewness in the dune height population becomes more positive during the rising and falling limbs of the flood hydrograph (Table 3.3), indicative of the generation of more larger dunes during the hydrograph (Figure. 3.11). Dune wavelength also increases during the rising limb of the hydrograph though it is noticeable that as mean wavelength increases slightly, the standard deviation and skewness both decrease. Although dune height increases with flow stage, dune wavelength is more responsive for individual dunes and consequently the dune form index (λ/H) increases through the hydrograph (Figure. 3.12c, table 3.3), indicating the generation of larger but 'flatter' bedforms. Dune leeside angle also increases in angle during the rising stage (Figures. 3.11d, 3.12d, Table 3.3) and decreases on the falling limb of the hydrograph. It is noticeable that the mean slipface angle during the period of high flow is 17° and 12° for the 1994 and 1995 hydrographs respectively. The higher leeside angles present during the peak flow, indicative of steeper leeside slopes even at these higher

year	flow stage	mean	standard deviation	skewness
Dune height (m)				
1994	low	0.36	0.27	1.07
	rising	0.65	0.47	2.16
	high	1.98	1.19	0.85
	falling	0.67	0.60	2.70
1995	low	0.63	0.51	1.63
	rising	0.84	0.45	1.16
	high	1.31	1.53	1.49
	falling	0.39	0.20	1.63
Dune wavelength (metres)				
1994	low	45.4	40.0	1.48
	rising	61.0	54.9	2.32
	high	34.9	25.7	2.12
	falling	38.1	31.5	2.27
1995	low	44.5	34.3	3.24
	rising	33.7	17.8	1.66
	high	48.4	28.1	1.85
	falling	46.3	32.6	1.92
Dune form index (λ/H)				
1994	low	19.1	25.6	1.75
	rising	35.4	39.2	2.32
	high	62.5	50.6	2.12
	falling	19.4	17.9	2.28
1995	low	21.8	16.9	3.24
	rising	26.5	18.6	1.66
	high	54.8	72.9	1.85
	falling	16.2	14.0	1.92
Leeside angle				
1994	low	7.1	5.4	1.34
	rising	7.0	4.3	0.35
	high	17.2	14.5	1.03
	falling	8.0	7.7	2.70
1995	low	8.0	7.4	2.16
	rising	10.5	7.2	1.36
	high	12.2	9.5	2.67
	falling	7.4	4.8	1.40

Table 3.3: Summary statistics for mean, standard deviation and skewness figures of dune height, wavelength, form index and mean leeside angle through the 1994 and 1995 hydrographs at Bahadurabad. Data are subdivided according to flow stage (see text for explanation)

transport stages, will cause more frequent and long-lived flow separation in the leeside of some dunes. This in turn may be expected to both create large-scale turbulence (see below), enhancing both bedload and suspended load transport, and change energy losses and bedform resistance (Ogink, 1988). Additionally, larger dunes and higher slipface angles are associated with greater mean flow velocities (Figure 3.13b,c) and consequently will generate larger shear gradients across the separation zone shear layer. These larger velocity gradients will generate greater turbulence and enhance sediment suspension associated with the larger bedforms at peak flow.

Hysteresis plots of dune height and wavelength at Bahadurabad (Figure 3.14) also illustrate that dunes respond rapidly to increases in flow velocity. Hysteresis in dune height (Figure 3.14a) displays both broad clockwise and anticlockwise rotation for the 1994 and 1995 hydrographs respectively, suggesting that the bedforms and hydraulic parameters may be either indirectly or directly related (Dalrymple and Rhodes, 1995). Dune wavelength hysteresis loops show an anticlockwise pattern (Figure 3.14b) with dune form index showing some flattening of dunes during the falling stage of 1994 but with little variation through the flood hydrograph in 1995. However, these plots also illustrate that there is little tendency for dunes to decrease in height as flow velocity increases, with dune height and wavelength increasing through the hydrograph. This demonstrates again that the majority of hydraulic conditions generate bedforms within the dune stability field and not in the transitional regime to upper-stage plane beds.

3.6 Flow associated with dunes

3.6.1 Mean flow field

Figure 3.15 demonstrates the pattern of mean flow over i) dunes with a steep leeside slope (leeside angle ~ 35°; H = 4.7m, λ = 163m; λ/H = 35), and ii) over a lower angled, flatter dune (leeside angle ~8°; H = 3.0m, λ = 80m; λ/H = 27). Both bedforms show a pattern of flow common to many dunes including:

- a region of slower downstream flow, with possibly flow reversals, in the dune leeside associated with flow expansion
- a zone of downward flow over the dune crest,
- upwards directed flow, of lower than mean downstream velocity, over the stoss side of the dune, and,
- flow acceleration over the dune crest

These patterns of mean flow match well with previous experimental and field work concerning flow over dunes (e.g. Raudkivi, 1966; van Mierlo and de Ruiter, 1988; Lyn, 1993; Nelson et al., 1993; McLean et al., 1994; Bennett and Best, 1995). It is evident from these plots that the mean flow patterns associated with these very large alluvial dunes, of both high and low leeside angle, bear many similarities to many past studies of smaller scale dunes; upwards directed flow in the lee of the dune may reach the flow surface, as witnessed by the many common 'boils' on the flow surface associated with dune fields (Coleman, 1969; Jackson, 1976; Best, 1996). This also suggests that the local leeside angle, which may largely determine the intensity and duration of flow separation and may be controlled by possible

short lived oversteepening of the leeside (possibly through the migration of secondary dunes over the primary dune crest), may be important in the generation of turbulence, energy losses and sediment suspension.

3.6.2 Turbulence and dunes

Many studies have noted the strong association between the occurrence of dunes and presence of large scale 'macroturbulence' within alluvial channels (Coleman, 1969), with several studies proposing that dune growth and stability are linked in some manner to this large-scale turbulence (e.g. Jackson, 1976; Yalin, 1992; Bennett and Best, 1995). At-a-point time series records obtained over very large dunes at Bahadurabad (~4m high, Figure 3.16) illustrate the occurrence of frequent upwellings of fluid over the dune trough. These upwellings, with positive vertical velocities and lower than average downstream velocity, have a periodicity ranging from 10-50 seconds. Records of the periodicity of these upwellings as they reach the surface (Figure 3.17a) and spectral analysis of the time series records (Figure 3.17b) show a mean periodicity of ~20 seconds. Use of a mean flow depth of 13.1 m and mean flow velocity of 1.32 m s^{-1}, allows comparison of the dimensionless recurrence period of the 'boils', T_b, with that proposed by past workers (Jackson, 1976; Yalin, 1992; Best, 1993), where

$$T_b = T_t . \overline{U} / h \sim 3\text{-}7 \qquad Eq\ 3.5$$

(T_t = measured burst period) which produces values between 0.58 and 5.1 with a mean of 2.1, in broad agreement with past work. However, the wide spread in values may be anticipated both due to vortex amalgamation in this complex flow field as well as eddy shedding form dunes of different size (primary and secondary dunes for instance) in the same mean flow conditions.

It is likely that the origin of this large-scale turbulence lies in i) eddy shedding of Kelvin-Helmholtz instabilities generated along the separation zone free shear layer present over steep dunes, and ii) temporal shear layer development associated with flow expansion downstream from lower angle dunes or local oversteepening of the leeside angle through secondary dune migration over the crest of primary dunes. It is clear that macroturbulence associated with bedforms is more intense at higher flow stages and is associated with larger, higher-angle leeside dunes and consequently greater velocity gradients across the leeside separation zone.

Figure 3.15 also illustrates the common pattern of high backscatter intensity, and hence suspended sediment concentration, associated with the leeside and lower stoss side of dunes. These higher backscatter values are associated with the regions of lower than average downstream velocity and positive vertical velocities generated by eddy shedding in the lee of the dune. It is evident this pattern is present both for low and higher angle dunes. Significant sediment suspension within the Jamuna is therefore often associated with large dune fields, a pattern also evident from backscatter records associated with bars (see Section 4.5)

3.7 Summary

- Dunes are the dominant bedform within all active channels and on bar margins/edges at all flow stages
- Dune height and wavelength range from 0.15-6.3 m and 4-350 m respectively
- Dunes are present at values of van Rijn's sediment mobility parameter of up to ~70 and in excess of the T~25 limit often suggested for the transition to upper-stage plane beds
- Dune leeside angle ranges from 3-50° with a mean of 9°. Dune leeside shape is compound and will produce a complex pattern of flow separation and turbulence generation
- Dune superimposition is common although there are no clear morphological relationships between the size of primary and secondary dunes. Secondary dunes may be superimposed on the stoss and leeside of primary dunes and may contribute to temporal oversteepening of the leeside angle of lower angle dunes
- Bedform response to flow stage is rapid with little lag effect but the variability in dune height and wavelength increase at higher flow stages
- Dunes create individual flow fields which control the local suspension of sediment, both over low and high angle leeside dunes
- Dunes are the dominant mode of bedload transport and therefore are of central importance in generating local bed morphology and initiating the formation of bars

4. Bar dynamics

4.1 Bar types and permanency

Bar and bank edges were traced from successive, bi-annual SPOT images (sheet 78, G11 and G12) for low (March) and high (September) flow for the period March 1991-March 1995. Figures 4.1a-d show the bar positions for the low flow period in successive years from 1992-1995 and the study bar can be seen emergent on Figure 4.1d. Bar types are predominantly 'unit' or 'longitudinal' bars (Smith, 1974; Church and Jones, 1982; Rundle, 1985) with a rhomboidal planform. Isolated mid-channel bars are less common in the Jamuna than bars associated with lower channel hierarchies (Bristow, 1987) which tend to accumulate into 'compound' or 'mosaic' bar complexes (Bluck, 1979) with a central portion of higher, vegetated, 'permanent' char surrounded by more mobile 'temporary' chars (Thorne et al., 1993). Sinuous anabranches often develop an inner point bar, which may become a mid-channel bar through chute-cutoff at high flow (Ashmore, 1991; Welford, 1994, Richardson and Thorne, SPR-16).

Bar migration and reworking occurs predominantly through erosion of the barhead and deposition at the bartail (Figures 4.2a-b) although upstream accretion onto the barhead is also common (Bristow, 1987; Lisle et al., 1991). Major bar complexes are rarely destroyed entirely as shown in Figures 4.2a-b. Migration rates of mid-channel bars are typically < 500 m yr^{-1}. The close correlation between areas of erosion and deposition for individual bars in the 55 km long G11-12 reach implies there is little short-term *net* aggradation in the braidbelt. There is a suggestion that smaller, isolated, mid-channel bars (< 2km long, see bars labelled A in Figure 4.2b) move at faster rates than the larger (> 5km long) bar complexes. Bars may be completely reworked as they pass through major nodes of flow convergence or channel confluences (see SPR-XX). New bars are commonly created by lateral accretion onto existing attached bars (Bluck, 1979, see bars labelled B in Figure 4.2b), by mid-channel deposition downstream of zones of significant bank erosion (Mosselman, 1995) or through rapid deposition downstream of a major flow constriction (Rundle, 1985; Macklin and Lewin, 1989 - see Mawa River example).

The overall morphology of the Jamuna in the 55km reach illustrated by SPOT images G11 and G12 is low sinuosity and moderately braided. The channel belt is dominated by two main channels (locally termed the west and east navigation channels) which bifurcate at the barheads of large (>15km long) mid-channel bar complexes and recombine at their bartails to form major zones of flow convergence and scour. This basic morphology is the X-shaped planform described by Carson and Griffiths (1987), Bridge (1993), Ferguson (1993) and Ashworth (1996) or 'hour-glass' shape described for the Jamuna by Thorne et al. (1993). The study bar site, 6 km north of Bahadurabad ghat, is immediately downstream of one of the locations of west and east channel convergence and therefore is a prime site for mid-channel bar growth with locally high sediment transport rates and downstream flow deceleration and divergence.

Figures 4.1a-d show that the position of this node of west and east channel convergence remained relatively stable between 1992 and 1995 despite the west channel becoming more sinuous upstream and eroding its outer bank. The channel downstream of the flow convergence is relatively 'clean' with no significant mid-channel bars from 1992-1994,

unlike the period 1994-1995, when a series of unattached bars were created. This period of widespread mid-channel bar growth may be related to the widening of the post-confluence channel (by up to 600 m along a 5 km strip of bank on the eastern margin, see Fig. 4.2b) which would result in a local increase in sediment supply and drop in flow competence.

Figures 4.3a-b show a close-up of the study bar site and its relationship to more local channel changes. The main development has been the growth and attachment of a large (~5km) mid-channel bar immediately north of Bahadurabad and which now forms the left margin of the Phulchari cross-channel and is emergent at high flow. The growth of the study bar does not *initially* influence the stability and position of the adjacent bar and bank edges although later morphological changes in the study reach may have caused the rapid bank erosion downstream at the Bahadurabad ghat (see Section 4.2 below).

4.2 Morphological development of mid-channel bars

Figures 4.4a-i illustrate the sequence of channel change at the special study site for selected periods between November 1993 and March 1996. All topographic data are reduced to SLW. The five transect lines that cover the zone of bar aggradation, together with two frequently surveyed lines immediately downstream, are plotted in Figures 4.5a-e for successive special surveys.

The study site is downstream of a major zone of flow convergence (see Figure 4.1d) and in November 1993 the main channel talweg was ~1 km wide with a low sinuosity and a simple parabolic cross-section (Figure 4.4a). During the peak flows of 1994 (Figure 2.1) the main channel widened to ~2 km and deposited a symmetrical, narrow, mid-channel bar ~ 1.5 km long at a maximum height of +2.9 m SLW (Figures 4.4b and 4.5a). The reach established a marked pool-bar-pool morphology as is characteristic of the initial stages of braiding (Ferguson and Werritty, 1983; Ashmore, 1991). Figure 4.4b suggests that the mid-channel bar initially developed as a central bar core and then grew by downstream accretion, as described by Leopold and Wolman (1957). This downstream growth occurred through migration of accretionary dune fronts across the bar top/margin (Figures 4.9 and 4.10), possibly in response to fluctuations in the hydrograph (Figure 2.1c). The flow structure associated with this period of bar growth is described in Section 4.5.

During the recession limb of the 1994 hydrograph the study bar deposited around its central core to create a broad bartop platform ~1km wide. This was accompanied by incision of both anabranches by up to 7 m (Figures 4.4c and 4.5a). This pattern of bar growth is again consistent with the classic description of braiding by Leopold and Wolman (1957), who observed that bar emergence is usually aided by anabranch incision after initial central bar deposition. The broadening of the bar morphology is associated with development of strong secondary flows in the well-defined anabranches on either side of the bar which are responsible for lateral sediment transport and accretion at the bar margins (see Section 4.5 and descriptions in Bristow, (1987); Ashworth et al., (1992); Bridge, (1993) and Richardson and Thorne, (SPR-16)). These secondary flows also cause formation of two bartail limbs (*cf.* Cant and Walker, 1978) which extend downstream from the main bar nucleus (Figures 4.4c and 4.6a), creating a sheltered, low velocity zone where significant volumes of fine sediment can accumulate. Peters (1993) suggests that deposition in such backwater areas may lead to

formation of highly cohesive "clay plugs". Grain size analysis of two volumetric bed samples taken in the bartail of the study bar (Table 4.1) reveals 7.8 and 11.0 % clay and 84.4 and 87.7 % silt, respectively, both with a median grain size, (D_{50}) of 0.011 mm.

Sample description	% < 2μm	% < 63μm	% > 63μm	D_{10} mm	D_{50} mm	D_{90} mm
Bartop, plug on BT5X032	11.0	98.7	1.3	0.0019	0.011	0.044
Bartop, plug at centre of bartail	7.8	92.1	7.9	0.0026	0.011	0.054
Washload, pump sample*	N.A.	71.2	28.8	N.A.	0.042	N.A.

Table 4.1: Grain size analysis of fine-grained surface sediment from the study bar (taken in February 1996) and channel washload.

*Mean grain size of pump samples taken at Bahadurabad (see SPR-014, Table 1c, p.29 for more details).

This indicates that the sediment trapped in zones of low velocity are dominantly fine silts which represent the finer fractions of the washload (D_{50} = 0.042 mm, see Table 4.1) but with sufficient quantity of clay to impart some cohesitivity to the sediment. Inspection of Jamuna SPOT images reveals this mid-channel bar morphology is extremely common (the fine-grained sediments trapped in the bartails often being used for intensive rice production (*cf.* Peters, 1993)) and the high preservation potential of this cohesive plug may be responsible for the long-term storage (depending on bar residence time) of the finest fractions of the sediment load.

The immobility of these cohesive sediments increases their preservation potential when the barhead migrates downstream. This feature is supported by results from a programme of 100MHz ground penetrating radar surveys on the bartop in February 1996 which revealed the preservation of a 0.5-0.75 m thick fine-grained layer (i.e. a strong radar reflectance) at approximately 6 m depth at the original site of bartail accretion (transect BT5X026, see Figures 2.1b and 4.6a) which had subsequently been overridden by the downstream migrating barhead (Figure 4.6b).

During the dry season of 1994-95 (Figure 4.4d) there was negligible channel change and only minor aeolian reworking of the exposed bar surface. The full cycle of bar creation, aggradation, accretion and emergence therefore took place during a single monsoon season and did not involve any downstream migration, as also observed by Leopold and Wolman (1957).

Land survey in March 1995 showed the bar surface morphology to be dominated by two dune fields that terminated in an abrupt accretionary front up to 3 m high (Figure 4.6a and Figure 4.10 later) and which were bordered by 0.5 high dunes wrapping around the bar margin. This accretionary front, with an avalanche face at the angle of repose, was also observed as it migrated over the bartop during the August 1994 survey (see Section 4.6 and Figure 4.9). The start of the 1995-96 monsoon runoff initiated a period of progressive lowering of the bartop (by up to 6m) and infilling of the eastern anabranch (Figures 4.4e and 4.5b). This is a common mode of development whereby the bartop flow reactivates the previous year's waning flow dune deposits (up to 4 m thick - see Section 4.6) and one anabranch eventually takes over as the dominant channel for bed material transport (Hoey and Sutherland, 1991;

92

Ashmore, 1993). The special survey conducted a month later (Figure 4.4f) shows that this pattern of rapid east anabranch aggradation is reversed and the channel re-scours to its former level (Figure 4.5c). Such a rapid switch between local scour and deposition has been observed in other braided rivers (e.g. Ashworth and Ferguson, 1986; Hoey and Sutherland, 1991; Goff and Ashmore, 1994) and is associated with the downstream migration of a major bar complex through the channel network (such as the attached bar centred on E470000, N785000, Figure 4.4e). Mobilisation of this attached bar complex may have been aided by the very high July peak discharge (see SPR-XX) which also caused up to 400 m of bank erosion of the 'permanent' char that borders the west anabranch (see Figures 4.4e and 4.4f and the cross-sectional changes at sections 30 and 28 in Figure 4.5c). Even during this period of significant channel change the study bar maintained its basic symmetrical morphology and remained fixed in its original position (although the bartail aggraded and extended downstream).

The 1995 monsoon hydrograph remained at a high level into late September (Figure 2.1c) and continued to cause significant channel change. The bed scour associated with the reactivation of the eastern anabranch propagated from section 25 (Figure 4.5c) down to beyond section 26 (Figure 4.5d). The downstream scouring of the eastern anabranch supplied sediment to promote bartail growth (~800m) and lateral accretion (~200m) into the western anabranch (Figure 4.5d). This deposition occurred as the talweg of the main channel developed a sinuous planform with flow in the eastern anabranch crossing over to the west via a shallow depositional zone at the tail of the study bar. The morphology of this cross-over point is highlighted by the ground penetrating radar survey in February 1996 which showed 3m high prograding slip faces, dipping east to west, superimposed by low amplitude dunes (see Figures 4.5b and 4.11). The concentration of flow into the west anabranch after passing over this depositional front led to bed scour (~2m) and more right bank retreat (~200m) immediately downstream (Figure 4.5d). The general pattern of channel change is similar to the model described by Ferguson and Werritty (1983, Figure 3, p. 185) for the braided River Feshie with scour pool enlargement and extension, oblique riffle growth and progradation and the overall development of a sinuous talweg planform. The study bar remains in its original position during this channel evolution but grows at the bartail through deposition at the cross-over point between the east and west anabranches.

During the falling limb of the hydrograph, the eastern anabranch continued to incise at its southern end and initiated new bar growth immediately downstream (Figure 4.4h). The study bar widened by ~200m (as also observed on the hydrograph falling limb in 1994) but shortened by ~800m as the east anabranch straightened and preferentially supplied sediment to the new mid-channel bar downstream.

The final bathymetric survey in March 1996 (Figure 4.4i) shows a deepening and narrowing of the scour hole that supplies sediment to the study reach and further downstream extension of the east anabranch (Figure 4.5e) to a point where it begins to divide again into two separate anabranches around the new mid-channel bar just upstream of Bahadurabad ghat. The study bar is still in the same position as the first stage of bar growth in August 1994 (Figure 4.4b) but it is difficult to quantify the change in bar height because complete land surveys are not available (hence the lower interpolated height in Fig. 4.4i). Both the west anabranch around the study bar and the Phulchari cross-channel have infilled (Figure 4.4i) and the morphology of the study reach resembles a point bar and chute cut-off channel pattern (see Richardson

and Thorne, SPR-16). The west anabranch downstream of the study bar continues to scour and propagate downstream aided by the flow divergence around the new mid-channel bar. This has ramifications for the downstream Bahadurabad ghat which is now a focus of major bank retreat.

4.3 Sediment balance in the study reach

The morphological changes described in Section 4.2 may be examined further by quantifying the spatial and temporal pattern of erosion and deposition for each survey period. Table 4.2 summarises the digitised magnitude of erosion and deposition for five survey periods for the seven transects over and immediately downstream of the study bar plotted in Figures 4.5a-e. Although periods of rapid, short-term scour and fill may have been missed by the surveys (Peters, 1993), the consistency of the mode and magnitude of channel change between successive transects suggests this may only be a minor source of error. It should be noted that because the transect lines are of different lengths within and between each Special Survey, the rates of erosion and deposition are also expressed as per unit length of transect line. This enables quantification of the spatial and temporal change in erosion and deposition and the approximate sediment budget for the study reach. Table 4.2 highlights three key features: (i) the spatial pattern (i.e. between surveys) of erosion and deposition is relatively consistent for each survey time period (no section has greater than twice the mean rate of channel change). This suggests that gross changes in the reach morphology are more important contributors to the sediment balance than local, short-term, scour and aggradation events, (ii) channel change in the zone of bar growth and evolution is strongly stage dependent with no apparent lag behind the hydrograph peak in erosion or deposition rates and a mean 'background' falling and low stage erosion and deposition rate of ~0.12 m^2 m^{-1} yr^{-1}, and (iii) there is no net aggradation or degradation of the study reach with a very close match (r^2 = 95.3%) between the rates of erosion and deposition. This suggests positive feedback between bar growth and local anabranch scour and widening (*cf.* Ashworth and Ferguson, 1986) with the study reach maintaining a stable channel capacity (*cf.* Neill, 1987; Laronne and Duncan, 1992; Ashworth, 1996).

Survey period & transect No.	Erosion	Erosion rate	Transect line length	Transect line erosion rate	Deposition	Deposition rate	Transect line length	Transect line deposition rate
	m^2	$m^2\ yr^{-1}$	m	$m^2m^{-1}yr^{-1}$	m^2	$m^2\ yr^{-1}$	m	$m^2m^{-1}yr^{-1}$
August 1994-March 1995								
24	45.4	77.7	960	0.081	27.9	47.8	500	0.096
34	44.1	75.4	705	0.107	50.3	86.2	820	0.105
25	48.6	83.2	680	0.122	56.6	97.0	815	0.119
33	52.3	89.5	630	0.142	58.5	100.1	800	0.125
26	52.2	89.3	770	0.116	47.9	81.9	730	0.112
30	46.5	79.6	710	0.112	40.6	69.5	450	0.154
28	*	*	*	*	*	*	*	*
Total	*289.1*	*494.7*		*0.680*	*281.9*	*482.5*		*0.711*
Mean	*48.2*	*82.5*		*0.113*	*47.0*	*80.4*		*0.119*
March 1995-June 1995								
24	36.4	118.9	515	0.231	61.7	201.5	980	0.206
34	39.7	129.7	440	0.295	67.3	219.7	1060	0.207
25	51.5	168.3	745	0.226	62.1	202.7	750	0.270
33	51.1	167.0	710	0.235	56.6	184.9	770	0.240
26	32.5	106.1	585	0.181	65.1	212.5	890	0.239
30	23.3	76.0	230	0.330	52.0	169.8	935	0.182
28	25.5	83.3	360	0.231	50.3	164.2	650	0.253
Total	*260.1*	*849.6*		*1.730*	*415.0*	*1355.3*		*1.596*
Mean	*37.2*	*121.3*		*0.247*	*59.3*	*193.6*		*0.228*
June 1995-July 1995								
24	93.9	928.3	2845	0.326	26.6	263.0	415	0.634
34	98.5	974.2	2705	0.360	15.8	156.6	140	1.118
25	68.4	676.6	1740	0.389	34.7	343.8	610	0.564
33	56.7	560.9	1980	0.283	44.8	442.8	750	0.590
26	54.3	537.2	1015	0.529	46.9	463.3	1270	0.365
30	54.4	537.9	950	0.566	52.9	523.4	960	0.545
28	48.3	477.6	505	0.946	62.8	620.5	825	0.752
Total	*474.5*	*4692.6*		*3.400*	*284.5*	*2813.3*		*4.568*
Mean	*67.8*	*670.4*		*0.486*	*40.6*	*401.9*		*0.653*
July 1995-September 1995								
24	37.9	300.1	1560	0.192	54.3	429.2	1150	0.373
34	39.8	314.9	1290	0.244	53.5	422.9	2005	0.211
25	57.5	454.6	1320	0.344	41.3	326.7	1380	0.237
33	59.2	468.1	1095	0.427	49.9	395.1	1455	0.272
26	67.7	535.9	1335	0.401	58.6	463.7	1585	0.293
30	57.7	456.6	1460	0.313	41.6	329.4	880	0.374
28	59.8	472.9	1195	0.396	51.1	404.6	705	0.574
Total	*379.6*	*3003.0*		*2.318*	*350.3*	*2771.6*		*2.333*
Mean	*54.2*	*429.0*		*0.331*	*50.1*	*395.9*		*0.333*
September 1995-February 1996								
24	49.9	108.2	905	0.120	31.1	67.5	540	0.125
34	57.7	125.2	1330	0.094	23.8	51.6	620	0.083
25	47.4	102.9	1140	0.090	11.9	25.8	180	0.143
33	38.9	84.5	1210	0.070	16.2	35.2	325	0.108
26	36.4	79.0	580	0.136	23.0	50.0	530	0.094
30	47.0	102.1	650	0.157	36.5	79.3	760	0.104
28	53.2	115.4	840	0.137	13.5	29.3	195	0.150
Total	*330.5*	*717.4*		*0.805*	*156.0*	*338.6*		*0.809*
Mean	*47.2*	*102.5*		*0.115*	*22.3*	*48.4*		*0.116*

68

Table 4.2: Rates of erosion and deposition for transects BT5X024, 34, 25, 33, 26, 30 and 28 over and immediately downstream of the study bar site (see Figure 2.1b). Note, the length of each transect line varies within and between surveys so the rates of erosion and deposition are also expressed per unit length of line. The February 1996 lines do not include land surveys (see Figure 4.5e).

The consistency in the temporal and spatial pattern of channel change in the study bar area suggests it may be possible to estimate aggregate and local sediment transport rates using either the 'morphological' or 'sediment continuity' method described in Ferguson and Ashworth (1992) and recently applied in braided rivers by Goff and Ashmore (1994), Martin and Church (1995), Lane et al., (1996) and Ashmore and Church (in press). However, these methods were developed for gravel-bed rivers, where it was possible to either directly measure the total sediment transport rate at the head of the study reach, or, to define a position in the reach where sediment transport rate tends to zero. In the case of the Jamuna, there are two difficulties with these criteria: (i) a high proportion of the bedload is associated with migrating dune bedforms which represent sediment throughput (Peters, 1993), and (ii) it is difficult to estimate the proportion of suspended load incorporated within the migrating dune bedform (*cf.* van Rijn, 1993; Kostaschuk and Ilersich, 1995). Nonetheless, both the 'morphological' and 'sediment continuity' methods may be used to compute a lower bound on the estimate of sediment transport rates in the Jamuna, particularly if the bedload transport rates associated with dune migration can be quantified from measurements of dune height, morphology and celerity (see Section 3.5.1). Although not part of this project, research development along this line my yield reliable order of magnitude estimates of sediment transport rate in very large and active braided rivers (Ashmore and Church, in press).

4.4 A model for mid-channel bar growth in the Jamuna

The observations of bar dynamics and channel change detailed in Sections 4.1-4.3 permit erection of a six stage model for mid-channel bar growth and channel evolution which may be more widely applicable in the Jamuna. The sequence is:

1. Development of straight, parabolic, main channel downstream of a major node of flow convergence (a 'Y' shaped planform, *cf.* Carson and Griffiths, (1987)).

2. Flow divergence (initiated by either bank widening or activation of a distributary offtake) and deposition of a symmetrical mid-channel bar caused by either (i) exceedance of the local transport capacity (Ashmore, 1991; Ashworth, 1996) and the progressive stacking of dunes, or (ii) growth of a local flow instability (Parker, 1976; Tubino, 1991).

3. Broadening of the initial bar nucleus and bartail extension through lateral accretion (Bristow, 1987; Ashworth et al., 1992), aggradation of the bartop by the downstream migration of dune accretionary fronts, and anabranch incision leading to bar emergence (Leopold and Wolman, 1957).

4. Preferential scour and propagation of one anabranch (Cheetham, 1979; Hoey and Sutherland, 1991), probably determined by the asymmetry of the upstream scour hole (Mosley, 1976), the morphology and degree of emergence of the barhead (Ashworth, 1996) and the direction of local transport pathways (Hoey and Sutherland, 1991).

5. Development of planform sinuosity of the talweg with the dominant anabranch crossing over to the minor anabranch via a submerged transverse bar (Ferguson and Werritty, 1983). Attachment of the transverse bar to the original bartail and progradation towards the bank edge causing anabranch scour and bank erosion (Lewin, 1976).

6. Further propagation of the dominant anabranch leading to abandonment of the minor anabranch upstream and its incorporation into the 'floodplain' (Richardson and Thorne, SPR-16). Possible channel bifurcation at the terminus of the anabranch scour front and development of a new mid-channel bar. Positive feedback and repetition of stages 1-6.

It should be noted that no downstream migration of the mid-channel bar is necessary for this sequence of channel evolution although the main morphological units will move if the node of flow convergence translates downstream (*cf.* Ashmore, 1993).

4. 5 Flow structure associated with bar growth

A number of linear (Engelund and Skovgaard, 1973; Parker, 1976; Fredsøe, 1978) and non-linear (Colombini et al., 1987; Tubino, 1991) stability analyses have been developed to predict the criteria for bar initiation, but few studies have been able to verify the flow structure in the field (Ashworth, 1996). Use of ADCP along all transect lines during the special survey of August 1994 permits quantification of the 3-D flow field at the stage of early bar growth in the study area (see Figure 4.4b).

Figures 4.7a-d show the magnitude and direction of the downstream velocity vector (*U-W*) and backscatter intensity for four transects that cover the area of the single feeder channel (BT5X036, 750 m upstream of the barhead), the barhead (BT5X036), the mid-bar (BT5X021, 250 m downstream) and the bartail (BT5X034, a further 500 m downstream). Figure 4.7a shows a central core of high velocity (up to 2.3 m s^{-1}) in the single channel approaching the barhead, with strongly convergent flow into the talweg where backscatter intensity is also the highest. As flow approaches the barhead (Figure 4.7b) it divides into two filaments of equal velocity (maximum ~2 m s^{-1}), with flow becoming strongly divergent (~60°) throughout the water depth. Backscatter intensity is high in the talweg and bar margin of each anabranch, with local peaks associated with dunes (see Section 3.6.2). Further down the bar, the flow accelerates down the east anabranch (up to 2.4 m s^{-1}) with a compensating deceleration (maximum 1.8 m s^{-1}) in the west anabranch (Figure 4.7c). The 'topographic forcing' of flow (Dietrich and Smith, 1983; Nelson and Smith, 1989) which causes flow divergence at the barhead is weakened by funnelling of the flow down the two anabranches and the introduction of streamline curvature effects (Prandtl, 1952) from the sinuous anabranch planform. This promotes production of secondary flows (Fujita and Komura, 1988; Weerakoon et al., 1991; Rhoads and Kenworthy, 1995) which are initially evident only in the west anabranch (Figure 4.7c), but become fully developed in both anabranches 500 m downstream at the bartail (Figure 4.7d). The inward near-bed secondary flow is likely to be responsible for lateral accretion and growth of the bartail limbs described in Section 4.2. The zone of low flow velocity (0.4 m s^{-1}) at the bartail is associated with low suspended sediment concentrations (Figure 4.7d), consistent with the accumulation of substantial fine-grained sediment (Section 4.2).

The overall pattern of flow structure at the early stages of bar growth is consistent with descriptions in the literature (Ashworth, 1996; M^{c}Lelland et al., 1996; Richardson et al., 1996), with topographic forcing of flow at the barhead causing flow divergence and anabranch curvature producing significant secondary flows (see models in Ashworth et al., 1992, Figure 25.3 and Richardson and Thorne SPR-16, Figure 1.5). The zone of flow divergence and deceleration most likely promotes dune stalling and stacking (see Section 4.6) with secondary flows in the anabranches causing lateral accretion and bartail growth.

A similar pattern of velocity is observed at peak flow in July 1995 (Figures 4.8a-f). As described in Section 4.2 and illustrated in Figures 4.4e-f and 4.5c, the June-July 1995 survey period showed rapid study bar aggradation and anabranch incision (particularly in the eastern anabranch). This resulted in the demarcation of a clear mid-channel bar morphology up to +4m SLW (Figure 4.5c). The high flow in July 1995 still submerged the symmetrical bar (Figures 4.8c-f) and initially divided it into two filaments of equal velocity around the barhead (Figures 4.8a-b) as also observed in August 1994 (Figure 4.7b). Similarly, the barhead also causes flow divergence through the 'topographic forcing' of flow. Further down the bar at transects BT5X025, 33 and 26 (Figures 4.8d-f), the combination of the obstructive nature of the barhead and the development of talweg curvature, causes a shift in the balance of flow between the two anabranches around the study bar and the increasing dominance of the eastern anabranch. This is clearly highlighted by the development of a core of high velocity at the outside bend of the eastern anabranch which is probably responsible for the erosion of the neighbouring mid-channel bar between July and September 1995 (see Figure 4.8f in particular and the channel change in Figure 4.5d). The change in the flow direction over and around the study bar during the high July flow is again similar to that observed in August 1994 with a progressive shift from flow divergence at the barhead to flow convergence at the bartail with the development of secondary flow. The pattern of backscatter intensity follows the change in downstream velocity with higher values in the eastern anabranch and on the eastern study bar margin where dune migration is particularly evident (Figures 4.8e-f).

4.6 Relationship between bedforms and bar growth

Section 3.2 demonstrates that dunes are ubiquitous in the Jamuna at all flow stages and their morphology is stage dependent. Since dunes are the dominant mode of bedload transport, they are intimately linked to bar creation and growth. Figure 4.9 shows a downstream survey line over the study bartop in August 1994 (which corresponds to the period of rapid bar aggradation - see Figures 4.4 and 4.7a-d). Dune height decreases as the flow shallows from the upstream talweg onto the barhead. The 3 m high accretionary front (labelled DF in Figure 4.9) was exposed at low flow in March 1995 (Figure 4.10) and represents the stacking of successive dunes as they migrate onto the barhead. Formation and migration of this accretionary front may be associated with short-term (days) fluctuations in discharge (stage changes of ±1m, see Figure 2.1c) at the hydrograph peak which provide the necessary flow depth and velocity to promote dune migration on the bartop platform.

As discussed in Section 4.2, after deposition of an initial bar core, bar growth is promoted by a combination of lateral accretion and stacking of successive dune fields which migrate both onto the barhead (Figure 4.9) but also wrap around the bar margin during waning flows. Lateral accretion can produce foresets up to 3 m high (Figure 4.11) which may subsequently

be superimposed by a series of 0.5-1 m high dunes (Figure 4.12) to produce a characteristic two-stage profile of subsurface alluvial architecture (Figure 4.11). The average D_{50} grain size of the preserved dunes is 0.24 mm (Table 4.3) which is very similar to the average talweg bed grain size (0.26 mm, Table 4.3). This suggests that there is minimal reworking/sorting of bed material once it is deposited on the bartop as the migrating dune bedforms stall.

Sample description	% < 63μm	D_{10} mm	D_{50} mm	D_{90} mm
Bartop, 10m from barhead[+]	0.78	0.22	0.33	0.47
Bartop, 10m from west edge, on BT5X026[+]	4.81	0.077	0.16	0.29
Trench on BT5X026, 1m depth, dune x-strats.[^]	0.28	0.14	0.23	0.33
Trench at bar margin, dune x-strats.[^]	2.18	0.13	0.24	0.33
Vibracore A, Core 3, 1.15m[†]	5.09	0.074	0.15	0.25
Vibracore B, Core 7, 1.40m[†]	0.53	0.14	0.24	0.33
Vibracore C, Core 8, 1.80 m[†]	0.18	0.22	0.33	0.50
Vibracore D, Core 8, 0.15 m[†]	0.72	0.21	0.33	0.48
Vibracore E, Core 9, 0.18 m[†]	9.59	0.064	0.23	0.36
Vibracore F, Core 9, 1.52 m[†]	0.65	0.13	0.20	0.33
Bed grab sample 1*	0.14	0.20	0.33	0.47
Bed grab sample 2*	0.94	0.10	0.18	0.32
Bed grab sample 3*	0.44	0.14	0.26	0.44

Table 4.3: Grain size of the study bar surface, subsurface and adjacent talweg from trenches, vibracore samples and Van Veen grab samples.

[+] Samples taken in February 1996 when the study bar was emergent

[^] Samples taken in February 1996 from two trenches excavated to 2 m. The trench face exposed on line BT5X026 is illustrated in Figure 4.12.

[†] Samples taken at several vibracore sites on the study bar in February 1996 (depth of sediment sample given in the Table)

[*] Samples taken on 12-14 August 1994 in the talweg of the east anabranch around the study bar at Bahadurabad using the Van Veen bed sampler.

4.7 Summary

A number of conclusions may be proposed from this study of bar dynamics:

- Mid-channel bars are the most common bar type in the Jamuna and exert considerable influence on the local flow structure, channel change and bank erosion
- Sand bars often form downstream of a zone of flow convergence and are initially deposited as a central symmetrical bar core, aligned sub-parallel to the primary flow direction
- The basic planform morphology of a mid-channel bar is rhomboidal with two protruding bartail limbs. This morphology is characteristic of all scales of mid-channel bars
- The bartail may be an important storage zone for fine sediment and can form highly cohesive and resistant 'plugs' which may be difficult to erode. Downstream migration of the barhead may preserve this plug and temporarily 'remove' the finest fractions from the channel and floodplain transport system
- Mid-channel bars grow through (i) flow divergence at the barhead and deposition at the bar margins, (ii) lateral accretion induced by secondary flows in the anabranches, (iii) vertical aggradation by successive stacking of dunes, and (iv) downbar migration of an accretionary dune field front. This front may only form during short-lived (days) fluctuations in discharge at the hydrograph peak
- Bar growth and channel change is not always accompanied by downstream migration of the bar nucleus. The basic bar morphology may thin and lengthen at high flow and broaden at low flow
- Channel change and the rate of sediment erosion and deposition is strongly stage dependent with no lag behind the hydrograph peak. The mean erosion and deposition rates are in balance throughout the hydrograph suggesting no net aggradation or degradation of the braidbelt
- There is a close relationship between bedform development, morphology and migration and the mechanics of bar growth. This is evidenced in both bed surveys and preserved subsurface alluvial architecture
- A six-stage model for mid-channel bar growth and morphological change in the study area is proposed which is consistent with observations in the literature and may be applied more widely in the Jamuna

List of references

Allen, J.R.L. 1982. *Sedimentary Structures: their character and physical basis*, Elsevier, Amsterdam, 539 pp.

Ashley, G.M. 1990. Classification of large-scale subaqueous bedforms: a new look at an old problem, *Journal of Sedimentary Petrology*, **60**, 1, 160-172.

Ashmore, P.E. 1982. Laboratory modelling of gravel, braided stream morphology, *Earth Surface Processes and Landforms*, **7**, 201-225.

Ashmore, P.E. 1991. How do gravel-bed rivers braid?, *Canadian Journal of Earth Sciences*, **28**, 326-341.

Ashmore, P.E. 1993, Anabranch confluence kinetics and sedimentation processes in gravel braided streams', In: Best, J.L. and Bristow, C.S. (eds.) *Braided Rivers*, Geological Society, London, Special Publication, **75**, 129-146.

Ashmore, P.E. and Church, M. in press. Sediment transport and river morphology: a paradigm for study, In: Klingeman, P.C., Beschta, R.L., Komar, P.D. and Bradley, J.B. (eds.), *Gravel-Bed Rivers in the Environment*, Wiley.

Ashworth, P.J. 1996. Mid-channel bar growth and its relationship to local flow strength and direction, *Earth Surface Processes and Landforms*, **21**, 103-123.

Ashworth, P.J. and Ferguson, R.I. 1986. 'Interrelationships of channel processes, changes and sediments in a proglacial river', *Geografiska Annaler*, **68A**, 361-371.

Ashworth, P.J., Ferguson, R.I. and Powell, M.D. 1992. Bedload transport and sorting in braided channels, In: Billi, P., Hey, R.D., Thorne, C.R. and Tacconi, P. (eds.), *Dynamics of Gravel-Bed Rivers*, John Wiley, Chichester, 497-513.

Baas, J.H. 1994. A flume study on the development and equilibrium morphology of small-scale bedforms in very fine sand, *Sedimentology*, **41**, 185-209.

Bennett, S.J. and Best, J.L. 1995. Mean flow and turbulence structure over fixed two-dimensional dunes: implications for sediment transport and bedform stability, *Sedimentology*, **42**, 491-513.

Best, J.L. 1993. On the interactions between turbulent flow structure, sediment transport and bedform development: some considerations from recent experimental research. In: Clifford, N.J., French, J.R. & Hardisty, J. (eds), *Turbulence: Perspectives on Flow and Sediment Transport* Wiley and Sons, Chichester, UK, 61-92.

Best, J.L. 1996. The fluid dynamics of small-scale alluvial bedforms, In: Carling, P.A. and Dawson, M.D. (eds.), *Advances in Fluvial Dynamics and Stratigraphy*, John Wiley and Sons, Chichester, UK. 68-125.

Best, J.L. and Bridge, J.S. 1992. The morphology and dynamics of low amplitude bedwaves on upper-stage plane beds and the preservation of planar laminae, *Sedimentology*, **39**, 737-752.

Bluck, B.J. 1979. Structure of coarse grained braided stream alluvium, *Transactions of the Royal Society of Edinburgh*, **70**, 181-221.

Bridge, J.S. 1993. The interaction between channel geometry, water flow, sediment transport and deposition in braided rivers, In: Best, J.L. and Bristow, C.S. (eds.), *Braided Rivers*, Geological Society, London, Special Publication, **75**, 13-71.

Bristow, C.S. 1987. Brahmaputra River: Channel migration and deposition, In: Ethridge, F.G., Flores, R.M. and Harvey, M.D. (eds.), *Recent Developments in Fluvial Sedimentology*, Society of Economic Paleontologists and Mineralogists, Special Publication, **39**, 63-74.

Cant, D.J. and Walker, R.G. 1978. Fluvial processes and facies sequences in the sandy braided South Saskatchewan River, Canada, *Sedimentology*, **25**, 625-648.

Carson, M.A. and Griffiths, G.A. 1987. Bedload transport in gravel channels, *Journal of Hydrology (NZ)*, **26**, 1-151.

Cheetham, G.H. 1979. Flow competence in relation to channel form and braiding, *Geological Society of America Bulletin*, **90**, 877-886.

Church, M. and Jones, D. 1982. Channel bars in gravel-bed rivers, In: Hey, R.D., Bathurst, J.C. and Thorne, C.R. (eds.), *Gravel-bed Rivers*, Wiley, Chichester, 291-324.

Coleman, J.M. 1969. Brahmaputra River: channel processes and sedimentation, *Sedimentary Geology*, **3**, 129-239.

Colombini, M., Seminara, G. and Tubino, M. 1987. Finite-amplitude alternate bars, *Journal of Fluid Mechanics*, **181**, 213-232.

Crickmore, M.J. 1970. Effect of flume width on bedform characteristics, Journal of the Hydraulics Division, American Society of Civil Engineers, 96, 473-496.

Dalrymple, R.W. and Rhodes, R.N. 1995. Estuarine dunes and bars, In: Perillo, G.M.E. (ed.), *Geomorphology and Sedimentology of Estuaries*, Elsevier, 359-422.

Dietrich, W.E. and Smith, J.D. 1983. Influence of the point bar on flow through curved channels, *Water Resources Research*, **19**(5) 1173-1192.

Engelund, F. and Skovgaard, O. 1973. On the origin of meandering and braiding in alluvial streams, *Journal of Fluid Mechanics*, **57**, 289-302.

Engel, P. & Lau, Y.L. 1980 Computation of bed load using bathymetric data, Journal of the Hydraulics Division, American Society of civil Engineers, 106,369-380.

Ferguson, R.I. 1993. Understanding braided processes in gravel-bed streams: progress and unresolved problems, In: Best, J.L and Bristow, C.S. (eds.), *Braided Rivers*, Special Publication of Geological Society of London, **75**, 73-87.

Ferguson, R.I. and Ashworth, P.J. 1992. Bedload and channel change in braided rivers, In: Billi, P., Hey, R.D., Thorne, C.R. and Tacconi, P. (eds.), *Dynamics of Gravel-Bed Rivers*, John Wiley, Chichester, 477-492.

Ferguson, R.I. and Werritty, A. 1983. Bar development and channel changes in the gravelly River Feshie, Scotland, In: Collinson, J.D. and Lewin, J. (eds.), *Modern and Ancient Fluvial Systems*, Special Publication of International Association of Sedimentologists, **6**, 181-193.

Fredsøe, J. 1978. Meandering and braiding of rivers, *Journal of Fluid Mechanics*, **84**, 609-624.

Fujita, I. and Komura, S. 1988. Visualization of the flow at a confluence, *Proceedings of the 3rd International Symposium on Refined Flow Modelling and Turbulence Measurements*, 611-618.

Goff, J.R. and Ashmore, P.E. 1994. Gravel transport and morphological change in braided Sunwapta River, Alberta, Canada, *Earth Surface Processes and Landforms*, **19**, 195-212.

Hoey, T.B. and Sutherland, A.J. 1991. Channel morphology and bedload pulses in braided rivers: a laboratory study, *Earth Surface Processes and Landforms*, **16**, 447-462.

Jackson, R.G. 1976. Sedimentological and fluid dynamic implications of the turbulent bursting phenomenon in geophysical flows, *Journal of Fluid Mechanics*, **77**, 531-560.

Julien, P.Y. and Klaassen, G.J. 1995. Sand-dune geometry of large rivers during flood, *Journal of Hydraulic Engineering*, **121**, 657-663.

Klaassen, G.J., Ogink, H.J.M. and van Rijn, L.C. 1986. Delft Hydraulics Research on bedforms, resistance to flow and sediment transport, In: *Proceedings 3rd International Symposium on River Sedimentation*, 25pp.

Klaassen, G.J., Vermeer, K. and Uddin, N. 1988. Sedimentological processes in the Jamuna (Lower Brahmaputra) river, Bangladesh, In: *Proceedings International Conference on Fluvial Hydraulics*, Budapest, Hungary, 381-394.

Klaassen, G.J and Masselink, G. 1992. Planform changes of a braided river with fine sand as bed and bank material, *Proceedings 5th International Symposium on River Sedimentation*, Karlsruhe, Germany, 459-471.

Klaassen, G.J., Mosselman, E., Masselink, G., Brühl, H., Huisink, M., Koomen, E. and Seymonsbergen, A.C. 1993. Planform changes in large braided sand-bed rivers, *Delft Hydraulics Publication 480*, December 1993.

Kornman, B.A. 1995. The effect of changes in the lee side shape of dunes on the flow field, turbulence and roughness, report on measurements. *Institute of Marine and Atmospheric Research, University of Utrecht, Report R 95-1.*

Kostaschuk, R.A. and Ilersich, S.A. 1995. Dune geometry and sediment transport: Fraser River, British Columbia, In: Hickin, E.J. (ed.), *River Geomorphology*, Wiley, Chichester, 19-36.

Lane, S., Chandler, J.H. and Richards, K.S. 1995. Developments in monitoring and modelling small-scale river bed topography, *Earth Surface Processes and Landforms*, **19**, 349-368.

Lane, S.N., Richards, K.S. and Chandler, J.H. 1996. Discharge and sediment supply controls on erosion and deposition in a dynamic alluvial channel, *Geomorphology*, **15**, 1-15.

Laronne, J.B. and Duncan, M.J. 1992. Bedload transport paths and gravel bar formation, In: Billi, P., Hey, R.D., Thorne, C.R. and Tacconi, P. (eds.), *Dynamics of Gravel-Bed Rivers*, John Wiley, Chichester, 177-205.

Leddy, J.O., Ashworth, P.J. and Best, J.L. 1993. Mechanisms of anabranch avulsion within gravel-bed braided rivers: observations from scaled physical models, In: Best, J.L and Bristow, C.S. (eds.), *Braided Rivers*, Special Publication of Geological Society of London, **75**, 119-127.

Leopold, L.B. and Wolman, M.G. 1957. *River Channel Patterns: Braided, Meandering and Straight*, United States Geological Survey, Professional Paper **262-B**.

Lewin, J. 1976. Initiation of bed forms and meanders in coarse-grained sediment, *Geological Society of America Bulletin*, **87**, 281-285.

Lisle, T.E., Ikeda, H. and Iseya, F. 1991. Formation of stationary alternate bars in a steep channel with mixed-size sediment: a flume experiment, *Earth Surface Processes and Landforms*, **16**, 463-469.

Lukanda, M., Peters, J.J. Swartenbroeckx, P. and Cornet, P. 1992. Applicability of sediment transport theories to large sandbed rivers, In: *Proceedings 5th International Symposium on River Sedimentation*, Karlsruhe, Germany, 327-337.

Lyn, D.A. 1993. Turbulence measurements in open-channel flows over artificial bed forms, *Journal of Hydraulic Engineering*, **119**, 306-326.

Macklin, M.G. and Lewin, J. 1989. Sediment transfer and transformation of an alluvial valley floor: the River South Tyne, Northumbria, UK., *Earth Surface Processes and Landforms*, **14**, 223-246.

Martin, Y. and Church, M. 1995. Bed-material transport estimated from channel surveys: Vedder River, British Columbia, *Earth Surface Processes and Landforms*, **20**, 347-361.

McLean, S.R., Nelson, J.M. and Wolfe, S.R. 1994. Turbulence structure over two-dimensional bedforms: implications for sediment transport. *Journal of Geophysical Research*, **99**, 12 729-12 747.

McLelland, S.J., Ashworth, P.J. and Best, J.L. 1994. *Velocity Correction Methods in Open Channels: Description, Critique and Recommendations*, FAP-24 Working Paper, August 1994, 16 pp.

McLelland, S.J., Ashworth, P.J. and Best, J.L. 1996. 'The origin and downstream development of coherent flow structures at channel junctions', In: Ashworth, P.J., Bennett, S.J., Best, J.L. and McLelland, S.J. (eds.), *Coherent Flow Structures in Open Channels*, Wiley, Chichester, 459-491.

Mosley, M.P. 1976. An experimental study of channel confluences, *Journal of Geology*, **84**, 535-562.

Mosselman, E. 1995. A review of mathematical models of river planform changes, *Earth Surface Processes and Landforms*, **20**, 661-670.

Mosselman, E., Koomen, M.H.E. and Seijmonsbergen, A.C. 1995. Morphological changes in a large braided sand-bed river, In: Hickin, E.J. (ed.), *River Geomorphology*, Wiley, Chichester, 235-249.

Murray, A.B. and Paola, C. 1994. A cellular model of braided rivers, *Nature*, **371**, 54- 57.

Neill, C.R. 1987. Sediment balance considerations linking long-term transport and channel processes, In: Billi, P., Hey, R.D., Thorne, C.R. and Tacconi, P. (eds.), *Dynamics of Gravel-Bed Rivers*, John Wiley, Chichester, 225-240.

Nelson, J.M. and Smith, J.D. 1989. Evolution and stability of erodible channel beds, In: Ikeda, S. and Parker, G. (eds.), *River Meandering*, American Geophysical Union, Water Resources Monograph, **12**, 321-377.

Nelson, J.M., McLean, S.R. and Wolfe, S.R. 1993. Mean flow and turbulence fields over two-dimensional bed forms. *Water Resources Research*, **29**, 3935-3953.

Ogink, H.J.M. 1988. Hydraulic roughness of bedforms, *Delft Hydraulics Report M2017*.

Parker, G. 1976. On the cause and characteristic scales of meandering and braiding in rivers, *Journal of Fluid Mechanics*, **76**, 457-480.

Parker, G. 1996. Some speculations on the relation between channel morphology and channel-scale flow structures, In: Ashworth, P.J., Bennett, S.J., Best, J.L. and McLelland, S.J. (eds.), *Coherent Flow Structures in Open Channels*, Wiley, Chichester, 423-459.

Peters, J.J. 1977. Sediment transport in the Zaire river, In: Nihoul, J.C.J. (ed.) *Bottom Turbulence*, 221-236.

Peters, J.J. 1993. Morphological studies and data needs, *Proceedings International Workshop on Morphological Behaviour of Major Rivers in Bangladesh*, FAP-24 Dhaka, 12 pp.

Peters, J.J. and Goldberg, A. 1989. Flow data in large alluvial rivers, In: *Proceedings HydroComp. '89 Conference on Computational Modelling and Experimental Methods in Hydraulics*, Elsevier, London, 77-86.

Prandtl, L. 1952. *Essentials of Fluid Dynamics*, Blackie, London, 452 pp.

Raudkivi, A.J. 1966. Bedforms in alluvial channels, *Journal of Fluid Mechanics*, **26**, 597-614.

Richardson, W.R.R. and Thorne, C.R. 1996. Study of secondary currents and morphological evolution in a bifurcated channel, *Final Study Report,SPR-16, FAP-24*, March 1996, 80 pp.

Richardson, W.R.R., Thorne, C.R. and Mahmood, S. 1996. Secondary flow and channel changes around a bar in the Brahmaputra River, Bangladesh, In: Ashworth, P.J., Bennett, S.J., Best, J.L. and McLelland, S.J. (eds.), *Coherent Flow Structures in Open Channels*, Wiley, Chichester, 520-543.

Rhoads, B.L. and Kenworthy, S.T. 1995. Flow structure at an asymmetrical stream confluence, *Geomorphology*, **11**, 273-293.

Rundle, A. 1985. Mechanisms of braiding, *Zeitschrift für Geomorphologie Suppl.-Bd*, **55**, 1-14.

Simons, D.B., Richardson, E.V., & Nordin, C.F. Jnr. 1965 Bedload equation for ripples and duncs, United States Geological Survey Professional Paper 462-H.

Southard, J.B. and Boguchwal, L.A. 1990. Bed configurations in steady unidirectional water flows. Part 2. Synthesis of Flume data, *Journal of Sedimentary Petrology*, **60**, 5, 458-479.

Smith, N.D. 1974, Sedimentology and bar formation in the upper Kicking Horse River, a braided meltwater system, *Journal of Geology*, **82**, 205-223.

Thorne, C.R., Russell, A.P.G., Alam, M.K. 1993. Planform pattern and channel evolution of the Brahmaputra River, Bangladesh, In: Best, J.L. and Bristow, C.S. (eds.), *Braided Rivers*, Geological Society, Special Publication, London, **75**, 257-276.

Tubino, M. 1991. Growth of alternate bars in unsteady flow, *Water Resources Research*, **27**, 37-52.

van Mierlo, M.C.L.M. and de Ruiter, J.C.C. 1988. Turbulence measurements above artificial dunes. *Rept. TOW A55 Q789*, pp. 1-42. Delft Hydraulics.

van Rijn, L.C. 1984. Sediment transport, part III: bed forms and alluvial roughness, *Journal of Hydraulic Engineering*, **110**, 1733-1755.

van Rijn, L.C. 1993. *Principles of Sediment Transport in Rivers, Estuaries and Coastal Seas*, Aqua Publications, Amsterdam.

Wan, Z. 1983. Some phenomenae associated with hyperconcentrated flow. In: Mutlu Sumer, B. & Müller, A (eds.) *Mechanics of Sediment Transport, Proceedings of Euromech 156*, Balkema, Rotterdam, 189-194.

Weerakoon, S.B., Kawahara, Y and Tamai, N. 1991. Three-dimensional flow structure in channel confluences of rectangular section, in *Proceedings of Technical Session on Study of Streams and Watersheds of High Irregularity*, 24th Congress, International Association of Hydraulic Research, Madrid, 373-380.

Welford, M.R. 1994. A field test of Tubino's model of alternate bar formation, *Earth Surface Processes and Landforms*, **19**, 287-297.

Williams, G.P. 1967. Flume experiments on the transport of a coarse sand, United States Geological Survey Professional Paper 562-B.

Wijbenga, J.H.A. and Klaassen, G.J. 1981. Changes in bedform dimensions under unsteady flow conditions in a straight flume, *Delft Hydraulics Publication* 260, 14pp.

Yalin, M.S. 1992. *River Mechanics*, Pergamon Press, 219 pp.

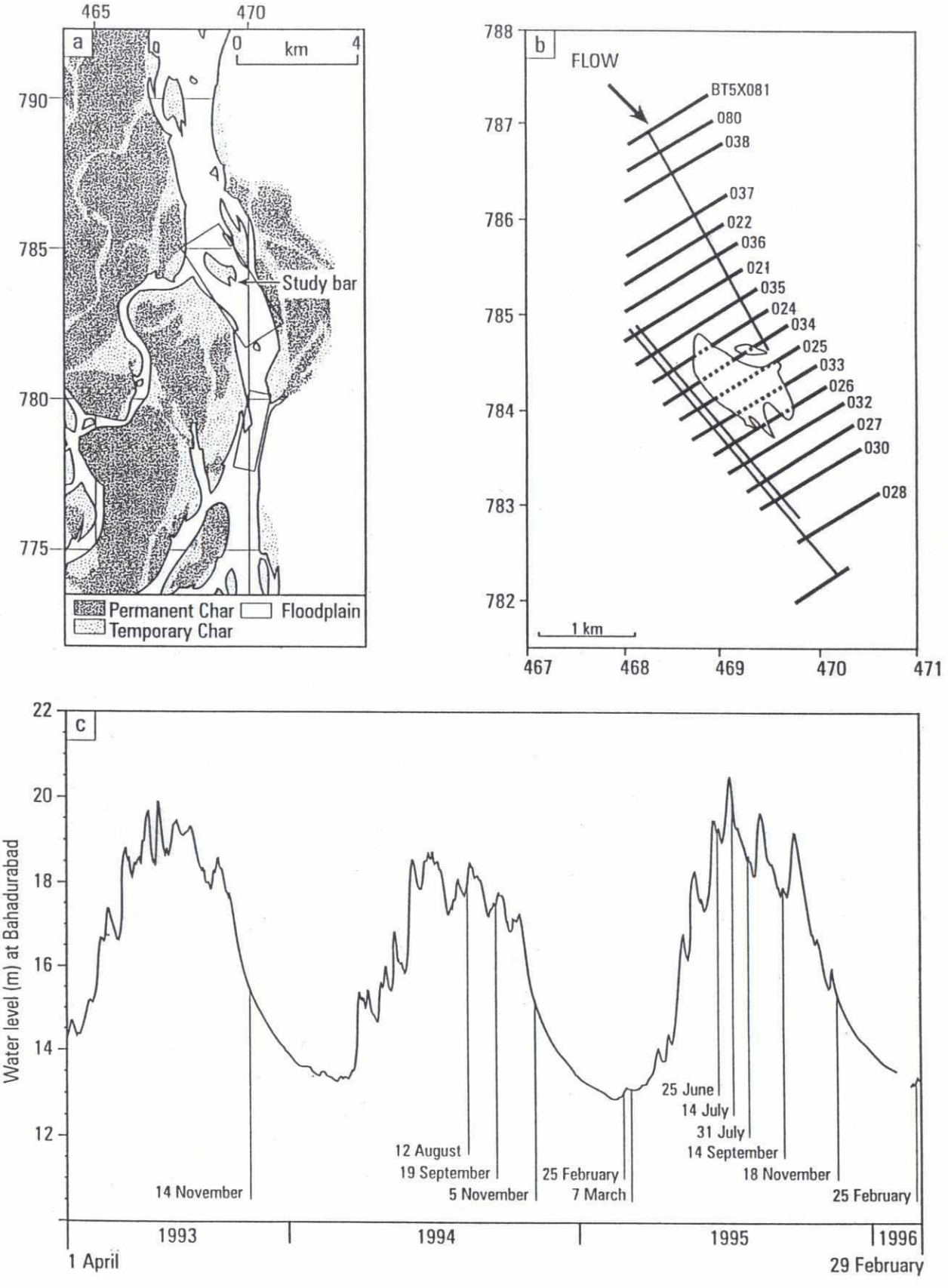

Figure 2.1: (a) Close-up of study reach morphology traced from G12 SPOT on 24/3/95 illustrating the dune and bar study sites (shown by boxes) at Bahadurabad, (b) Special Survey lines over and around the study bar between 7-13 March 1995, (c) flood hydrographs at Bahadurabad from November 1993 to February 1996 highlighting the water level during survey periods. Only the mean date of each survey period is shown (see Table 2.2).

a

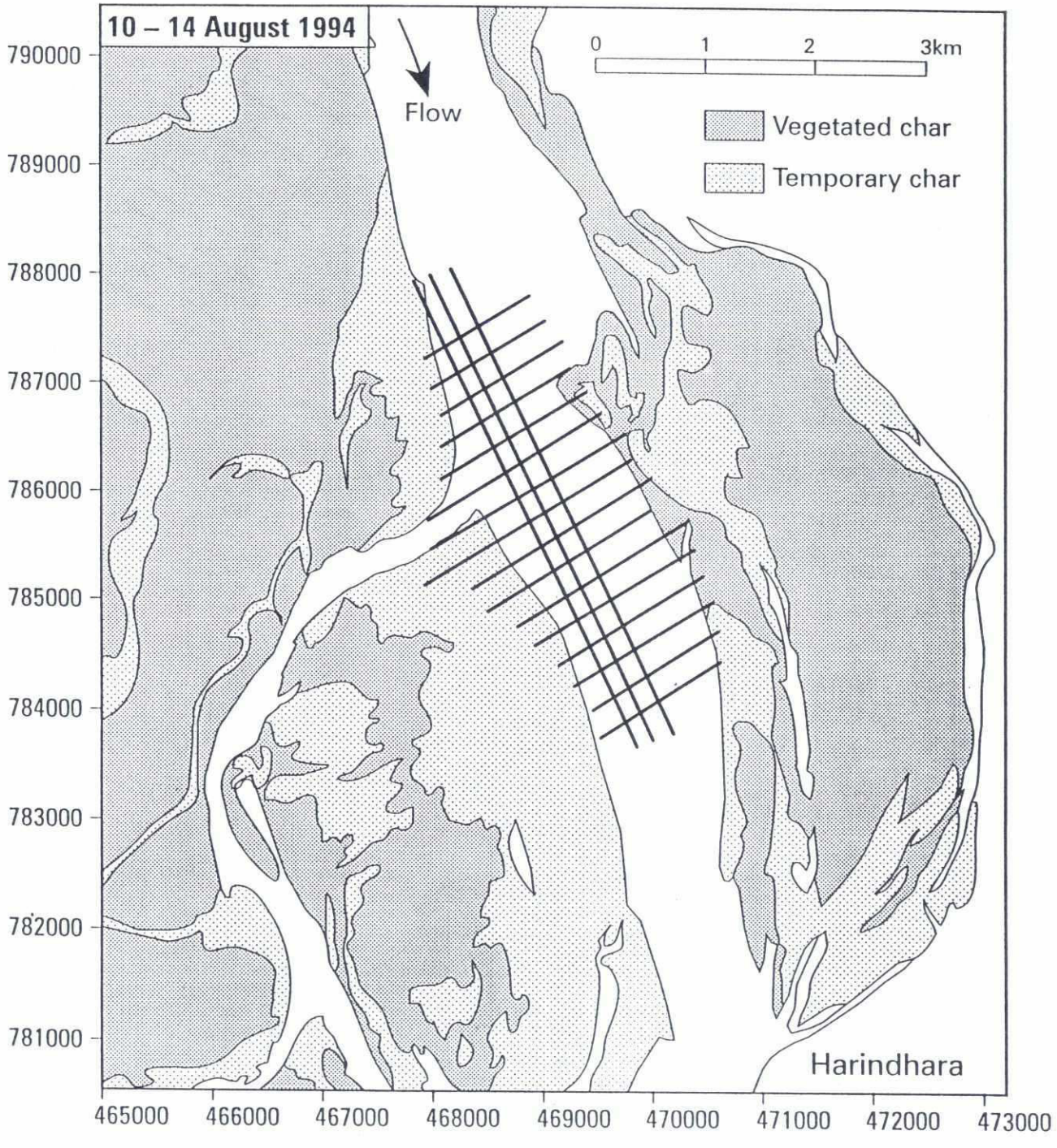

Figure 2.2: (a) Special survey lines undertaken for the bar morphology study on 10-14 August 1994. Lines are superimposed onto 3/3/94 SPOT image. Coordinates are in BTM.

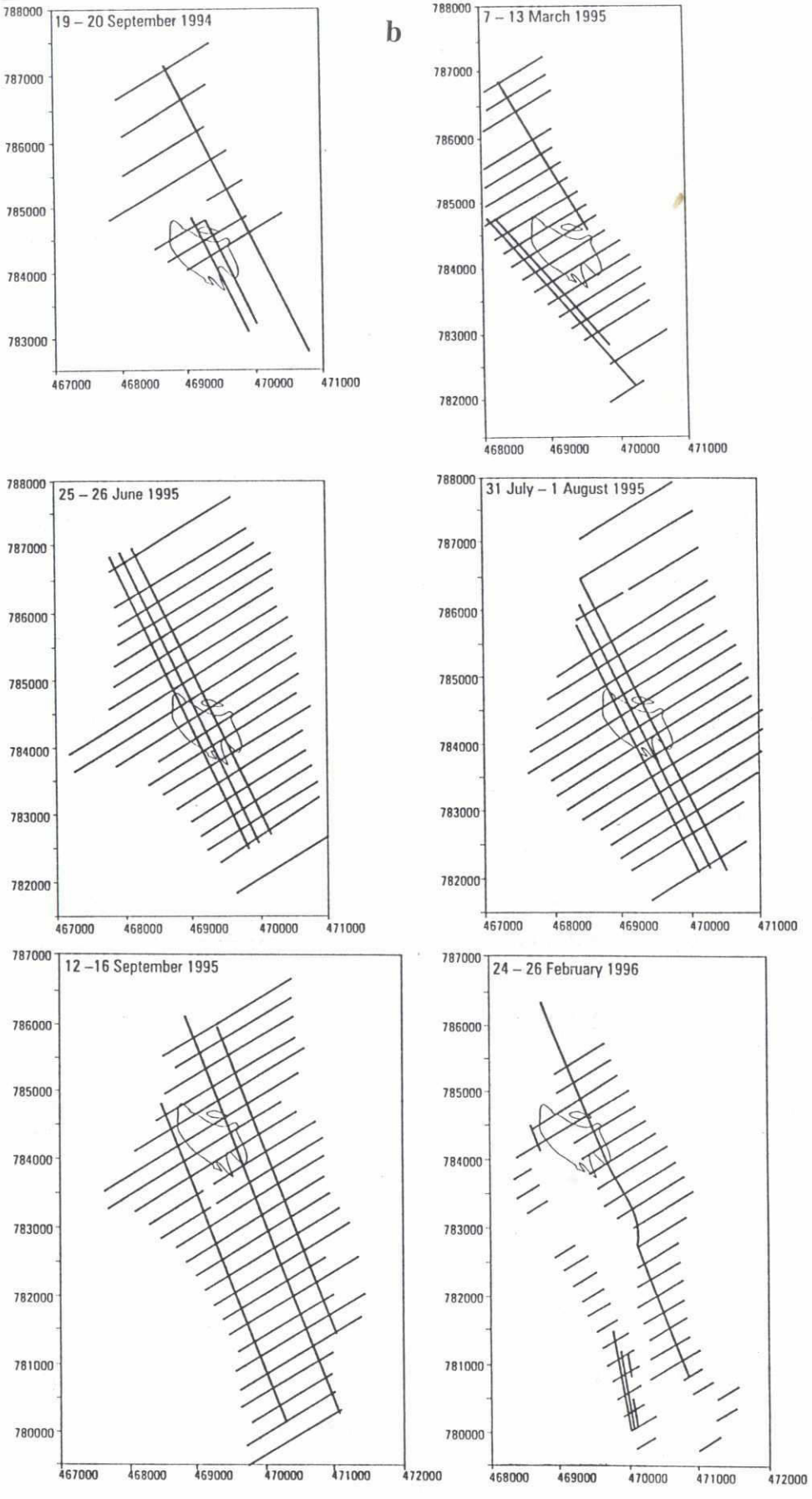

Figure 2.2: (b) Runs lines undertaken for all other special surveys for the bar morphology study at Bahadurabad. Coordinates are in BTM. The position of the study bar as land surveyed on 12/3/95 is plotted on each diagram for reference (although the bar extended laterally and downstream in some subsequent surveys - see Section 4.2).

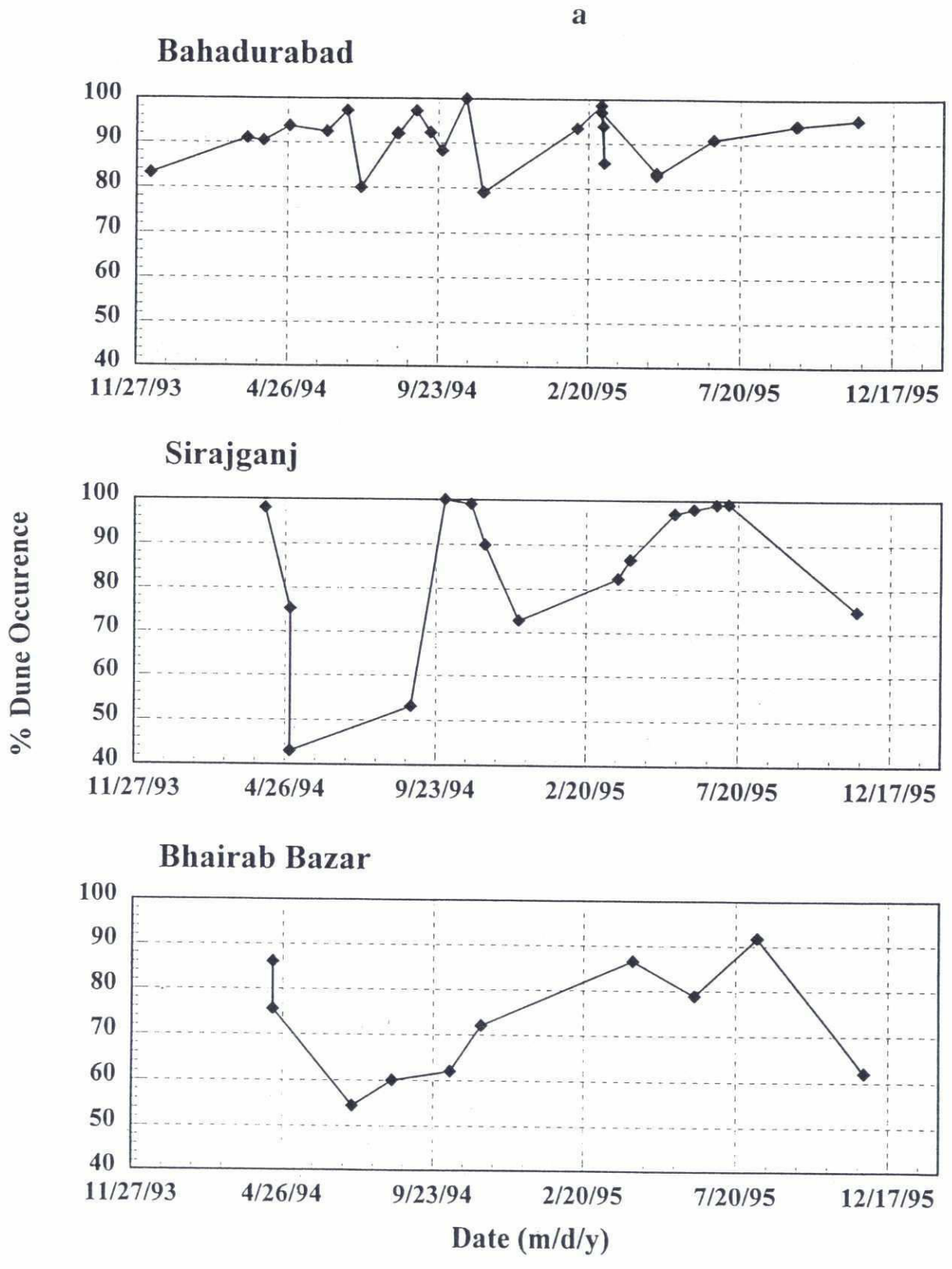

Figure 3.1: (a) The percentage occurrence of dunes in the main channels at Bahadurabad, Sirajganj and Bhairab Bazar for the study period between November 1993 to December 1995

b

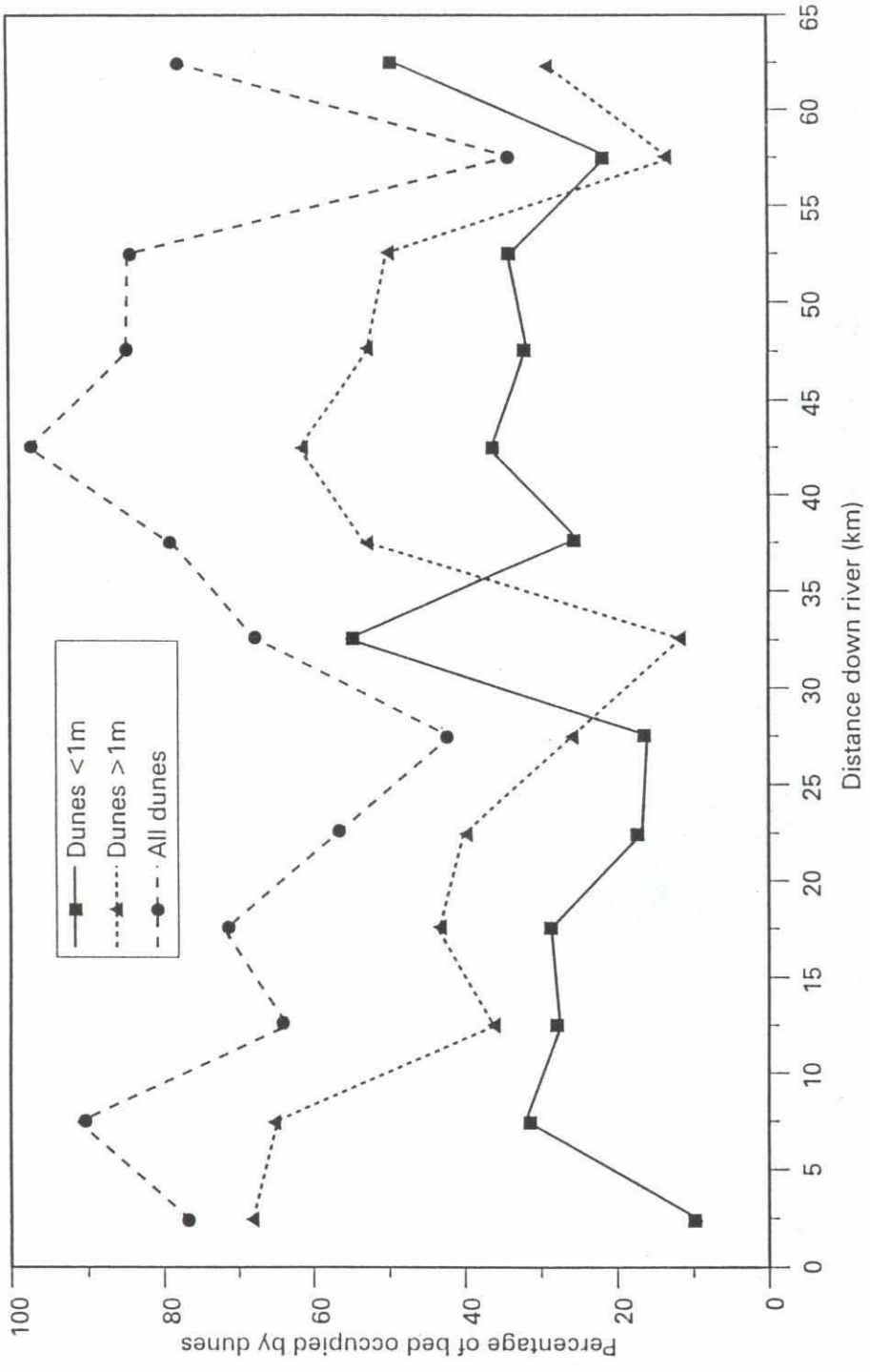

Figure 3.1: (b) The percentage occurrence of dunes along a downstream transect from Sirajganj-Aricha

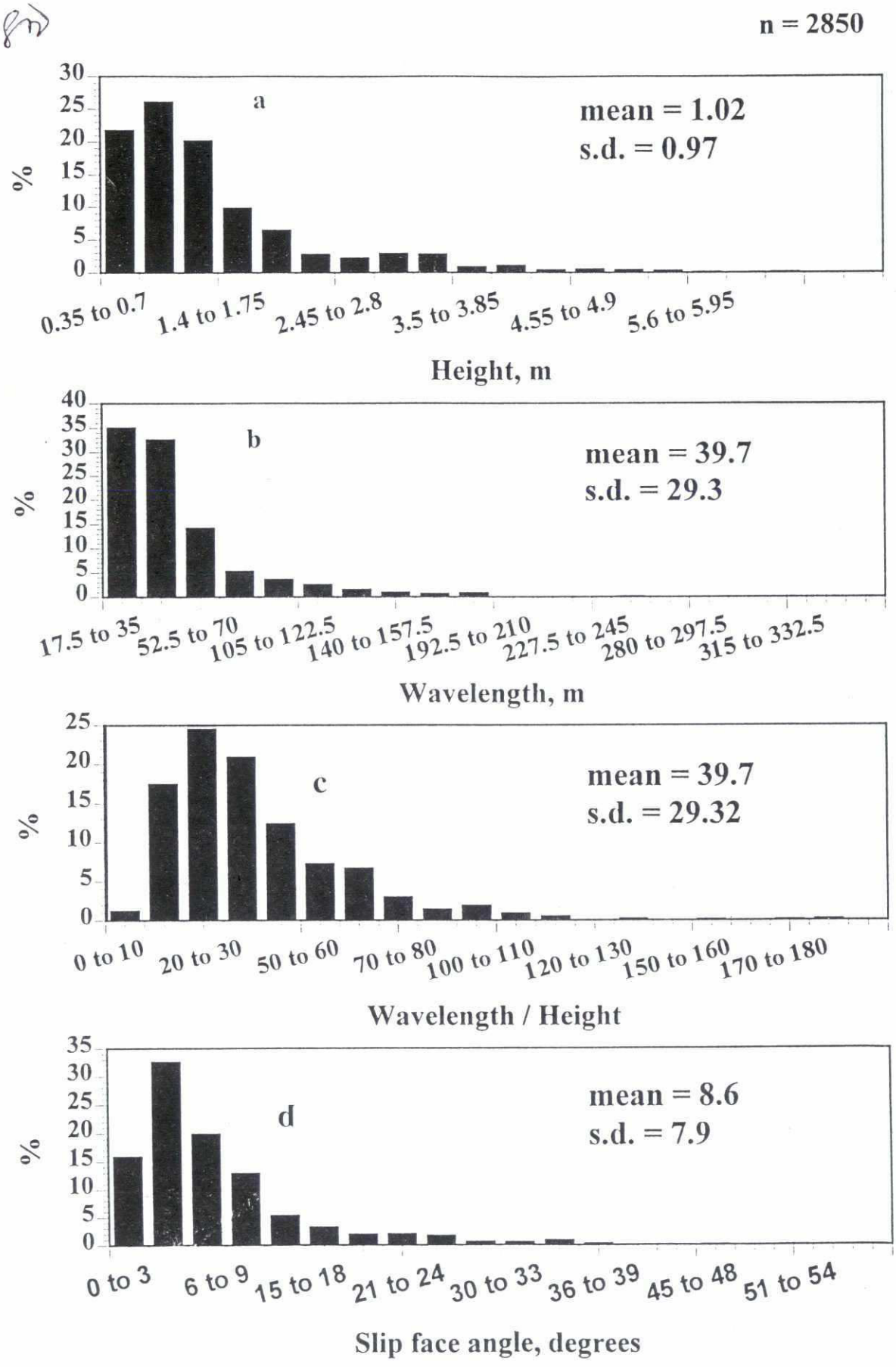

Figure 3.2: Histograms of: (a) dune height (b) dune wavelength (c) dune form index (wavelength/height) and (d) leeside angle, for all three sites for all study periods

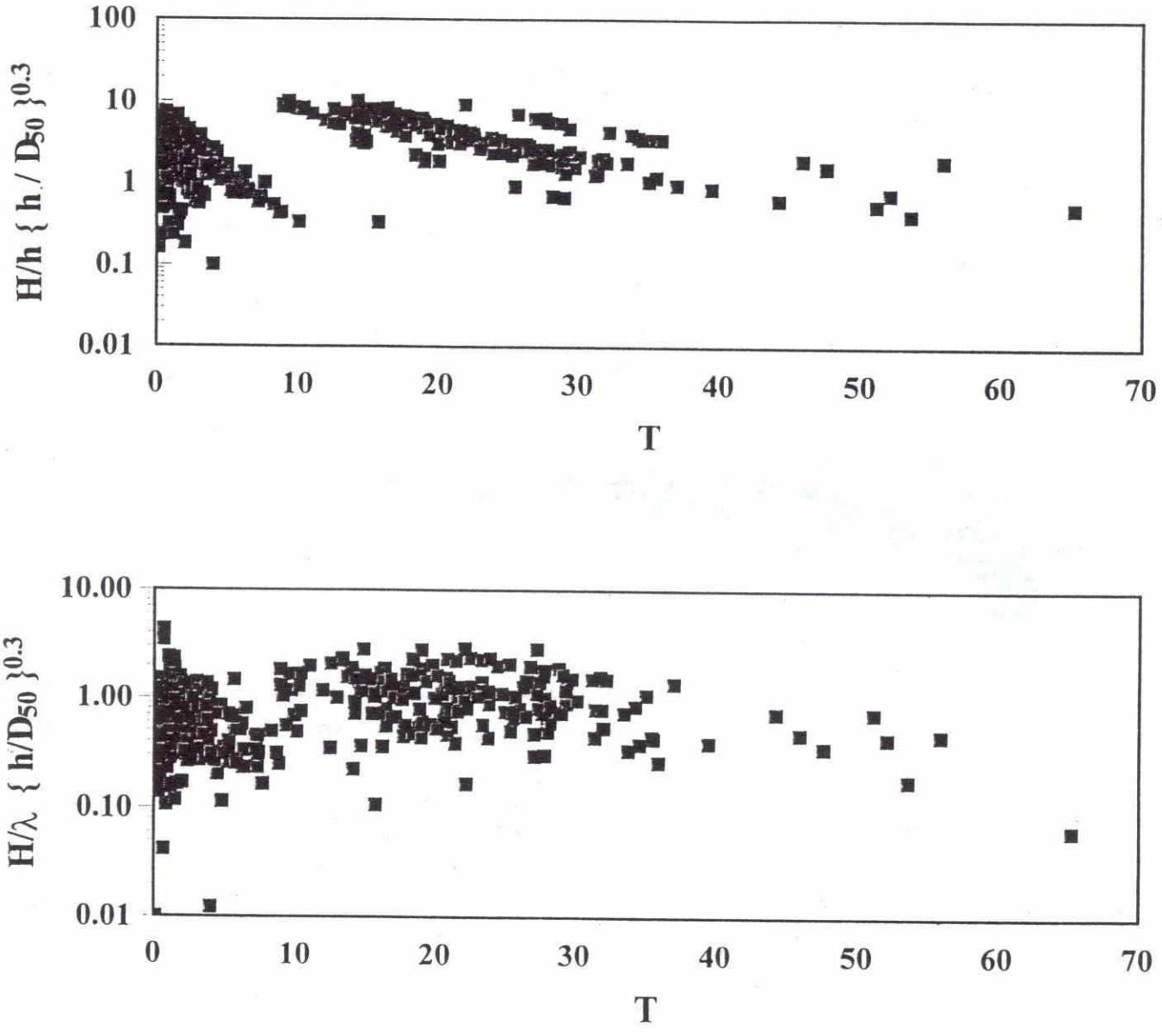

Figure 3.3: Plots of van Rijn's sediment mobility parameter, T, versus (a) bedform height and (b) bedform steepness

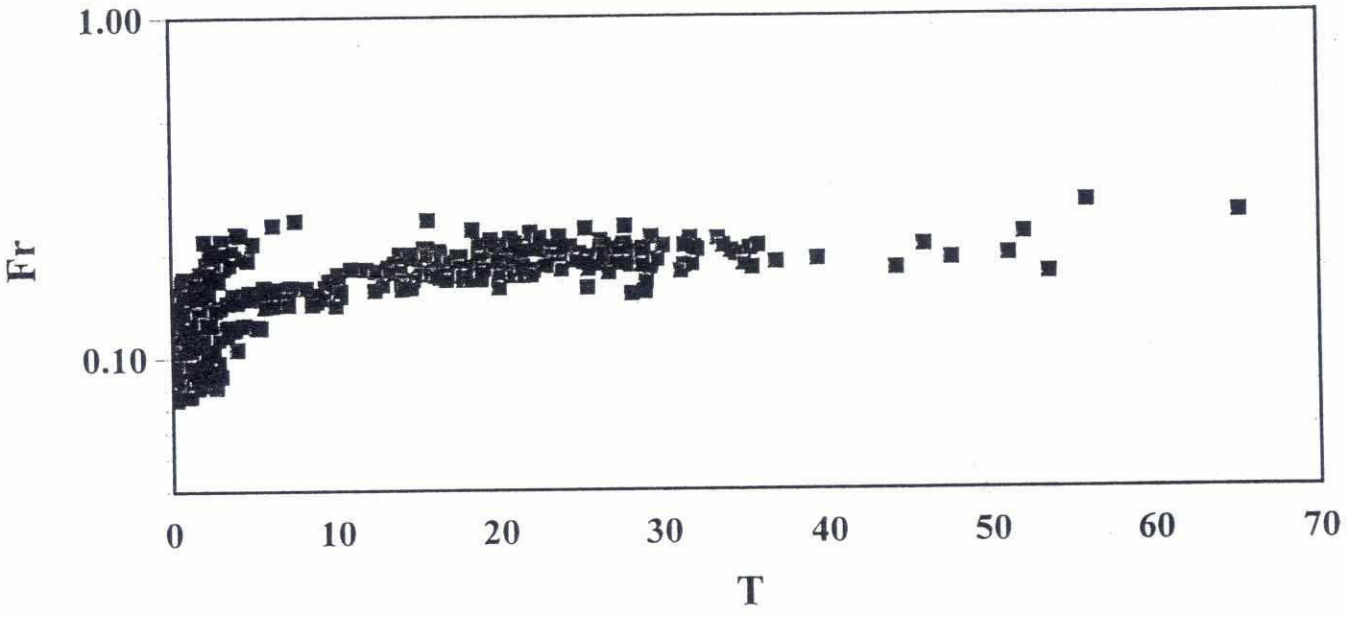

Figure 3.4: Plot of van Rijn's sediment mobility parameter, T, versus local Froude number, Fr (Fr $= \overline{U} / \sqrt{gh}$)

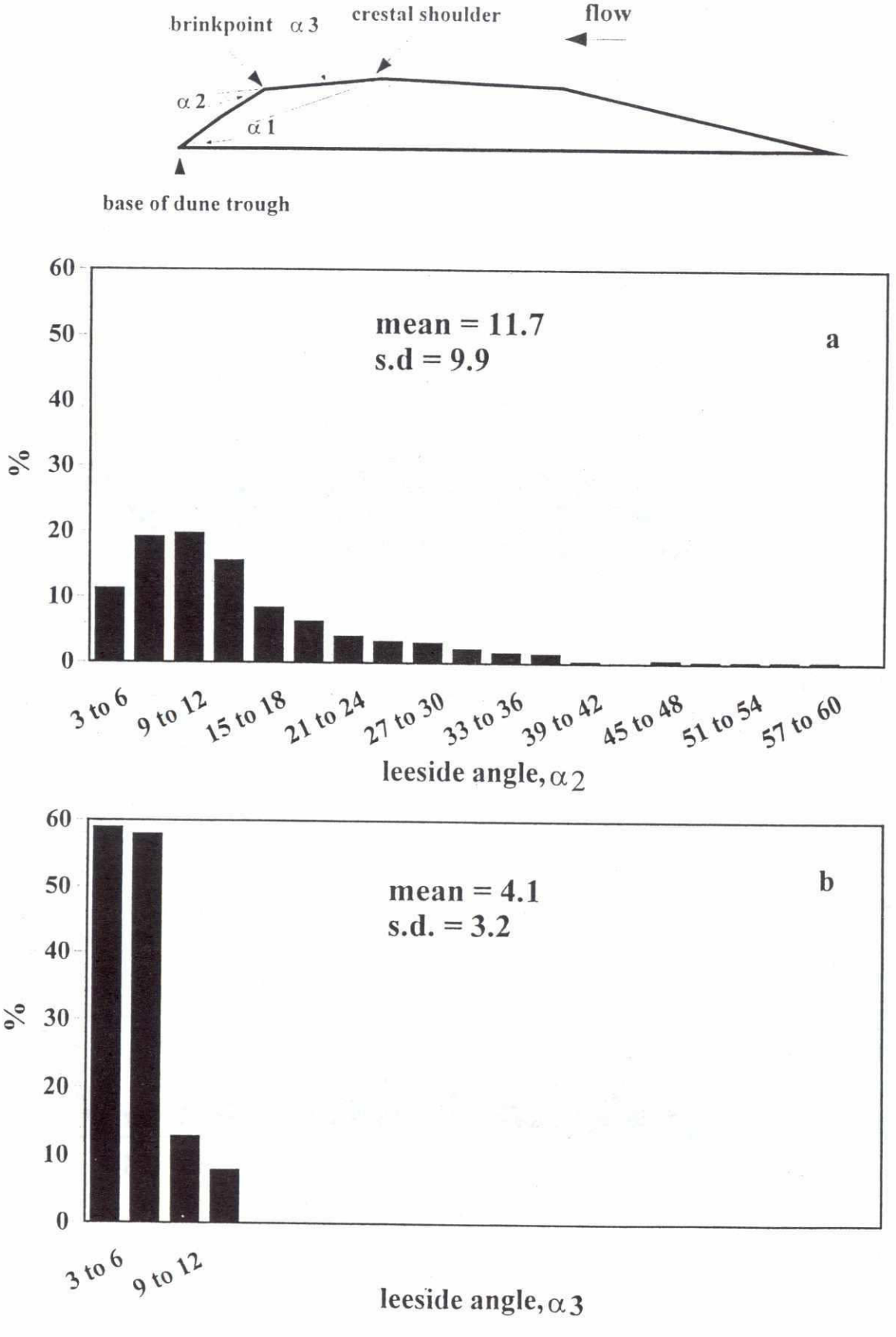

Figure 3.5: Histograms of the leeside angle defined by (a) the angle at the brinkpoint, a2, and (b) the angle at the crestal shoulder (a 3). See inset diagram for definitions of a 1, a 2 and a 3. The histogram of leeside angle a 1 is shown in Figure 3.2d.

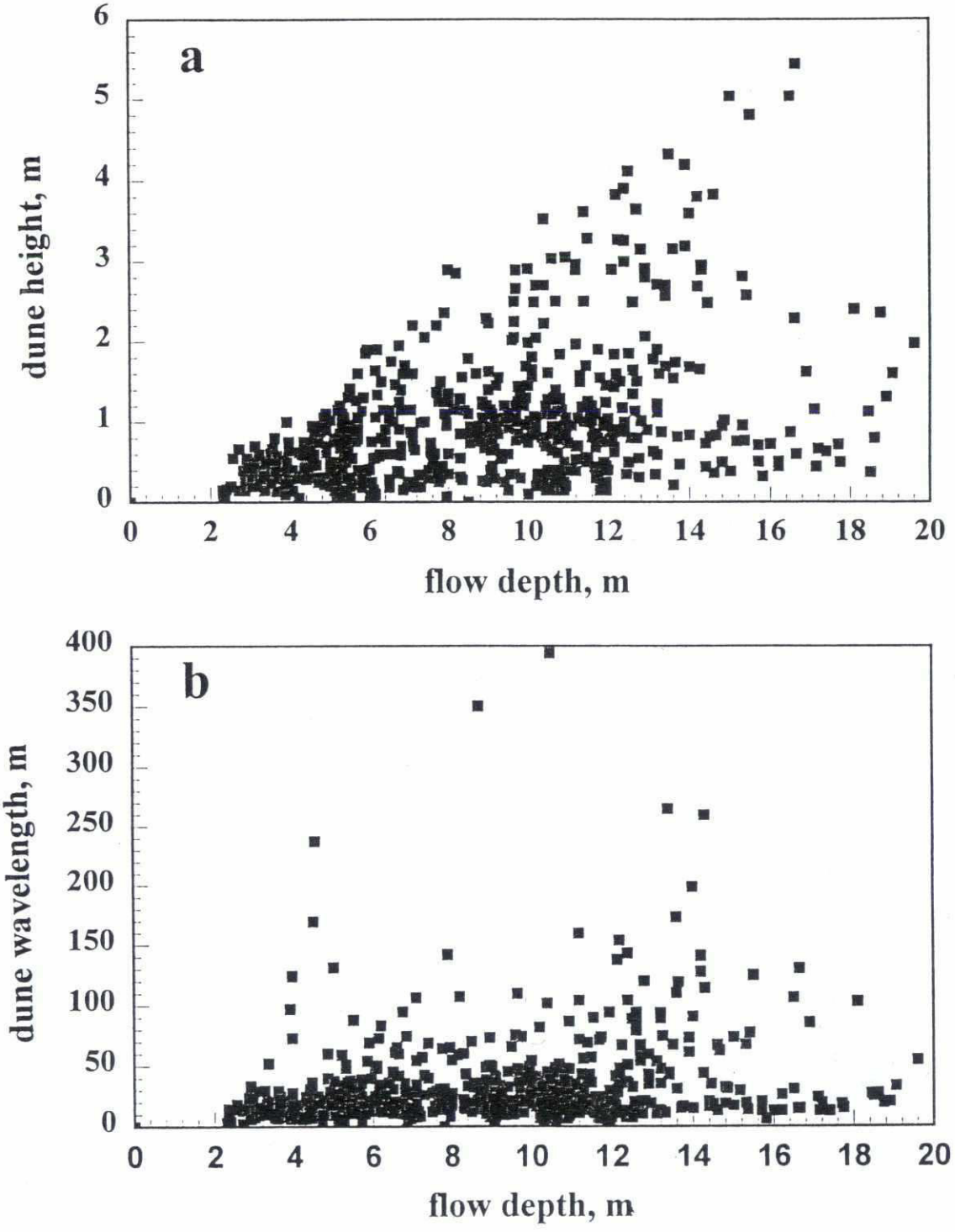

Figure 3.6: Plots of (a) dune height and (b) dune wavelength as a function of flow depth for all three study sites throughout the study period.

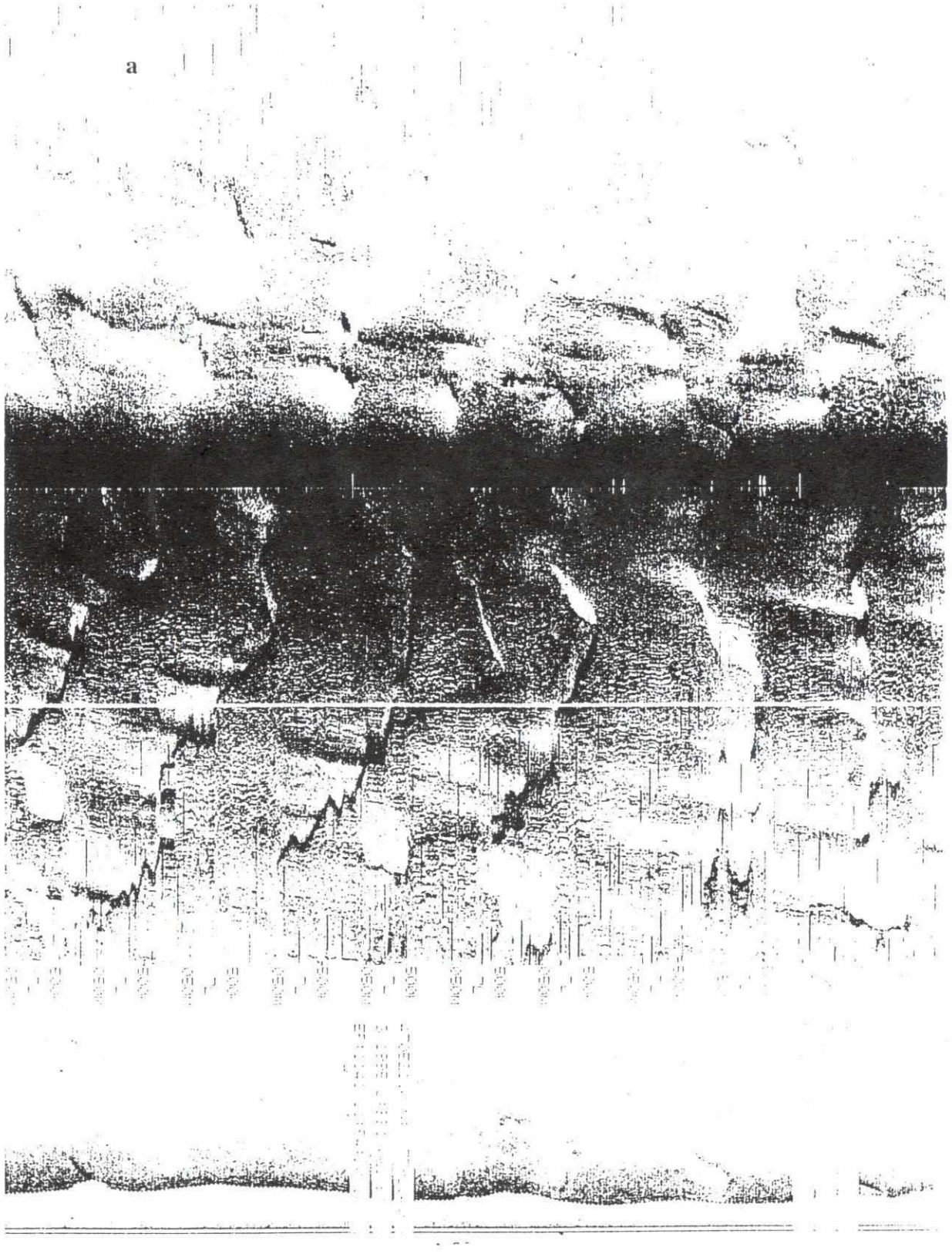

Figure 3.7: (a) Side scan sonar image obtained at low flow (March 1995) at Bahadurabad illustrating clear dune crestlines, (b) Composite tracing of dune crestline morphology derived from side scan image (March 1995) showing an area approximately 1km in length and 200m wide. Note the sinuosity of both the larger and smaller wavelength dunes

b

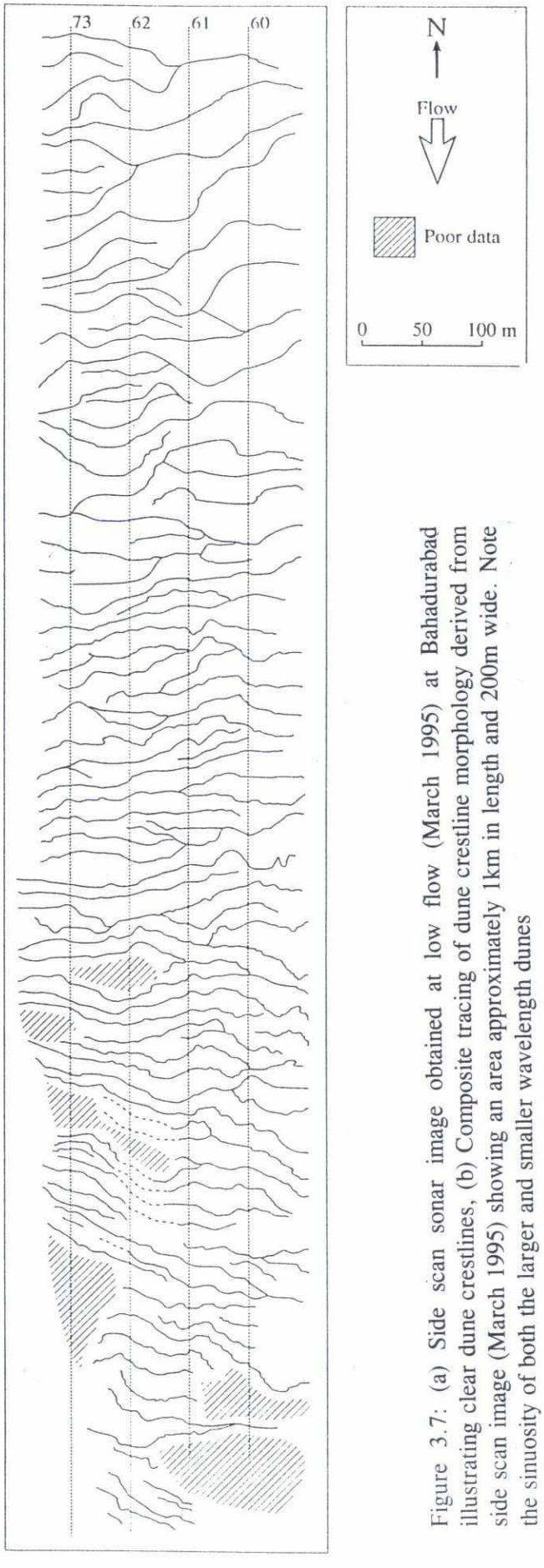

Figure 3.7: (a) Side scan sonar image obtained at low flow (March 1995) at Bahadurabad illustrating clear dune crestlines, (b) Composite tracing of dune crestline morphology derived from side scan image (March 1995) showing an area approximately 1km in length and 200m wide. Note the sinuosity of both the larger and smaller wavelength dunes

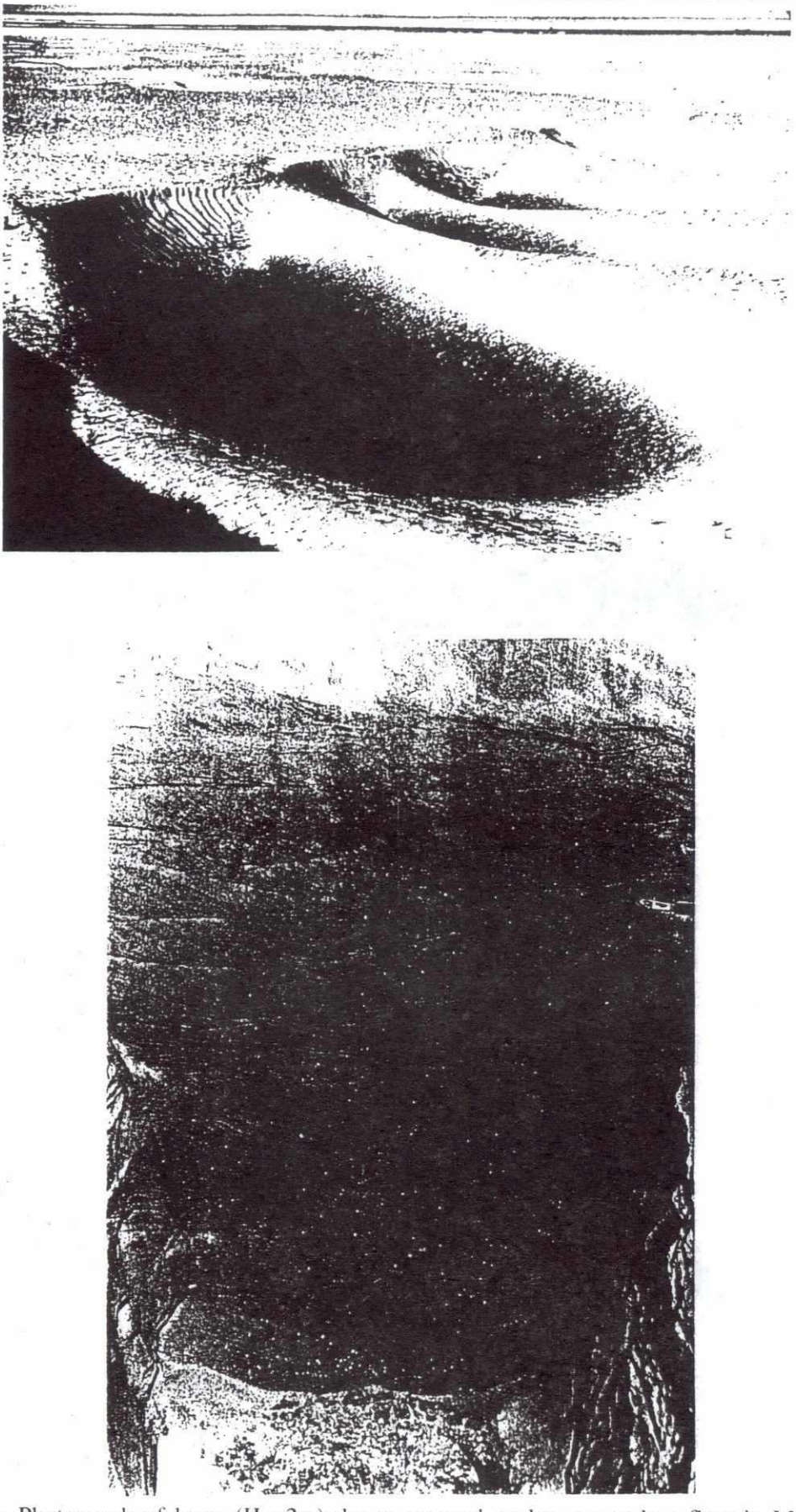

Figure 3.8: Photograph of large (H ~ 2m) dunes exposed on bar top at low flow in March 1995 illustrating a sinuous crestline with distinct spurs and troughs in the dune morphology. Bartop dunes such as these are common and illustrate that dunes are found both in the talwegs and on bar margins and tops.

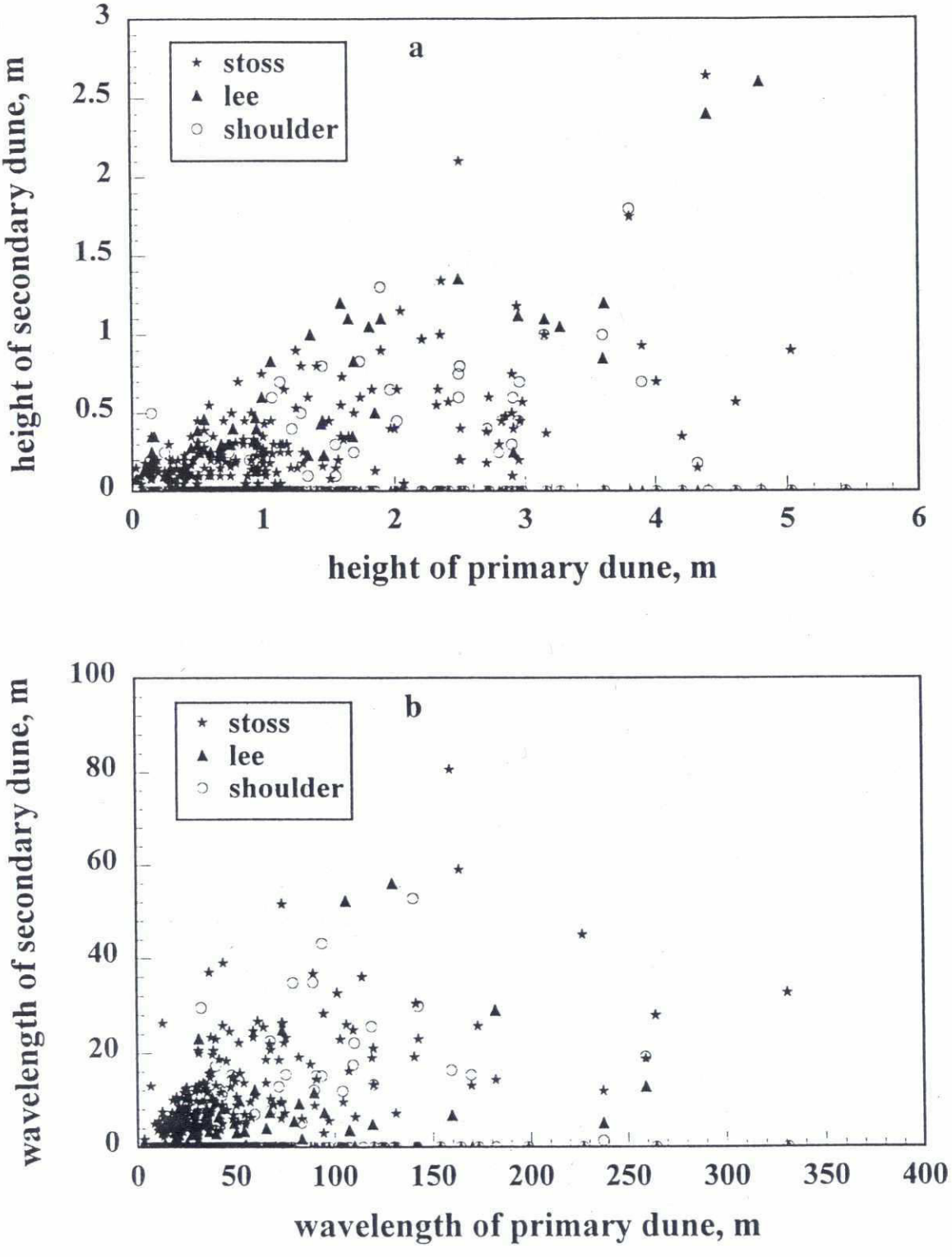

Figure 3.9: Scatterplots of (a) height of primary dunes -vs- height of secondary dunes and (b) wavelength of primary dunes -vs- wavelength of secondary dunes, subdivided according to position on the primary dune (leeside, stoss side or crestal shoulder)

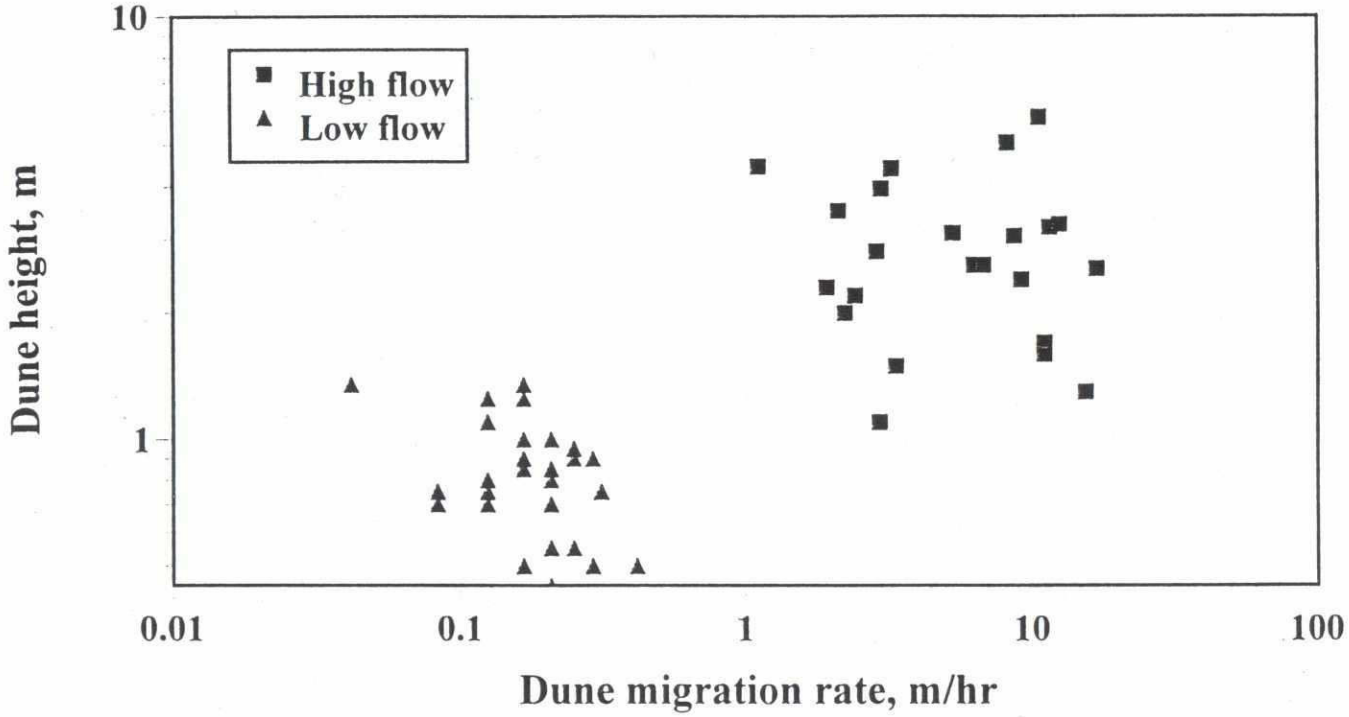

Figure 3.10: Scatterplot of dune migration rate -vs- dune height at Bahadurabad for high flow stage.

a

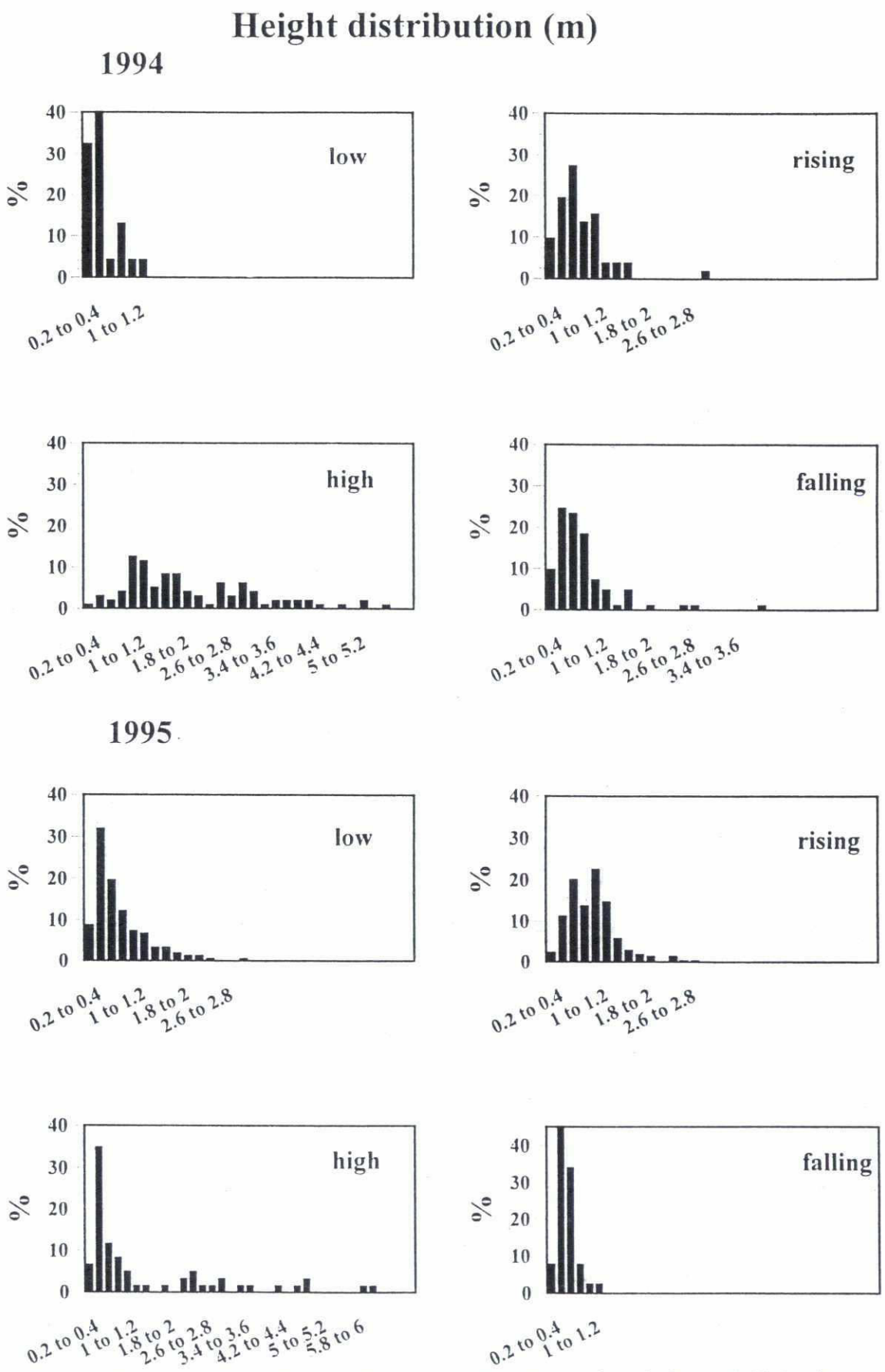

Figure 3.11: Histograms of (a) dune height, (b) wavelength, (c) form index and (d) leeside angle through the 1994 and 1995 flood hydrographs. Each year is divided into low flow (< 1.5 m s^{-1}), high flow (> 1.5 m s^{-1}) and rising and falling limbs of the hydrograph (> 1.5 m s^{-1}).

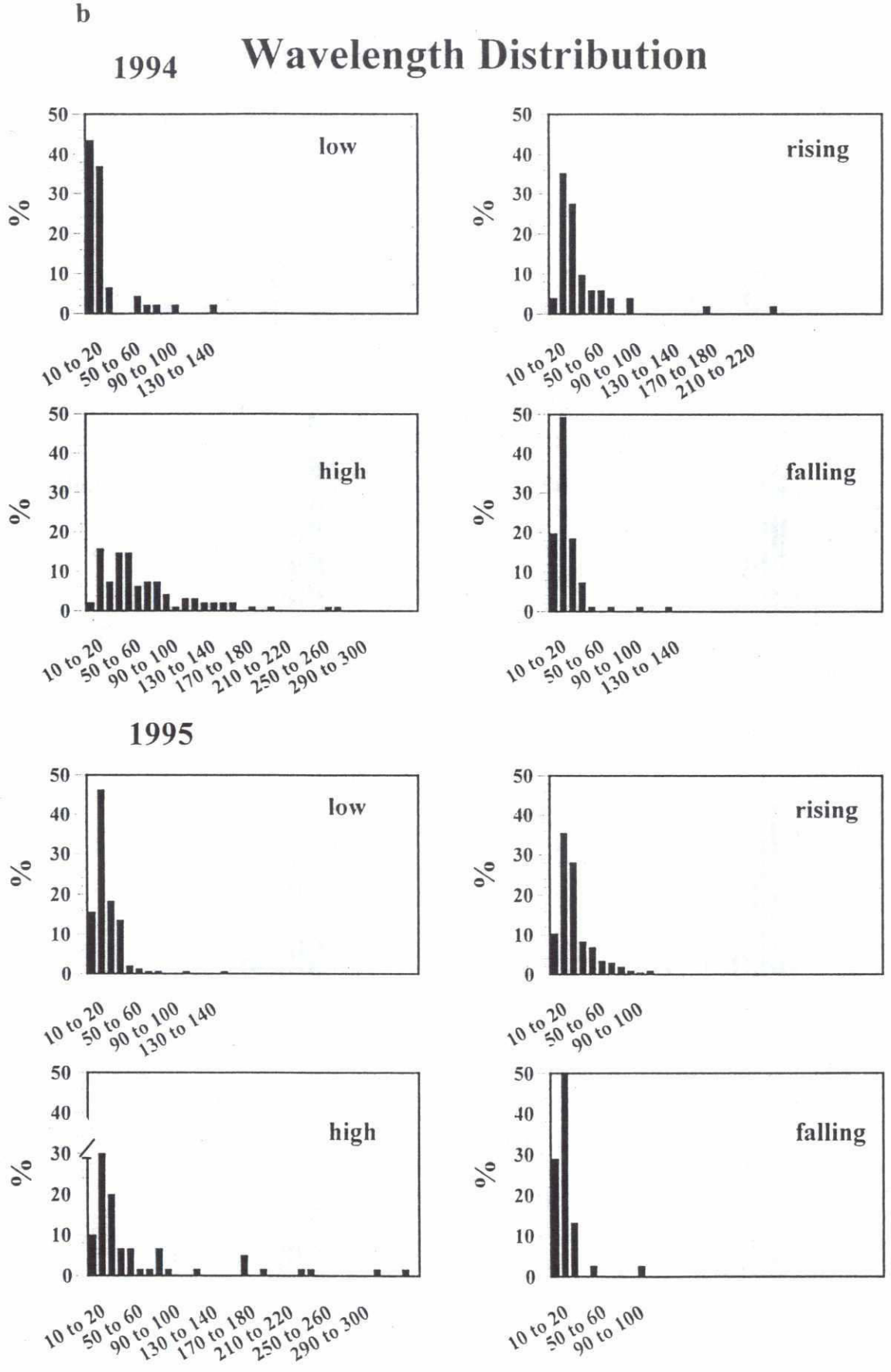

Figure 3.11: Histograms of (a) dune height, (b) wavelength, (c) form index and (d) leeside angle through the 1994 and 1995 flood hydrographs. Each year is divided into low flow (< 1.5 m s^{-1}), high flow (> 1.5 m s^{-1}) and rising and falling limbs of the hydrograph (> 1.5 m s^{-1}).

c

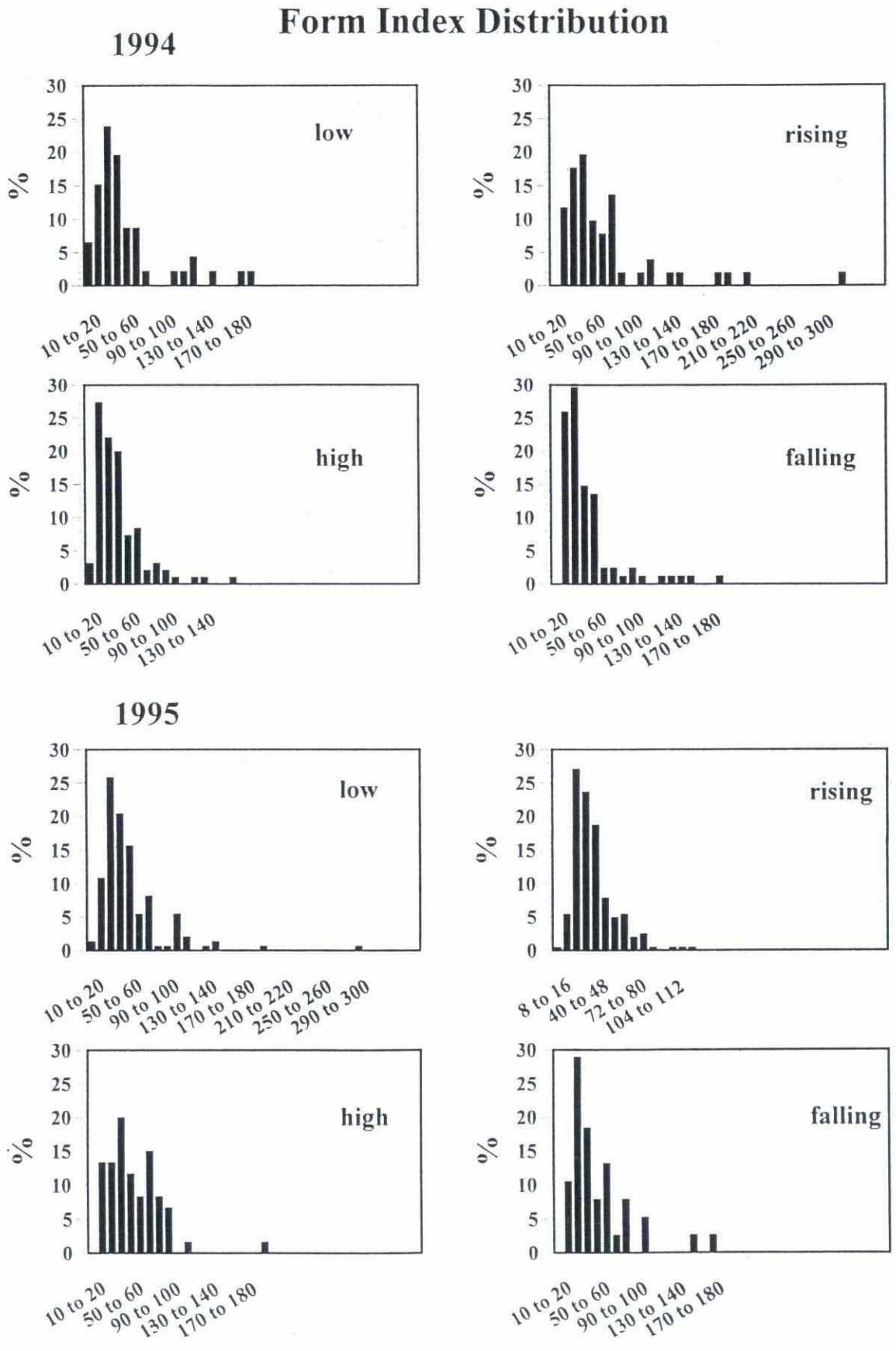

Figure 3.11: Histograms of (a) dune height, (b) wavelength, (c) form index and (d) leeside angle through the 1994 and 1995 flood hydrographs. Each year is divided into low flow (<1.5 m s^{-1}), high flow (>1.5 m s^{-1}) and rising and falling limbs of the hydrograph ($>$ 1.5 m s^{-1}).

d

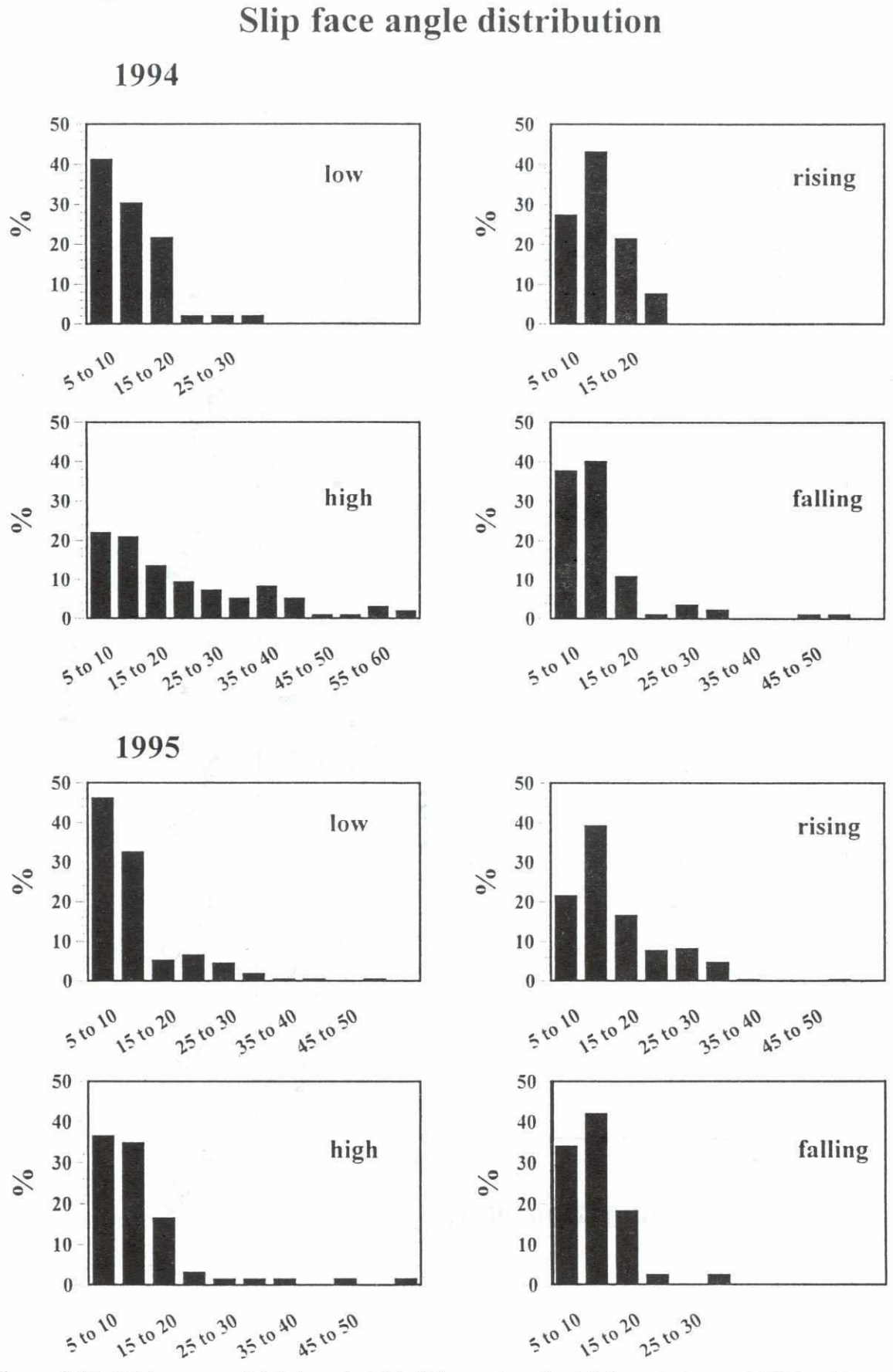

Figure 3.11: Histograms of (a) dune height, (b) wavelength, (c) form index and (d) leeside angle through the 1994 and 1995 flood hydrographs. Each year is divided into low flow (< 1.5 m s^{-1}), high flow (> 1.5 m s^{-1}) and rising and falling limbs of the hydrograph (> 1.5 m s^{-1}).

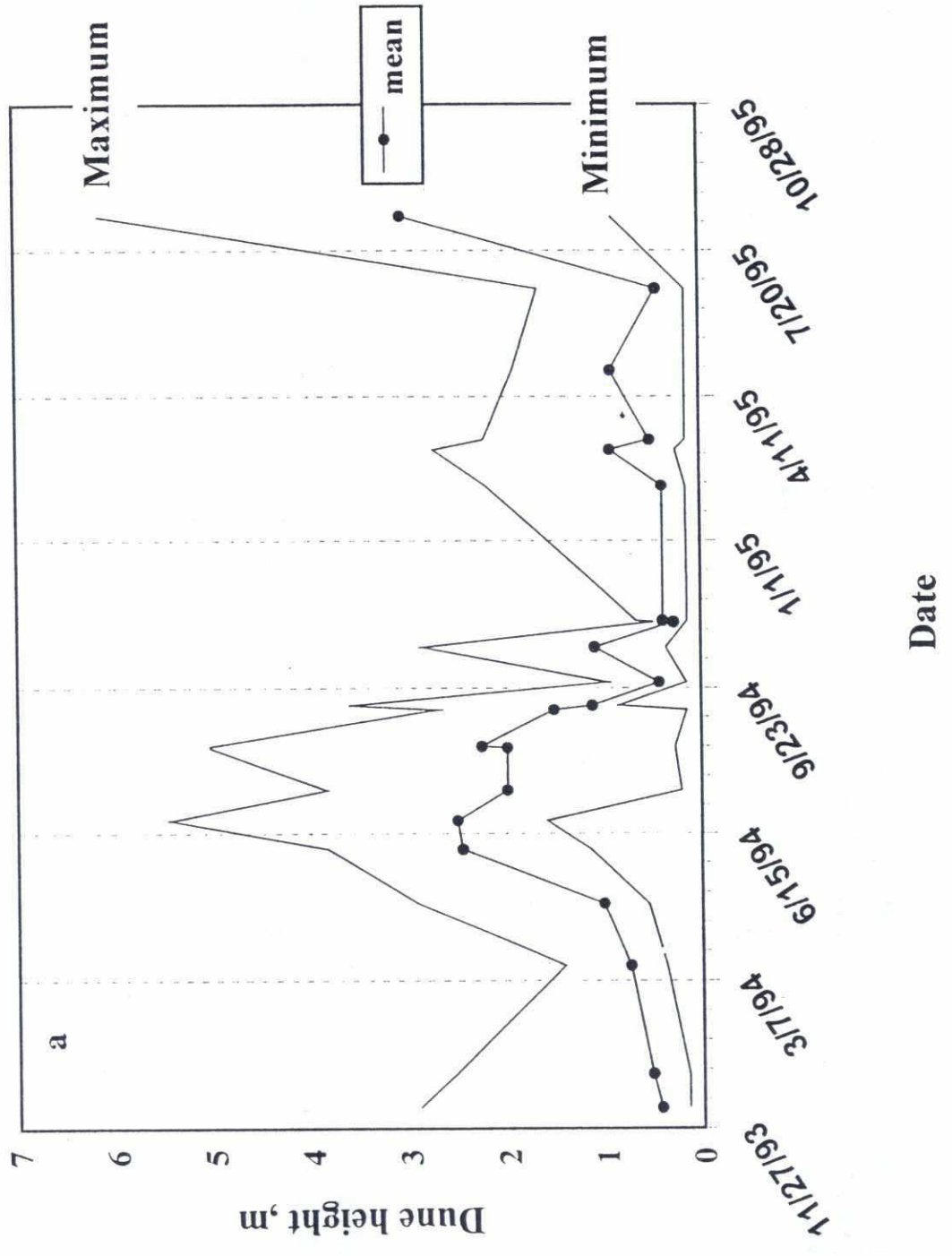

Figure 3.12: Temporal variation in the mean, maximum and minimum values of (a) dune height, (b) wavelength, (c) form index and (d) leeside angle through the 1994 and 1995 flood hydrographs.

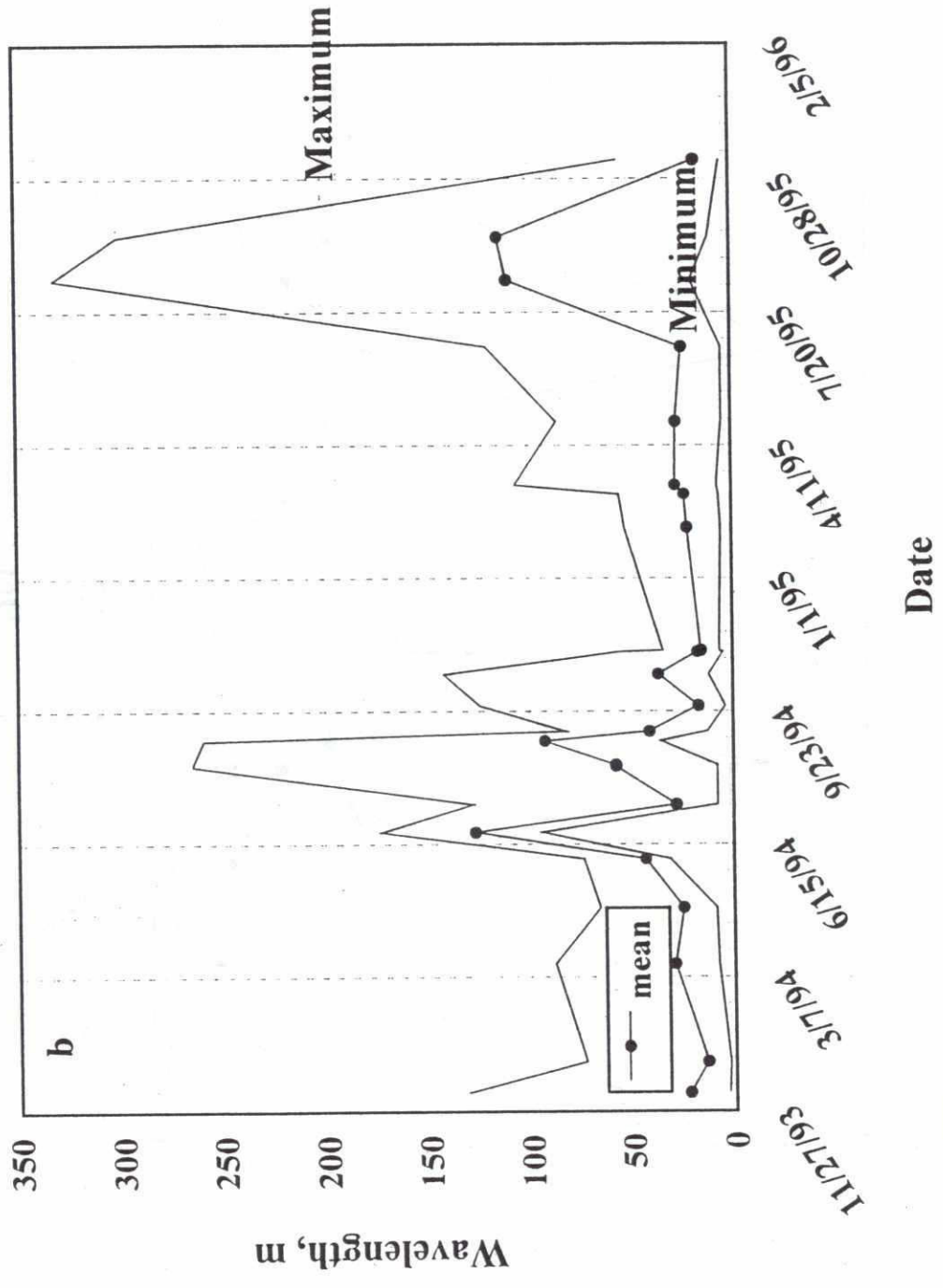

Figure 3.12: Temporal variation in the mean, maximum and minimum values of (a) dune height, (b) wavelength, (c) form index and (d) leeside angle through the 1994 and 1995 flood hydrographs.

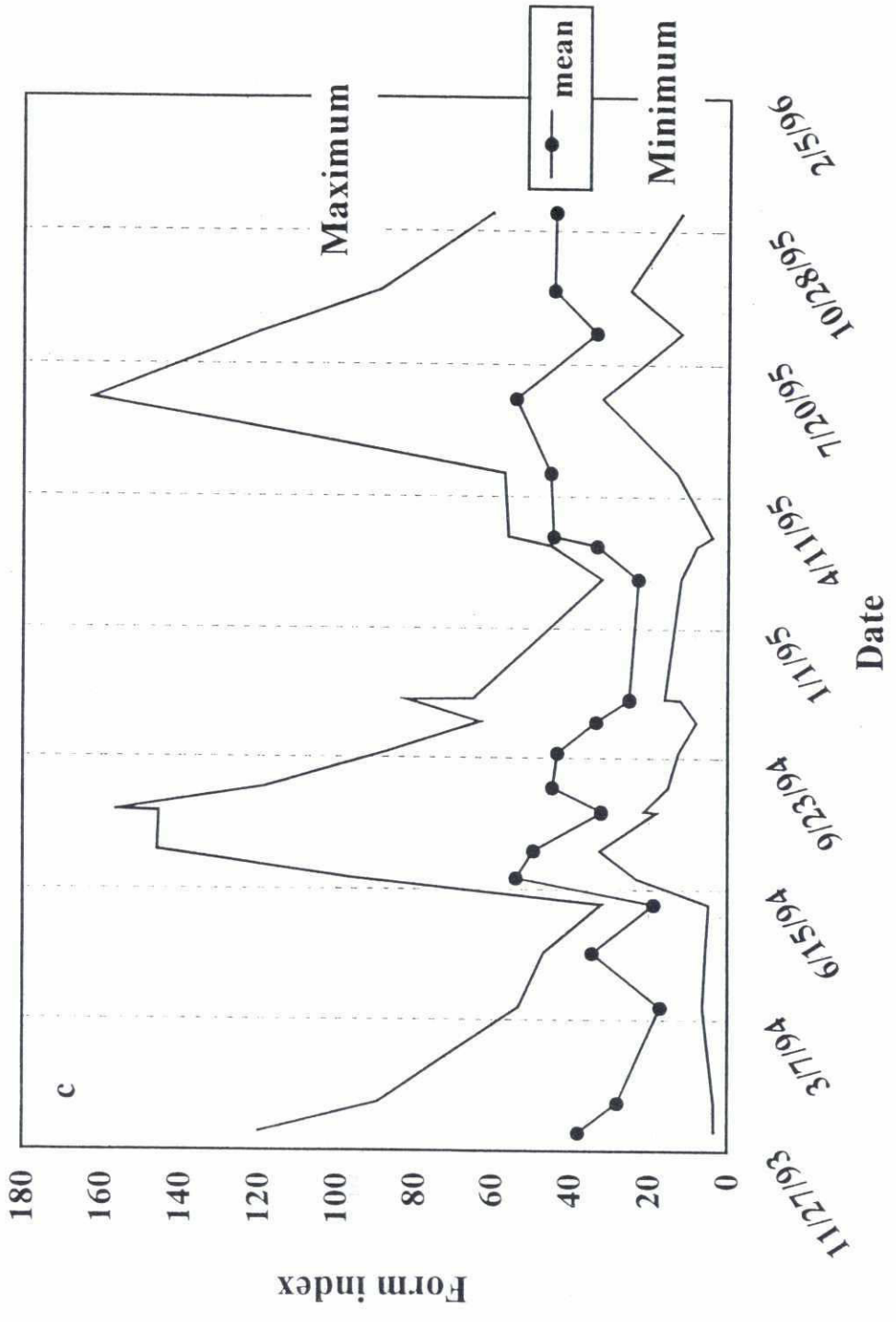

Figure 3.12: Temporal variation in the mean, maximum and minimum values of (a) dune height, (b) wavelength, (c) form index and (d) leeside angle through the 1994 and 1995 flood hydrographs.

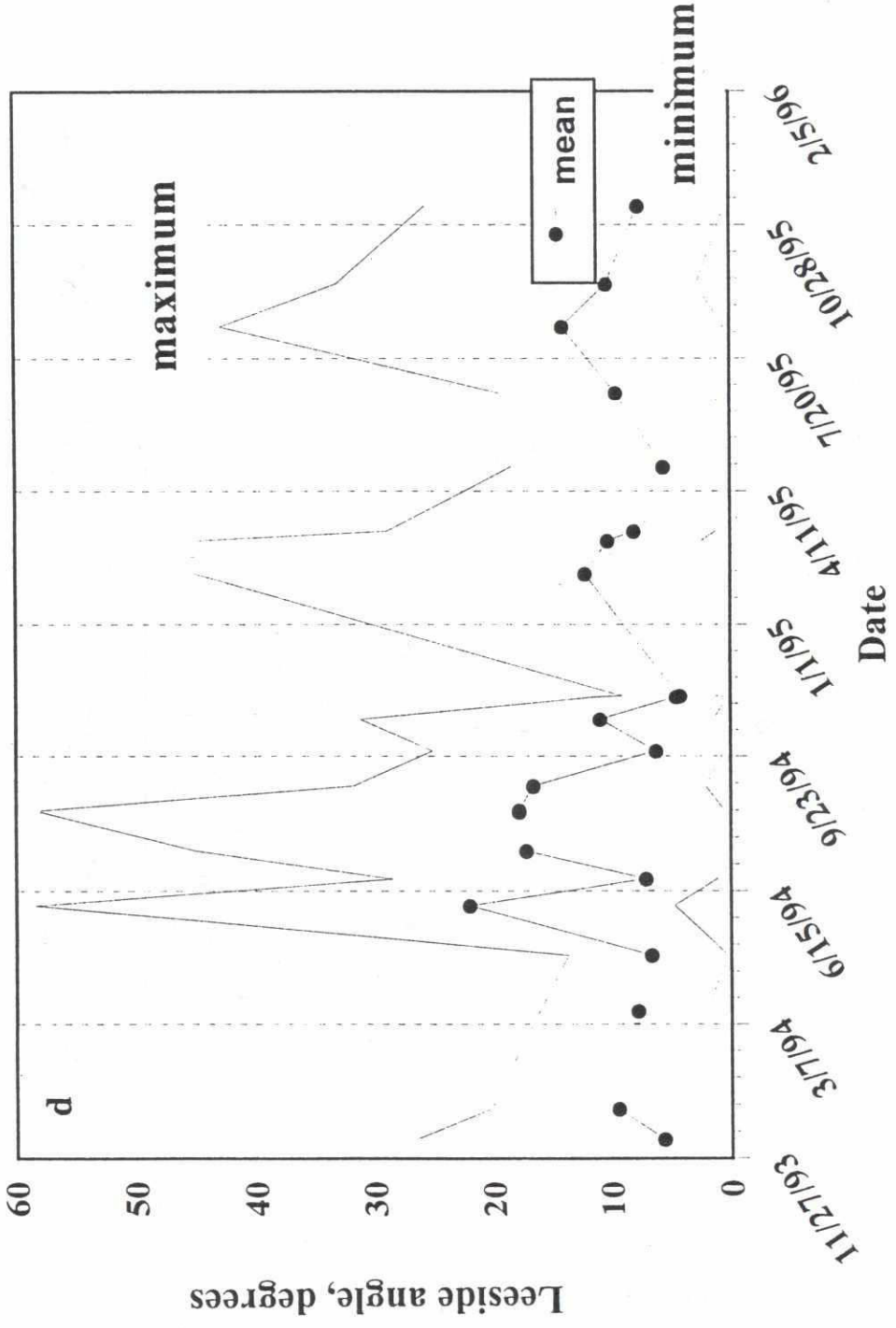

Figure 3.12: Temporal variation in the mean, maximum and minimum values of (a) dune height, (b) wavelength, (c) form index and (d) leeside angle through the 1994 and 1995 flood hydrographs.

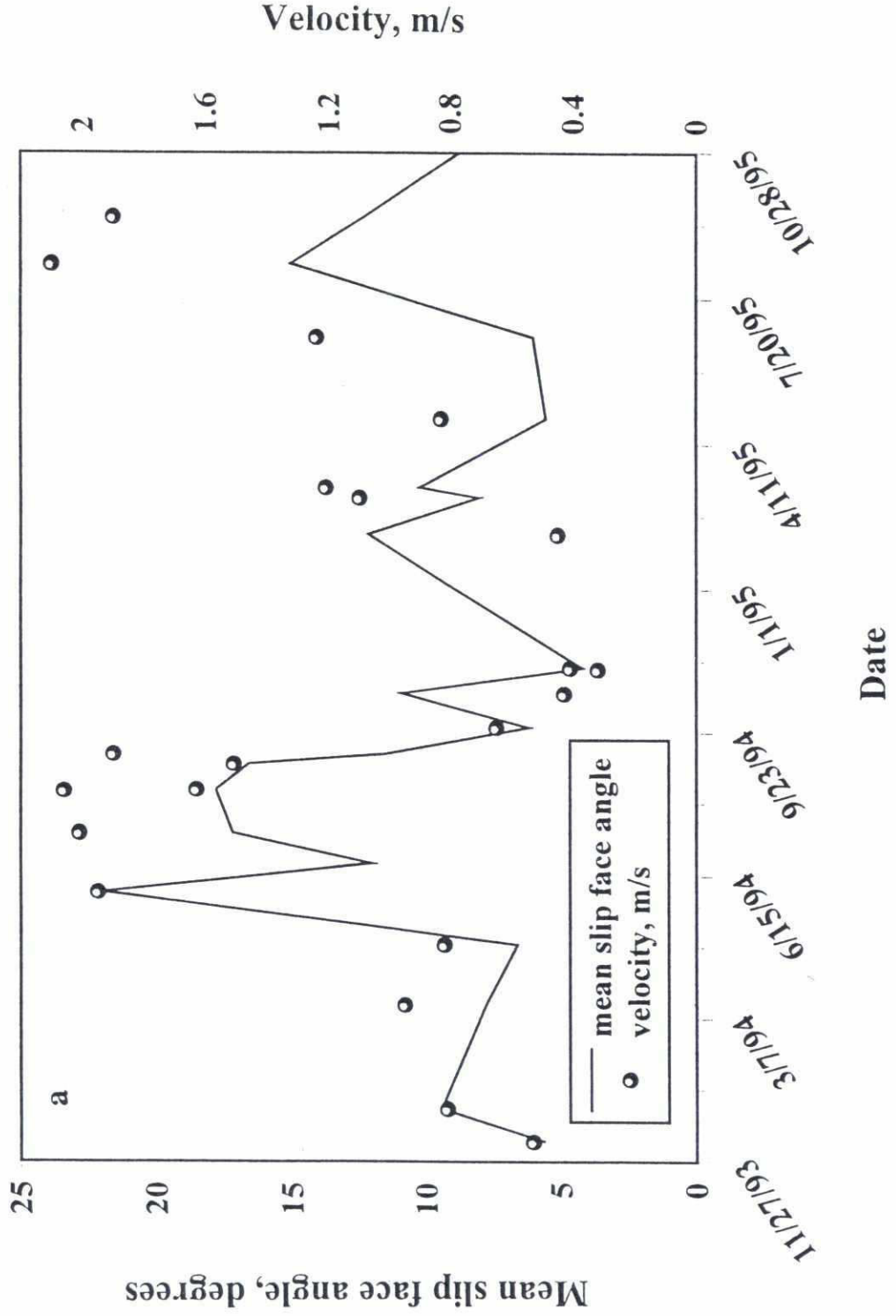

Figure 3.13 Plots of leeside angle as a function of a) time and b) mean downstream velocity; (c) dune height as a function of mean downstream velocity.

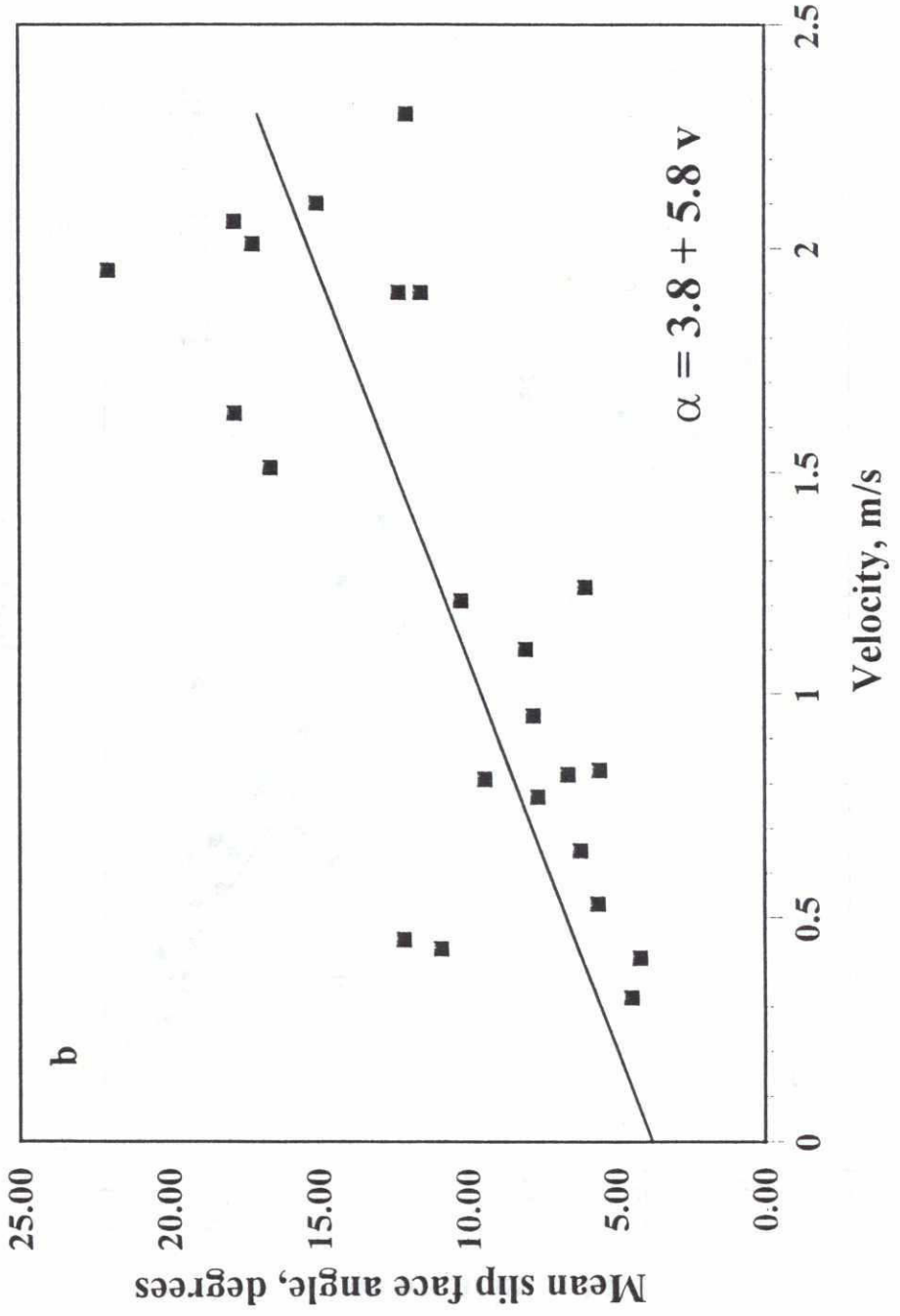

Figure 3.13 Plots of leeside angle as a function of a) time and b) mean downstream velocity; (c) dune height as a function of mean downstream velocity.

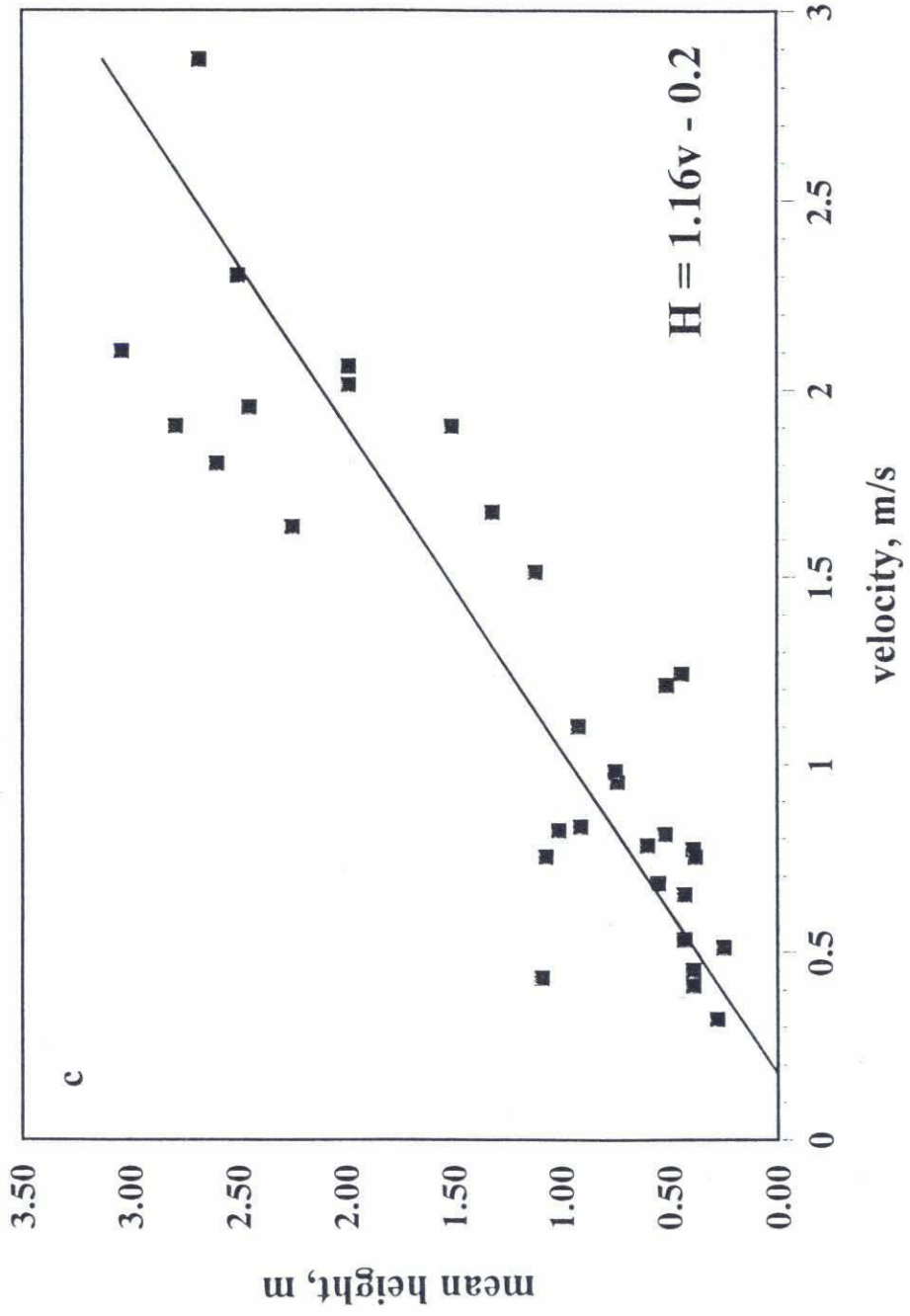

Figure 3.13 Plots of leeside angle as a function of a) time and b) mean downstream velocity; (c) dune height as a function of mean downstream velocity.

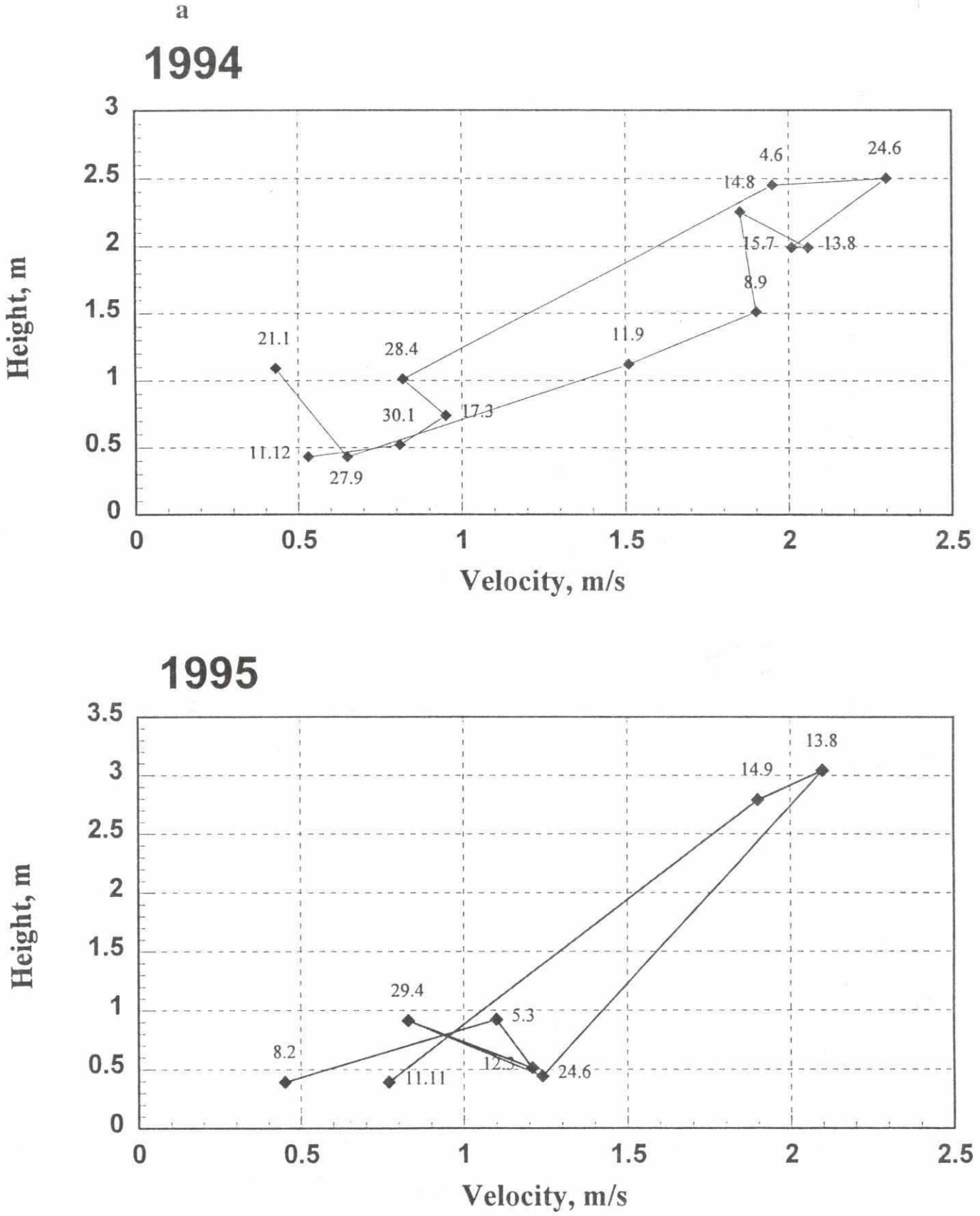

Figure 3.14: Hysteresis plots for 1994 and 1995 hydrographs at Bahadurabad for (a) dune height, (b) dune wavelength and (c) dune form index plotted as a function of mean flow velocity derived from ADCP records.

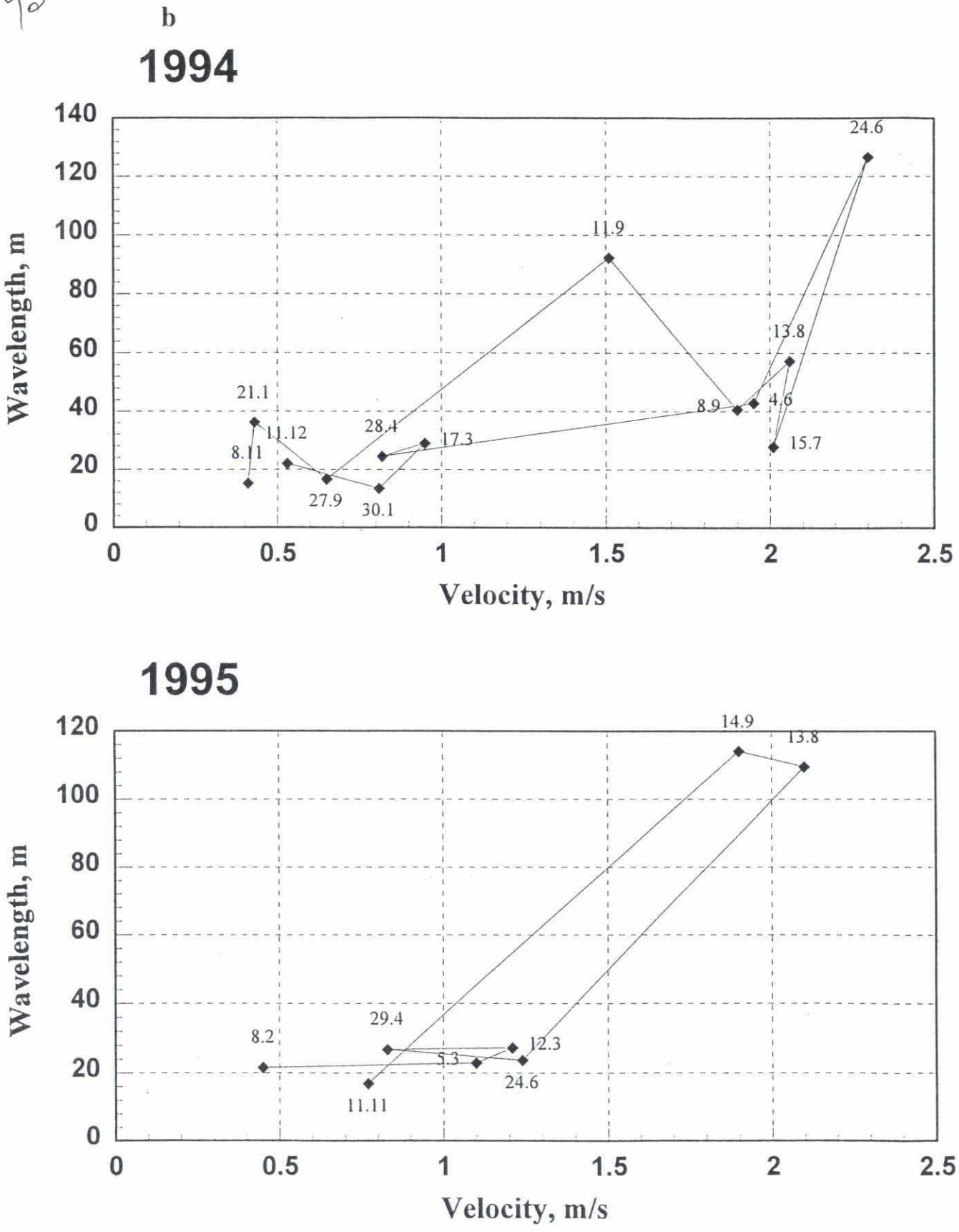

Figure 3.14: Hysteresis plots for 1994 and 1995 hydrographs at Bahadurabad for (a) dune height, (b) dune wavelength and (c) dune form index plotted as a function of mean flow velocity derived from ADCP records.

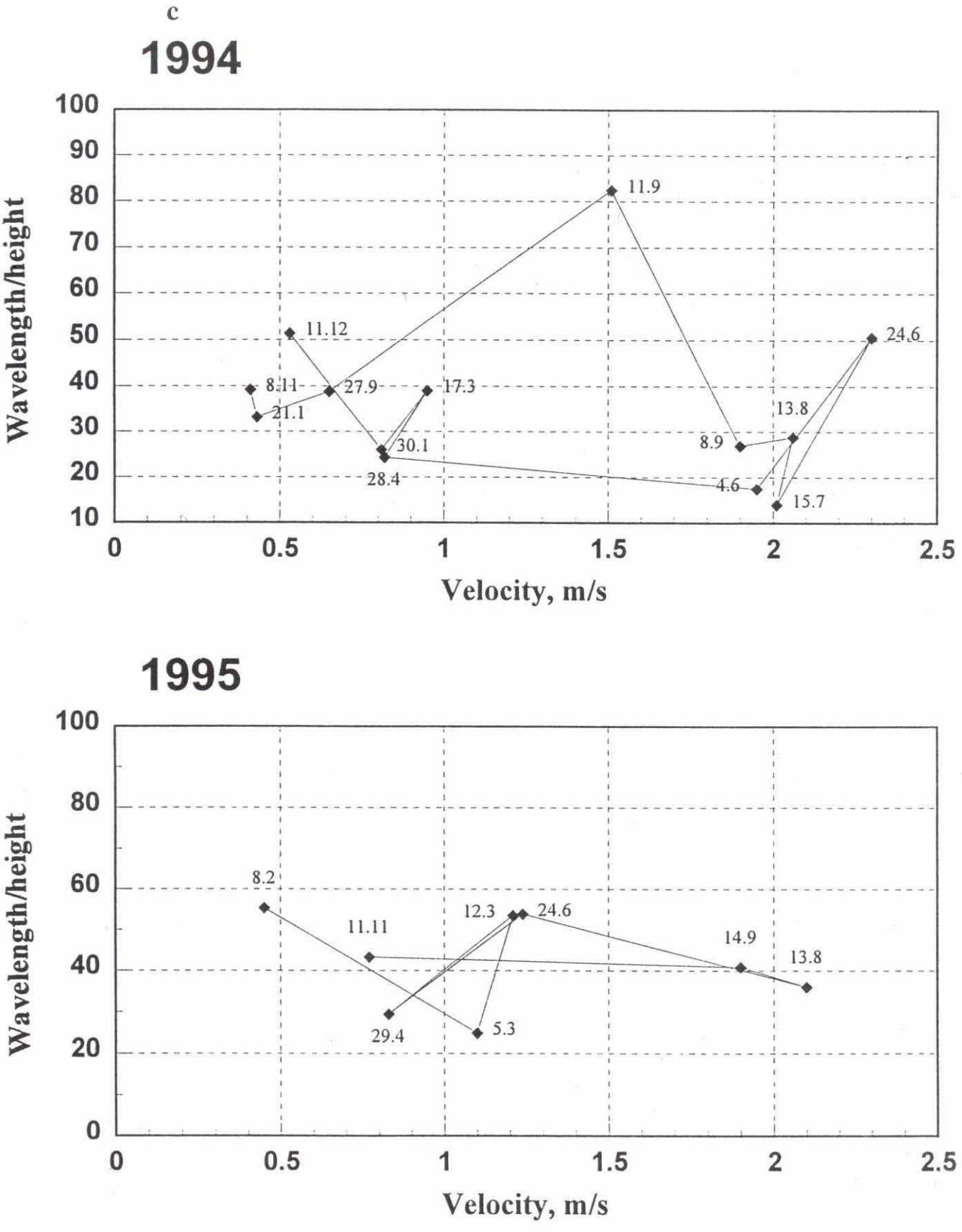

Figure 3.14: Hysteresis plots for 1994 and 1995 hydrographs at Bahadurabad for (a) dune height, (b) dune wavelength and (c) dune form index plotted as a function of mean flow velocity derived from ADCP records.

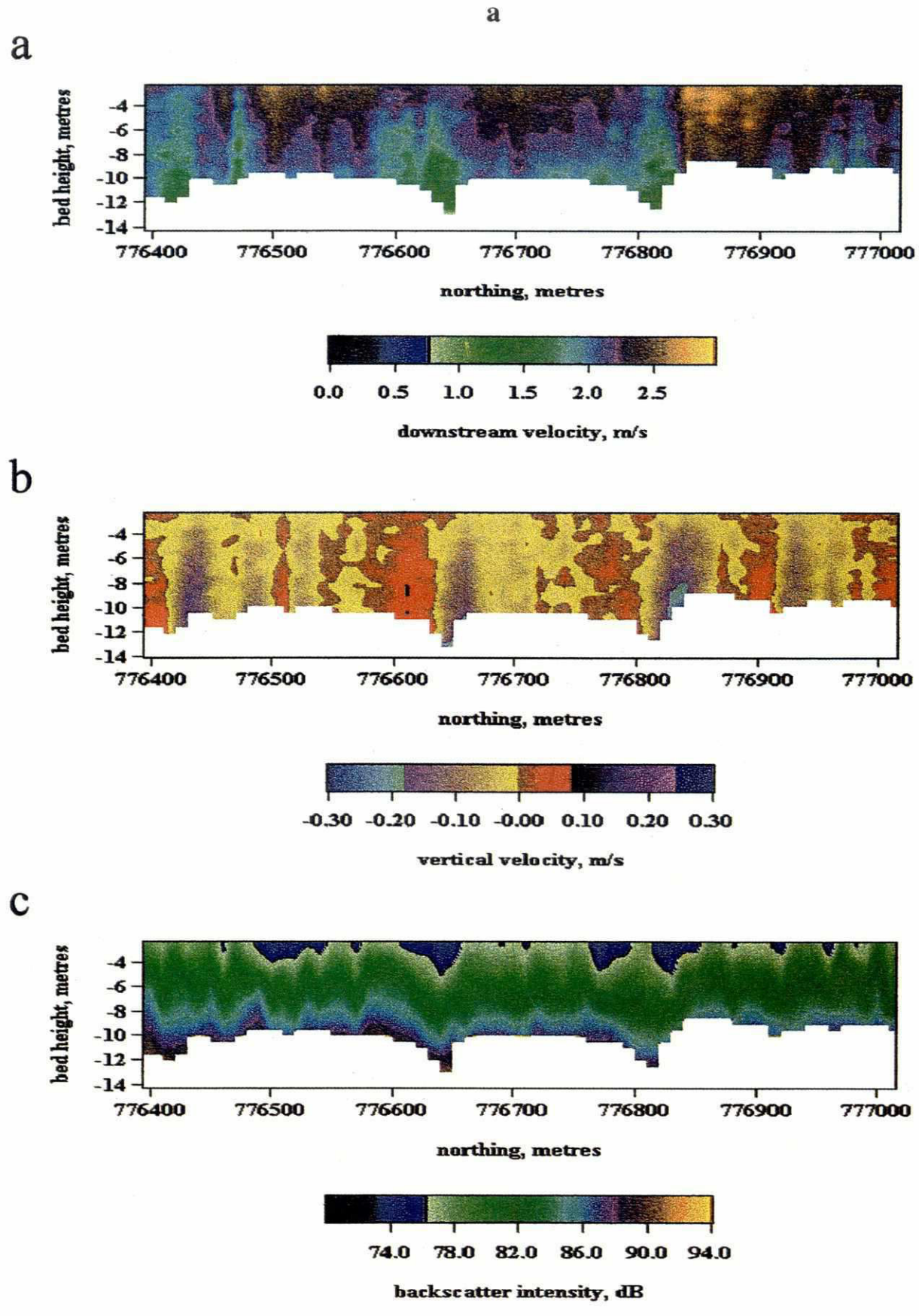

Figure 3.15: Plots of downstream and vertical flow velocities and backscatter intensities over a) steep and b) low-angle leeside dunes at Bahadurabad.

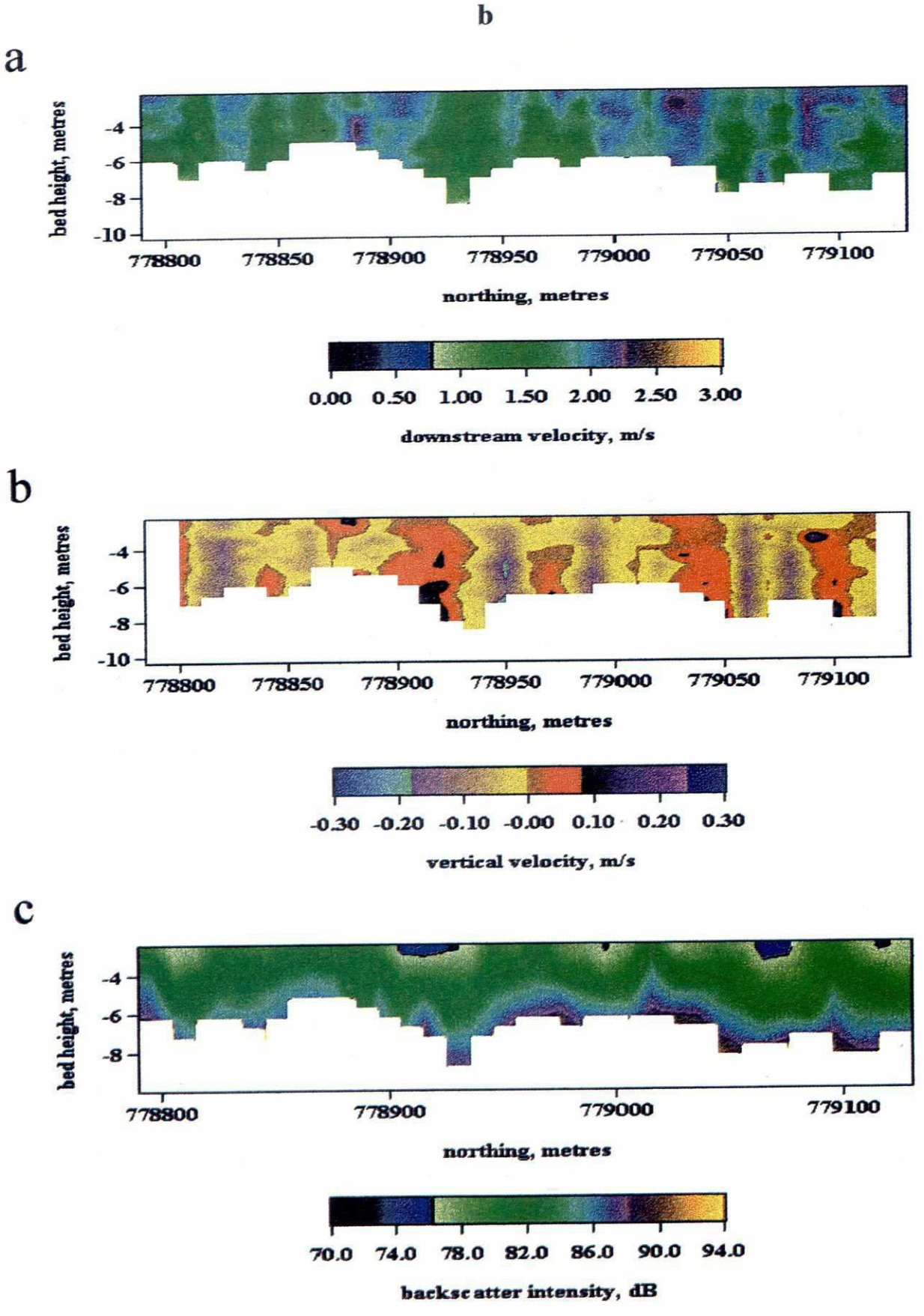

Figure 3.15: Plots of downstream and vertical flow velocities and backscatter intensities over a) steep and b) low-angle leeside dunes at Bahadurabad.

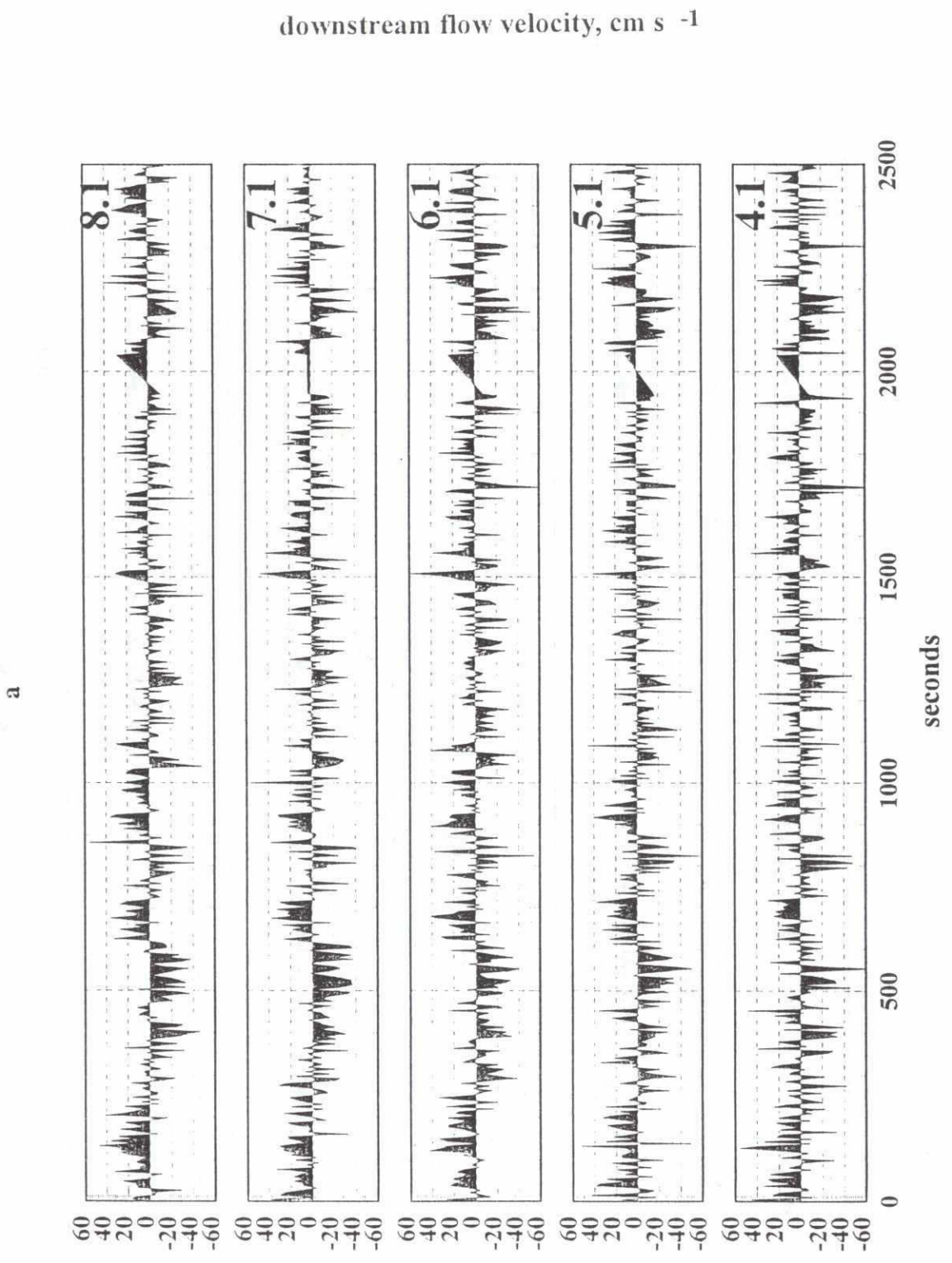

Figure 3.16: At-a-point time series records of (a) downstream and (b) vertical velocities at 5 heights above a dune trough (bold figures denote height above bed in metres). These plots illustrate the occurrence of low downstream velocity upwellings associated with the dune leeside. Both velocities are expressed as deviations from the mean at-a-point temporal average velocity; absolute velocities are shown in Figure 3.15(a).

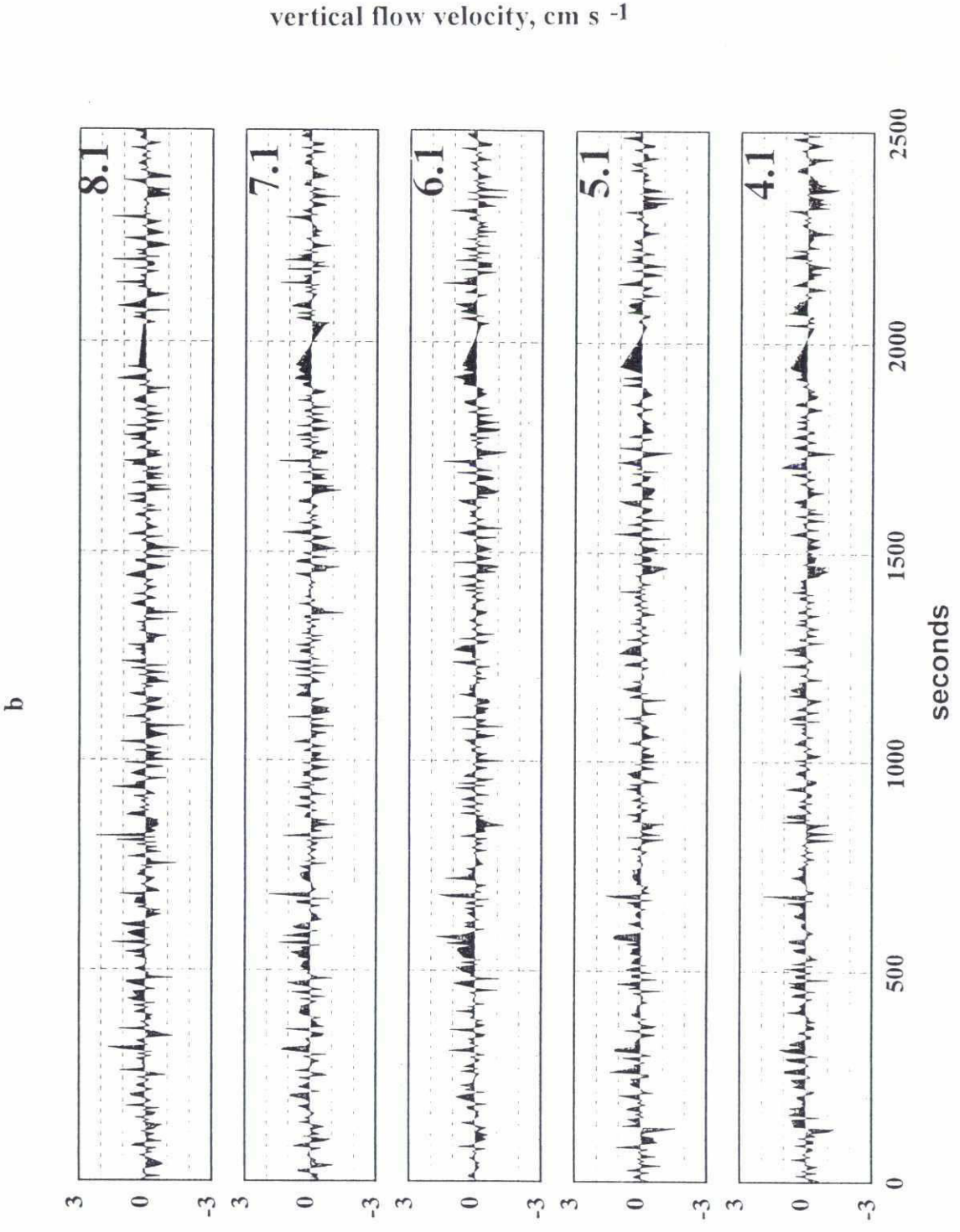

Figure 3.16: At-a-point time series records of (a) downstream and (b) vertical velocities at 5 heights above a dune trough (bold figures denote height above bed in metres). These plots illustrate the occurrence of low downstream velocity upwellings associated with the dune leeside. Both velocities are expressed as deviations from the mean at-a-point temporal average velocity; absolute velocities are shown in Figure 3.15(a).

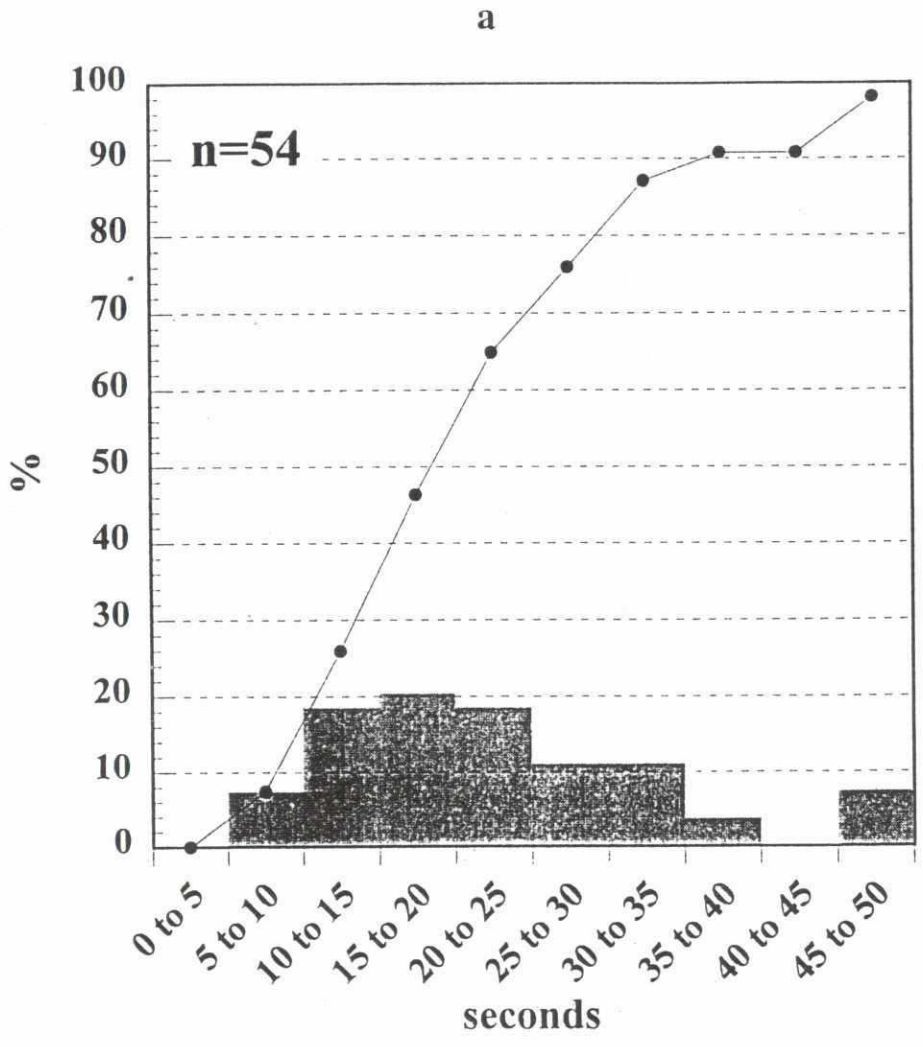

Figure 3.17: Temporal occurrence of 'boils' associated with dunes at Bahadurabad, August 1994 estimated from a) visual records of 'boil' surface upwellings and b) spectral analysis of ADCP downstream and vertical velocity records over a dune crest and trough.

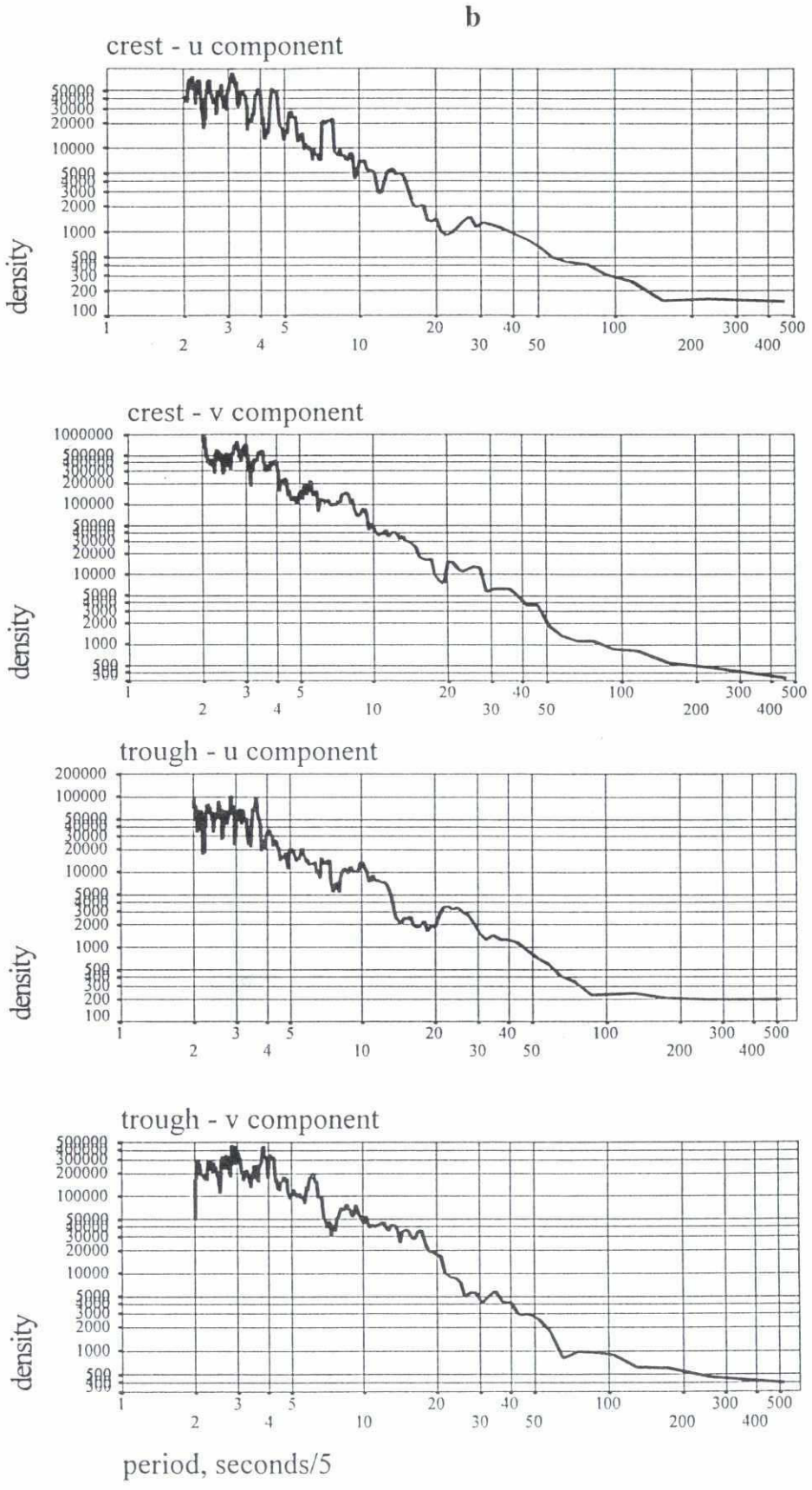

Figure 3.17: Temporal occurrence of 'boils' associated with dunes at Bahadurabad, August 1994 estimated from a) visual records of 'boil' surface upwellings and b) spectral analysis of ADCP downstream and vertical velocity records over a dune crest and trough.

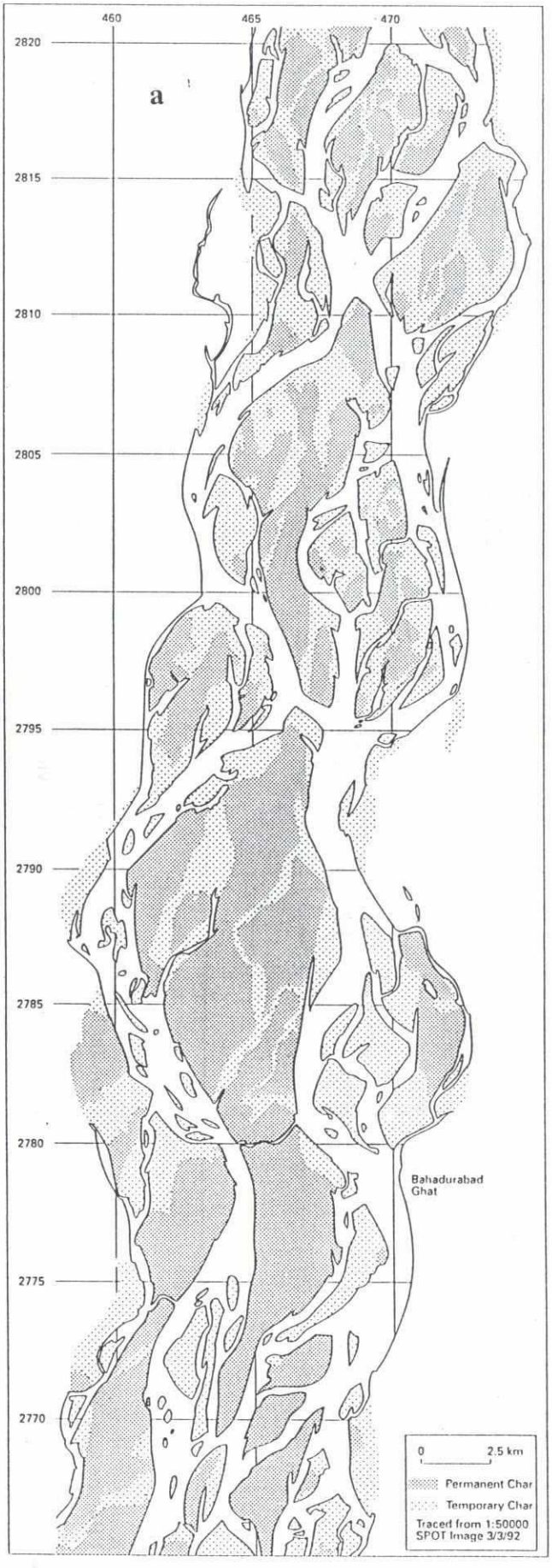

Figure 4.1: Morphology of a 55 km reach of the braided Jamuna River traced from 1:50000 SPOT images G11 and G12 during low flow on (a) 3/3/92, (b) 12/3/93, (c) 3/3/94, and (d) 24/3/95. Coordinates are SPOT. Note the position of the study bar in (d) downstream of a major flow convergence.

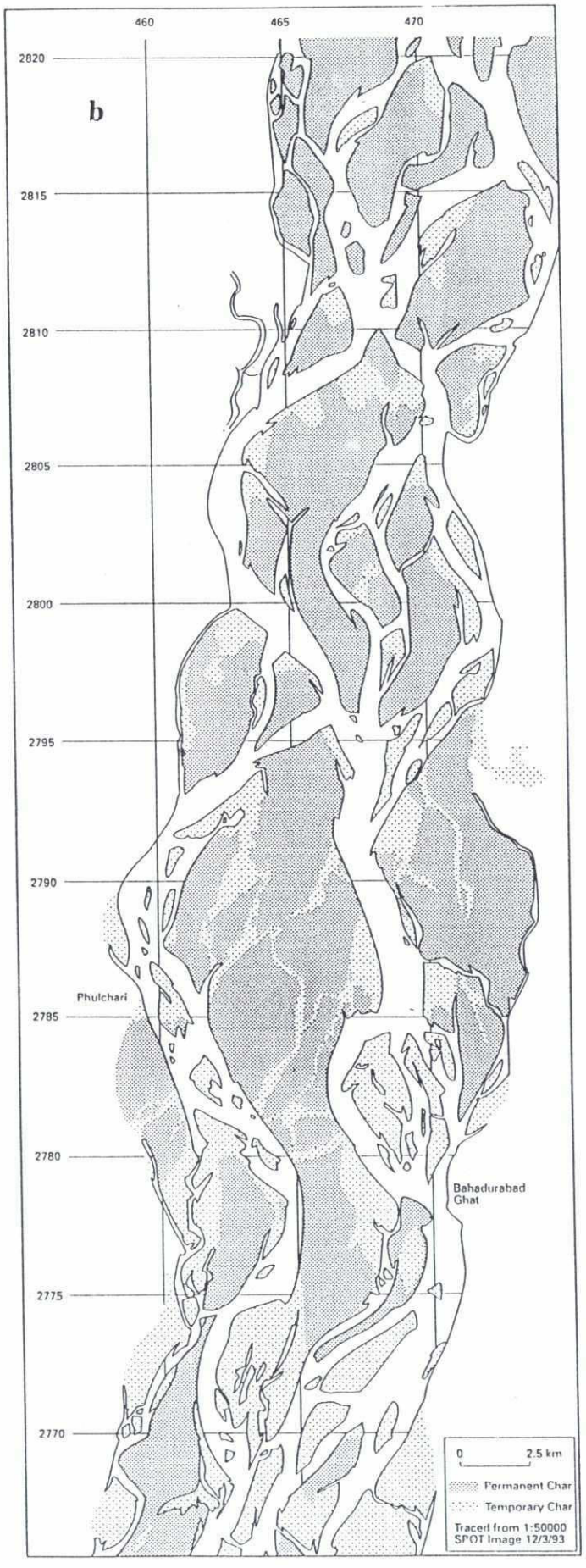

Figure 4.1: Morphology of a 55 km reach of the braided Jamuna River traced from 1:50000 SPOT images G11 and G12 during low flow on (a) 3/3/92, (b) 12/3/93, (c) 3/3/94, and (d) 24/3/95. Coordinates are SPOT. Note the position of the study bar in (d) downstream of a major flow convergence.

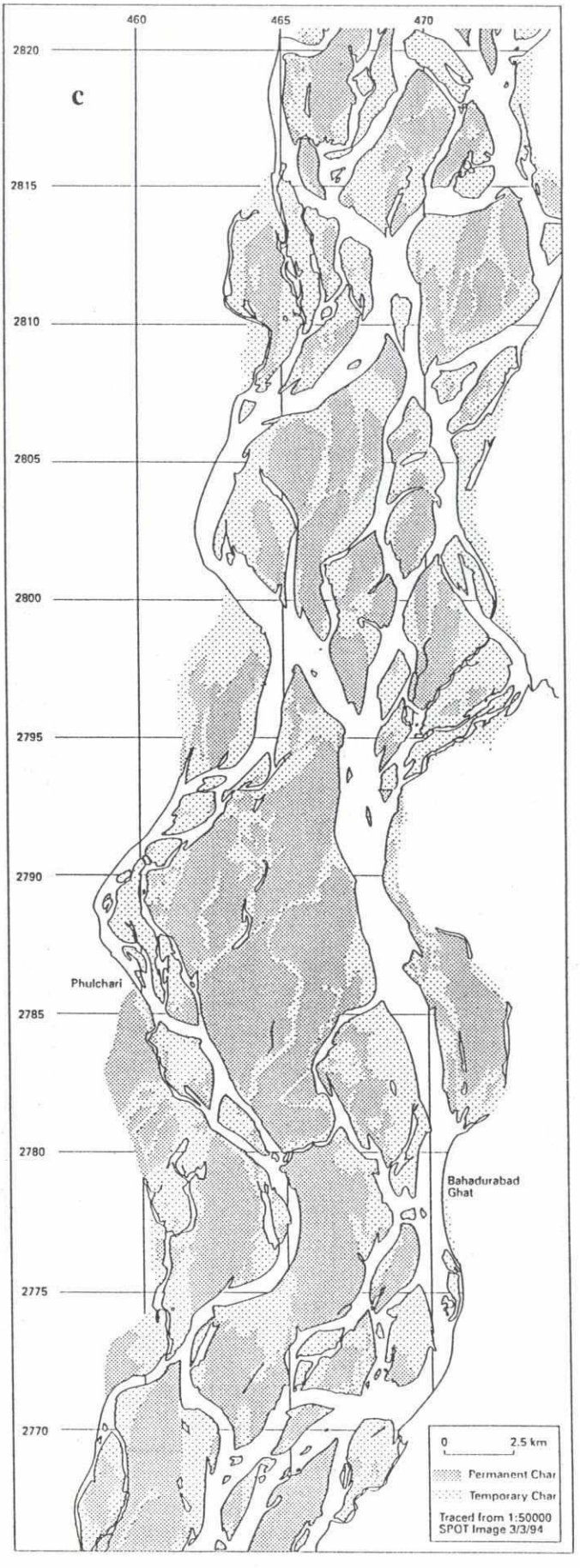

Figure 4.1: Morphology of a 55 km reach of the braided Jamuna River traced from 1:50000 SPOT images G11 and G12 during low flow on (a) 3/3/92, (b) 12/3/93, (c) 3/3/94, and (d) 24/3/95. Coordinates are SPOT. Note the position of the study bar in (d) downstream of a major flow convergence.

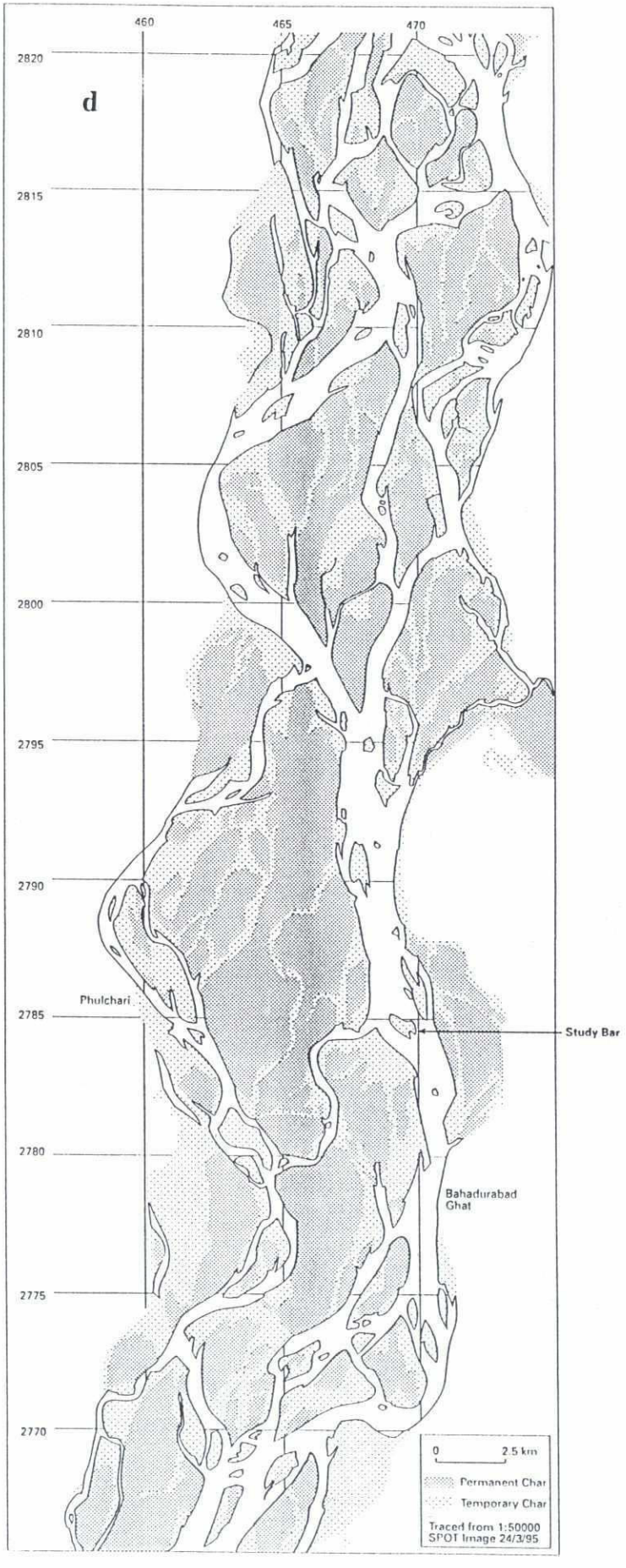

Figure 4.1: Morphology of a 55 km reach of the braided Jamuna River traced from 1:50000 SPOT images G11 and G12 during low flow on (a) 3/3/92, (b) 12/3/93, (c) 3/3/94, and (d) 24/3/95. Coordinates are SPOT. Note the position of the study bar in (d) downstream of a major flow convergence.

a

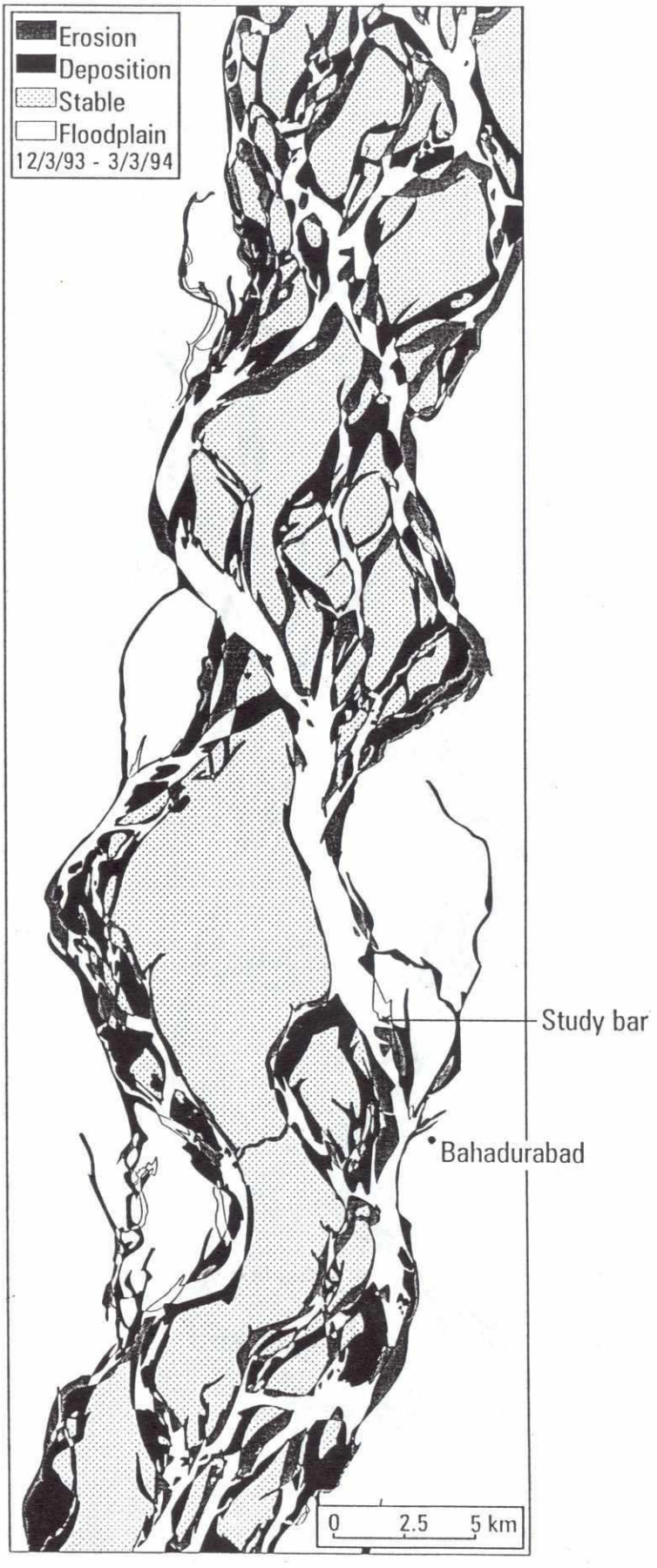

Figure 4.2: (a) Channel change and bar migration from 12/3/93-3/3/94. Bar positions are traced from G11 and G12 1:50000 SPOT images.

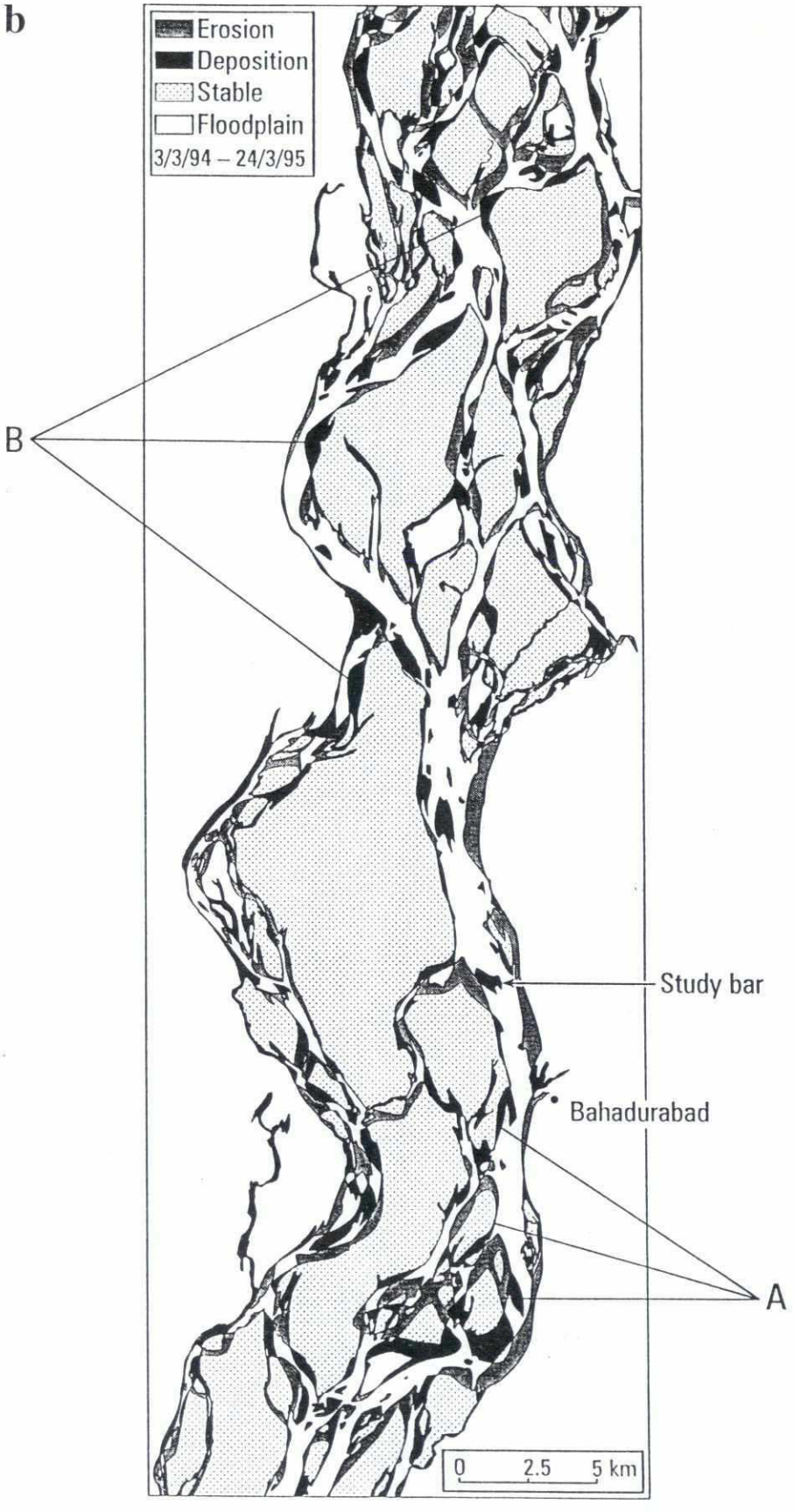

Figure 4.2: (b) Channel change and bar migration from 3/3/94-24/3/95. Bar positions are traced from G11 and G12 1:50000 SPOT images. The bars labelled A show the characteristic barhead erosion and bartail deposition, the bars labelled B migrate upstream by accretion of secondary lobes onto the barhead and margin.

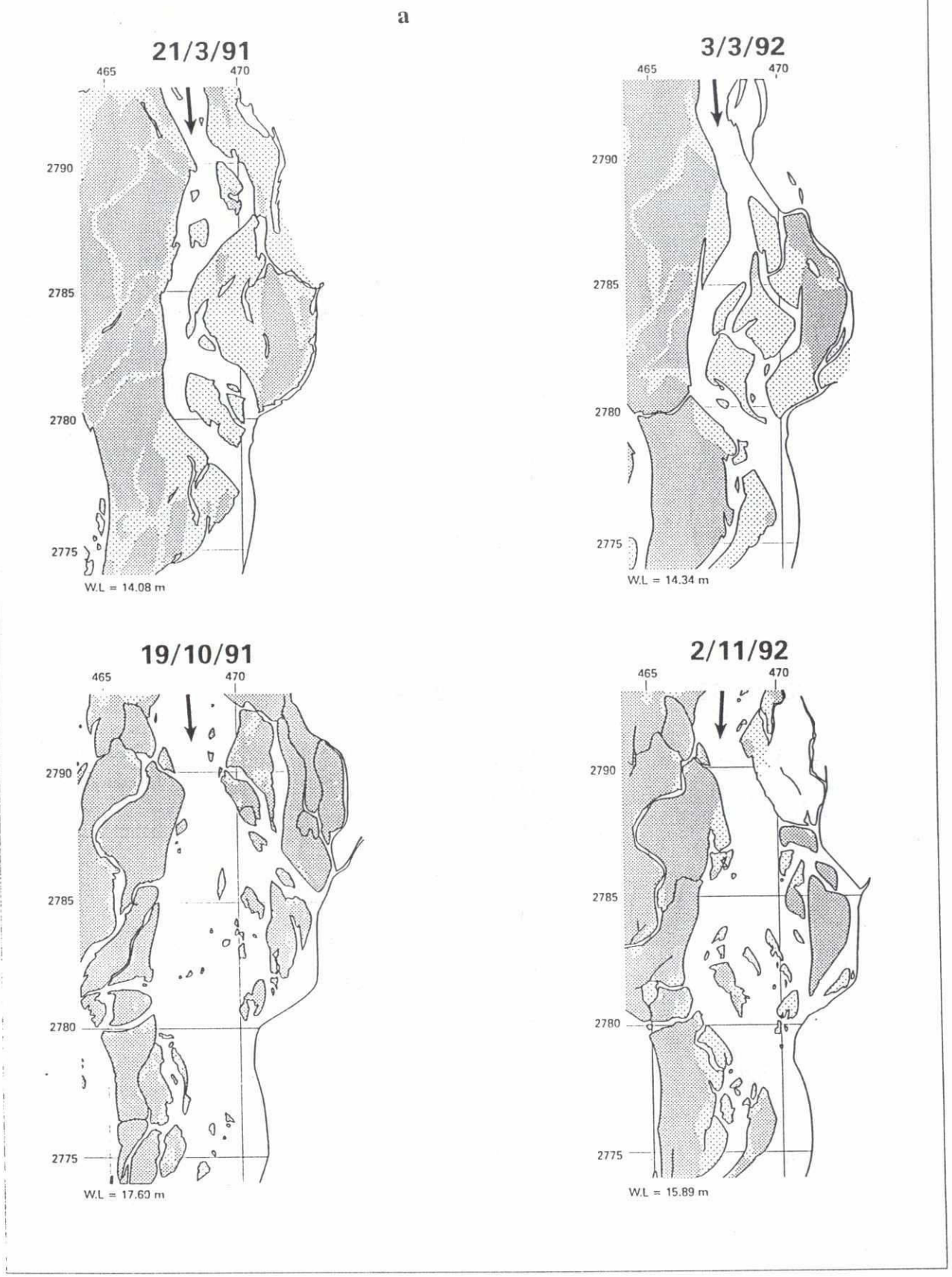

Figure 4.3: (a) and (b) Bar morphology and channel change in the study area north of Bahadurabad ghat from March 1991-March 1995. Diagrams are traced from biannual 1:50000 SPOT images approximately coinciding with low and high flow in the monsoon hydrograph (see Figure 2.1c). The mean water level at the time of satellite imagery is shown. Coordinates are SPOT.

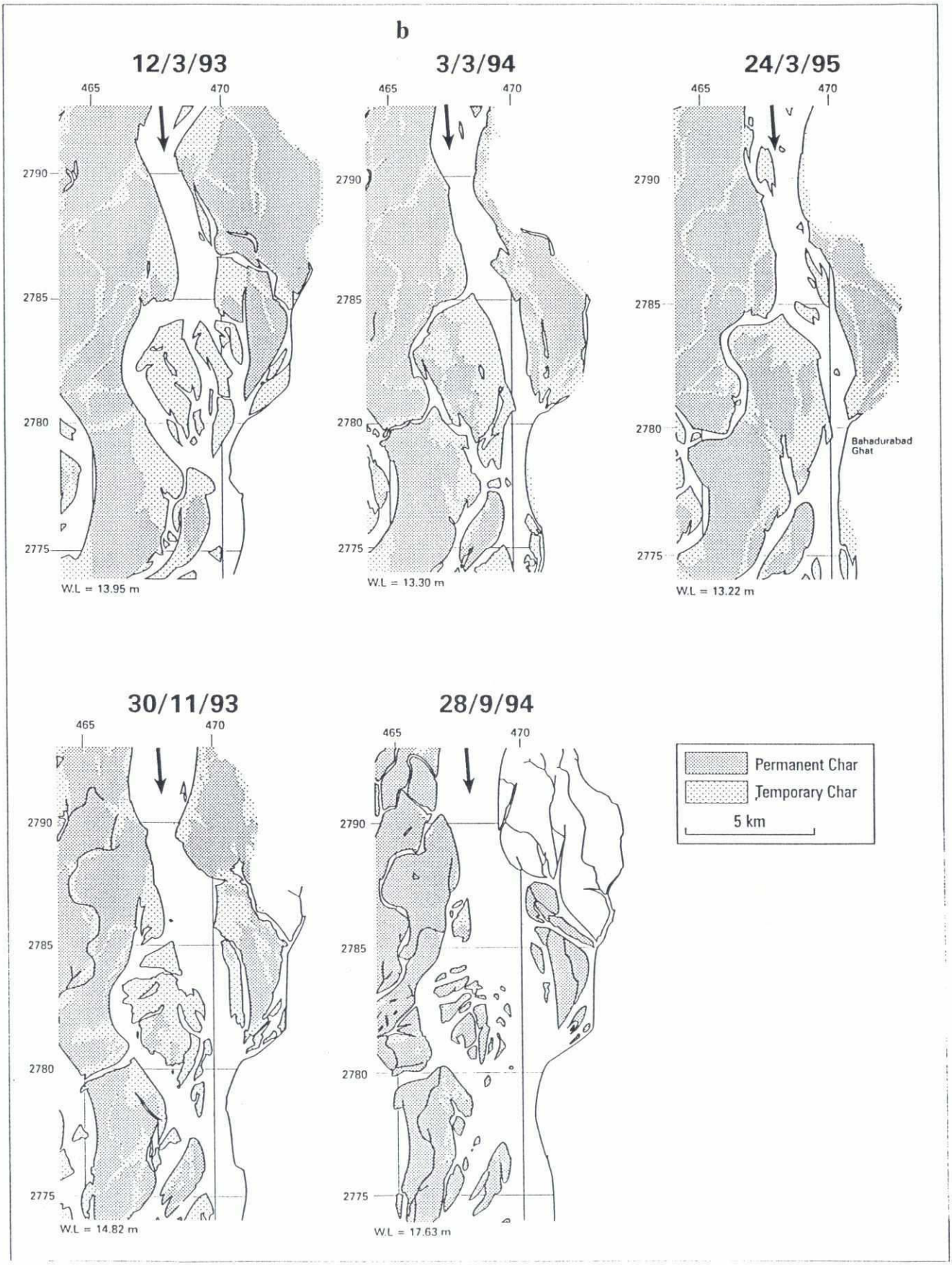

Figure 4.3: (a) and (b) Bar morphology and channel change in the study area north of Bahadurabad ghat from March 1991-March 1995. Diagrams are traced from biannual 1:50000 SPOT images approximately coinciding with low and high flow in the monsoon hydrograph (see Figure 2.1c). The mean water level at the time of satellite imagery is shown. Coordinates are SPOT.

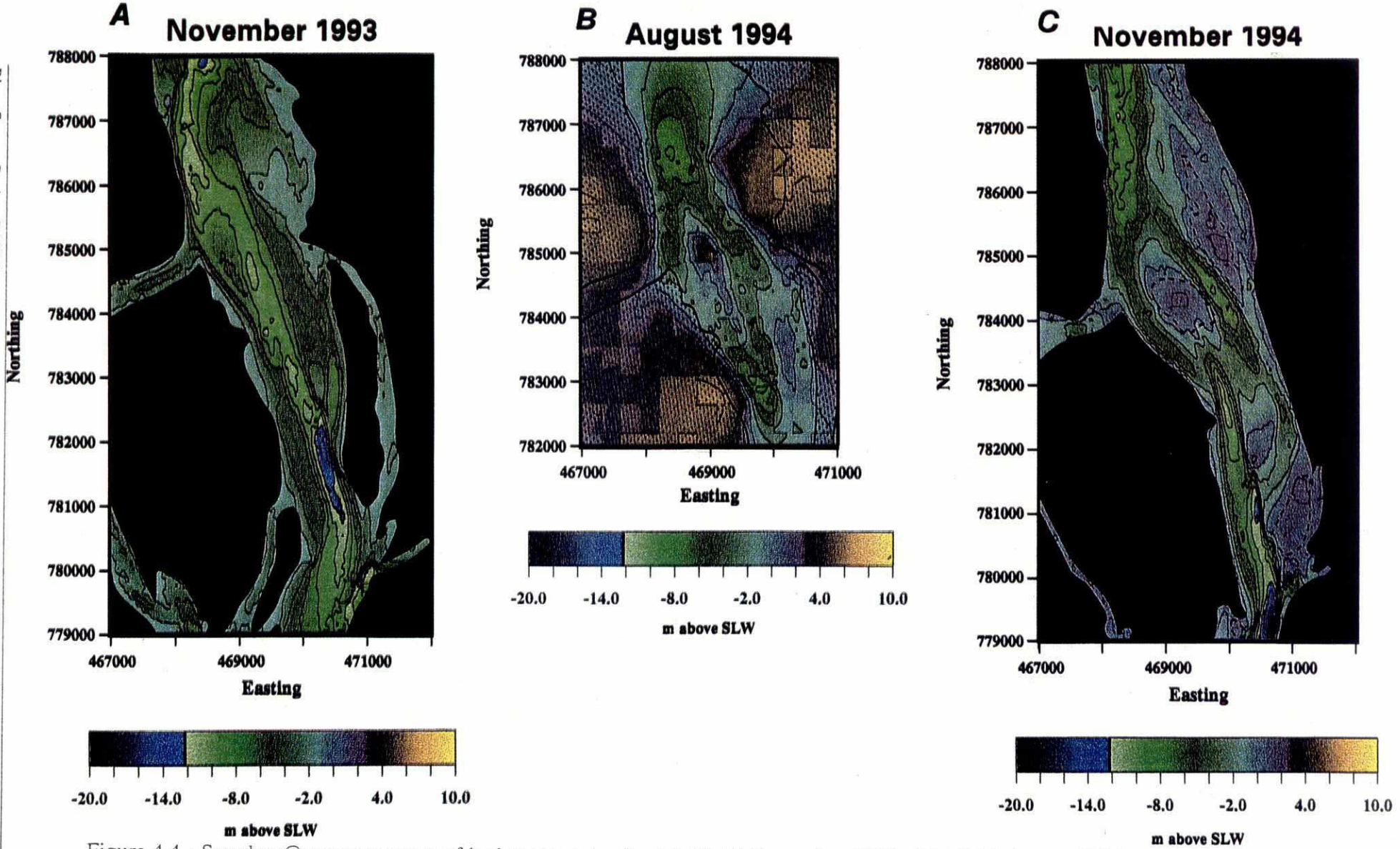

Figure 4.4 : Spyglass@ contour maps of bed topography for (a) 10-18 November 1993, (b) 10-14 August 1994, (c) 1-10 November 1994, (d) 7-8, 13 March 1995, (e) 25-26 June 1995, (f) 31 July/1 August 1995, (g) 12-16 September 1995, (h) 11-25 November 1995, (i) X-X March 1996. The area of bed survey is different for special and bathymetric surveys (see Table 2.2) but all the figures are plotted at the same scale. All heights are reduced to SLW to enable comparison between dates. The position of the water edge for each bathymetric survey period is digitised from the bed contour at the relevant SLW level (emergent bar shown as black). These water edges are also used to define the approximate water margin for special surveys (emergent bar highlighted with dotted fill). The land survey over the study bar in February 1996 is incomplete so the bartop contours are unrealistically low.

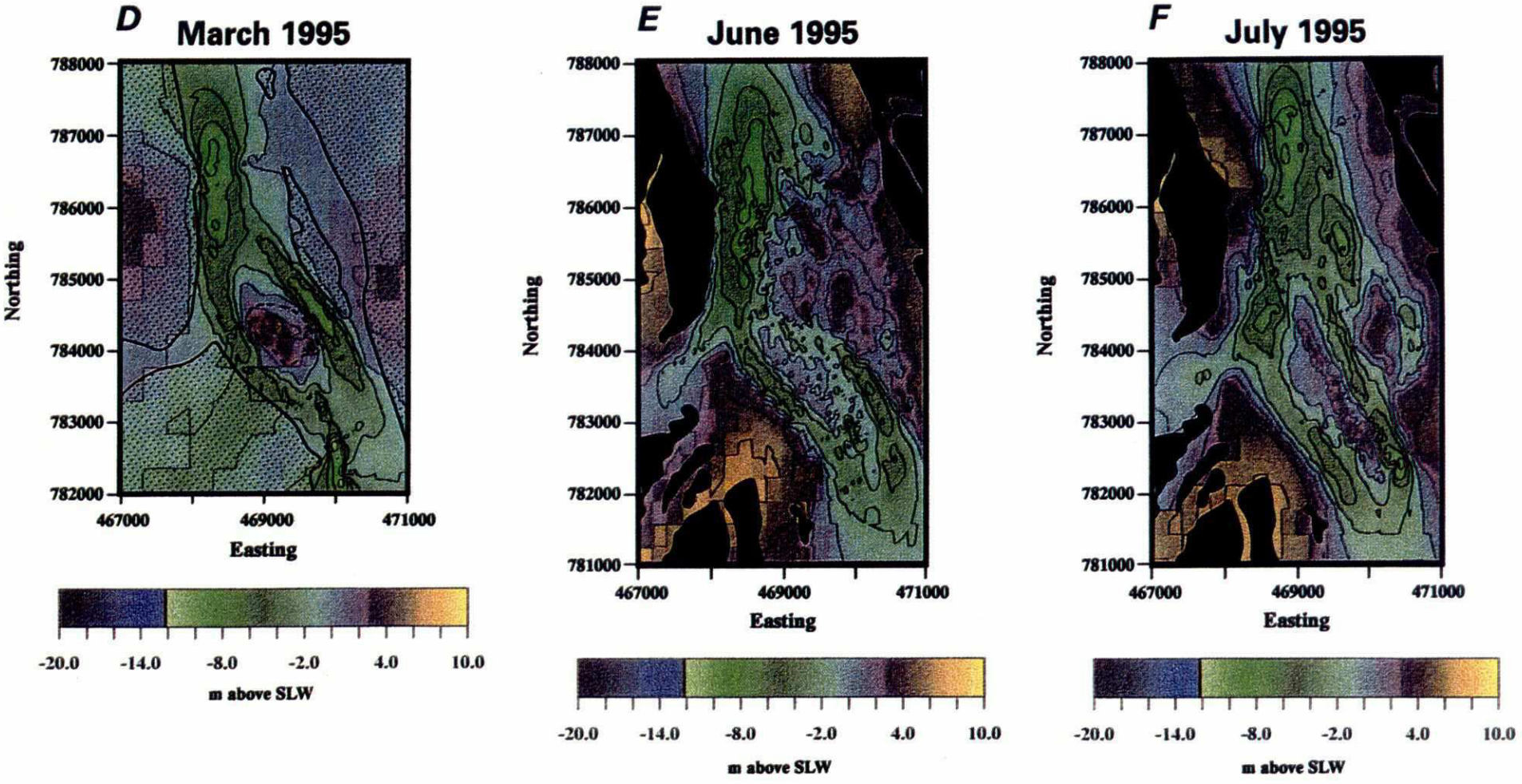

Figure 4.4 : Spyglass@ contour maps of bed topography for (a) 10-18 November 1993, (b) 10-14 August 1994, (c) 1-10 November 1994, (d) 7-8, 13 March 1995, (e) 25-26 June 1995, (f) 31 July/1 August 1995, (g) 12-16 September 1995, (h) 11-25 November 1995, (i) X-X March 1996. The area of bed survey is different for special and bathymetric surveys (see Table 2.2) but all the figures are plotted at the same scale. All heights are reduced to SLW to enable comparison between dates. The position of the water edge for each bathymetric survey period is digitised from the bed contour at the relevant SLW level (emergent bar shown as black). These water edges are also used to define the approximate water margin for special surveys (emergent bar highlighted with dotted fill). The land survey over the study bar in February 1996 is incomplete so the bartop contours are unrealistically low.

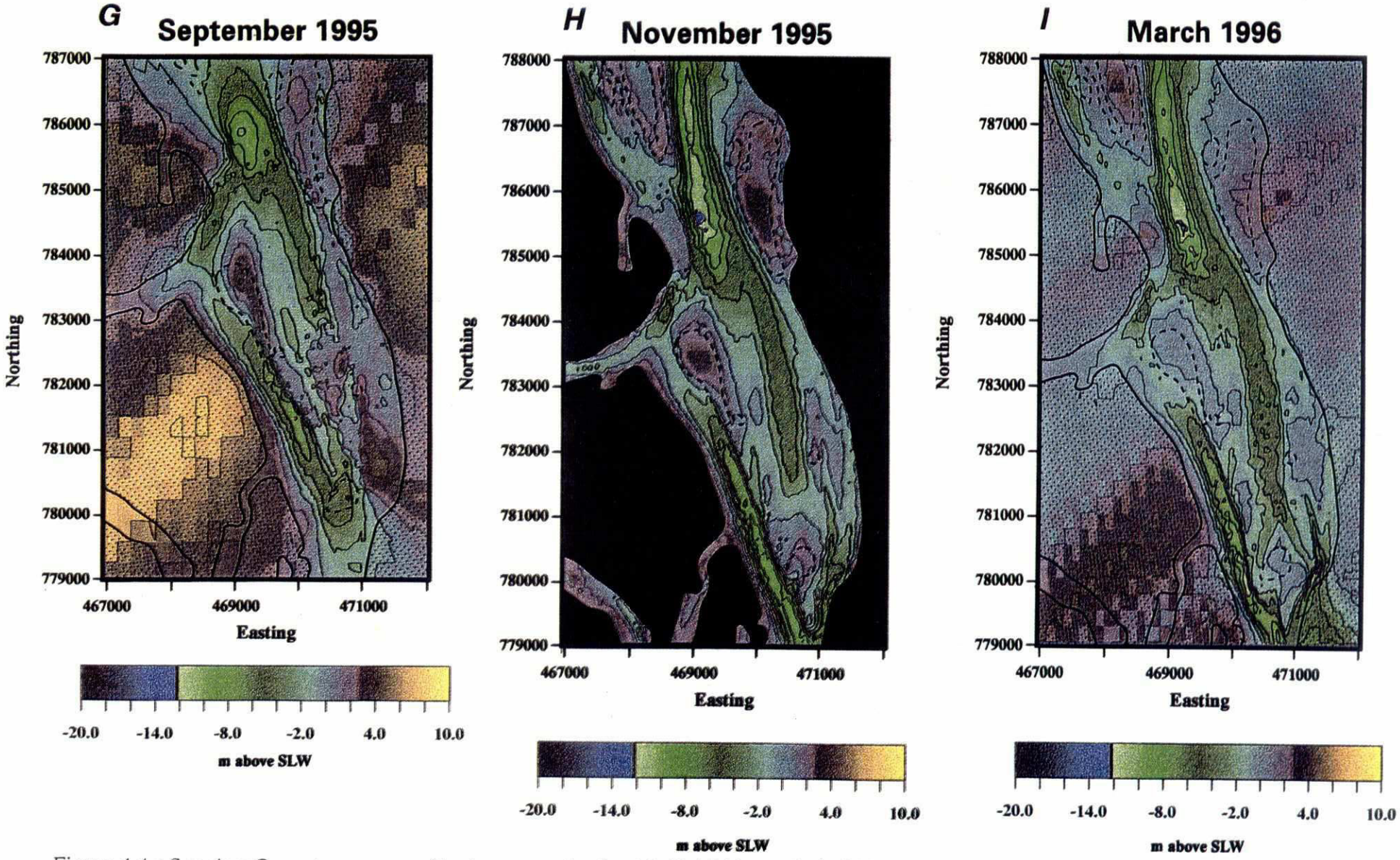

Figure 4.4 : Spyglass@ contour maps of bed topography for (a) 10-18 November 1993, (b) 10-14 August 1994, (c) 1-10 November 1994, (d) 7-8, 13 March 1995, (e) 25-26 June 1995, (f) 31 July/1 August 1995, (g) 12-16 September 1995, (h) 11-25 November 1995, (i) X-X March 1996. The area of bed survey is different for special and bathymetric surveys (see Table 2.2) but all the figures are plotted at the same scale. All heights are reduced to SLW to enable comparison between dates. The position of the water edge for each bathymetric survey period is digitised from the bed contour at the relevant SLW level (emergent bar shown as black). These water edges are also used to define the approximate water margin for special surveys (emergent bar highlighted with dotted fill). The land survey over the study bar in February 1996 is incomplete so the bartop contours are unrealistically low.

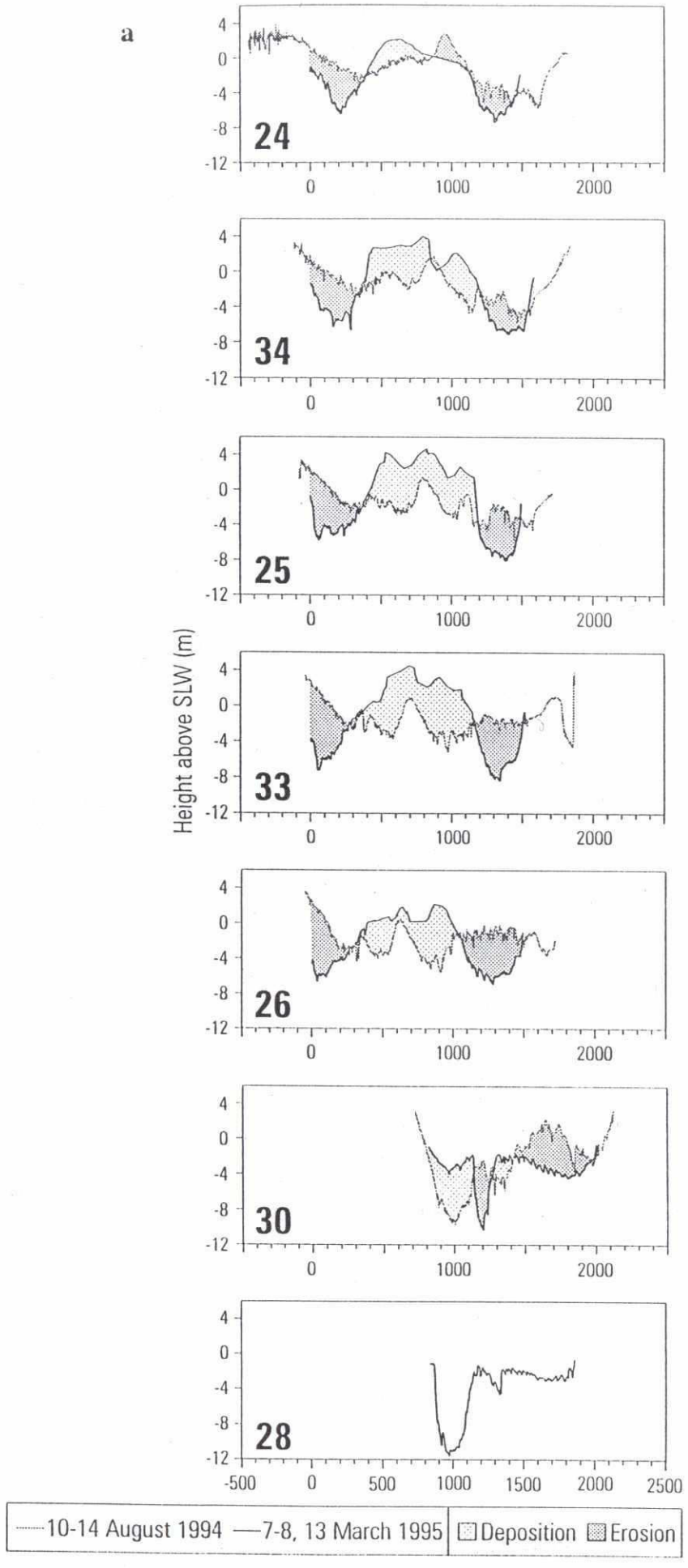

Figure 4.5: Superimposed cross-sections for the five bar transects (BT5X024, 34, 25, 33, and 26) and BT5X030 and 28. 750 and 1250 m downstream of BT5X026 respectively (see Figure 2.1b). The periods of special survey are (a) 10-14 August 1994→7-8, 13 March 1995, (b) 7-8, 13 March 1995→25-26 June 1995, (c) 25-26 June 1995→31 July/1 August 1995, (d) 31 July/1 August 1995→12-16 September 1995, and (e) 12-16 September 1995→24-26 February 1996. The area of each block of erosion and deposition is given in Table 4.2 later. Note that the February 1996 land survey is incomplete.

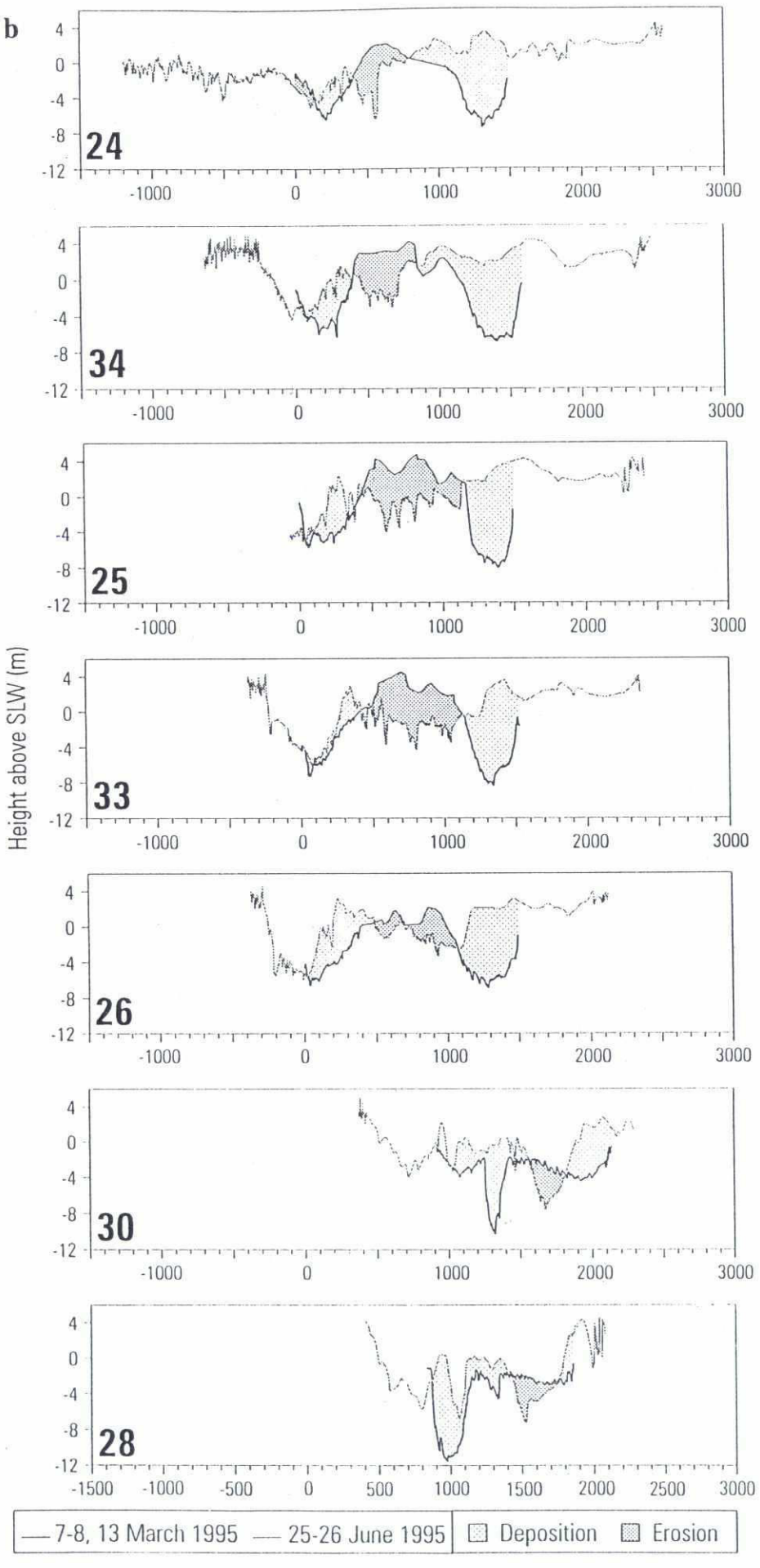

Figure 4.5: Superimposed cross-sections for the five bar transects (BT5X024, 34, 25, 33, and 26) and BT5X030 and 28, 750 and 1250 m downstream of BT5X026 respectively (see Figure 2.1b). The periods of special survey are (a) 10-14 August 1994→7-8, 13 March 1995, (b) 7-8, 13 March 1995→25-26 June 1995, (c) 25-26 June 1995→31 July/1 August 1995, (d) 31 July/1 August 1995→12-16 September 1995, and (e) 12-16 September 1995→24-26 February 1996. The area of each block of erosion and deposition is given in Table 4.2 later. Note that the February 1996 land survey is incomplete.

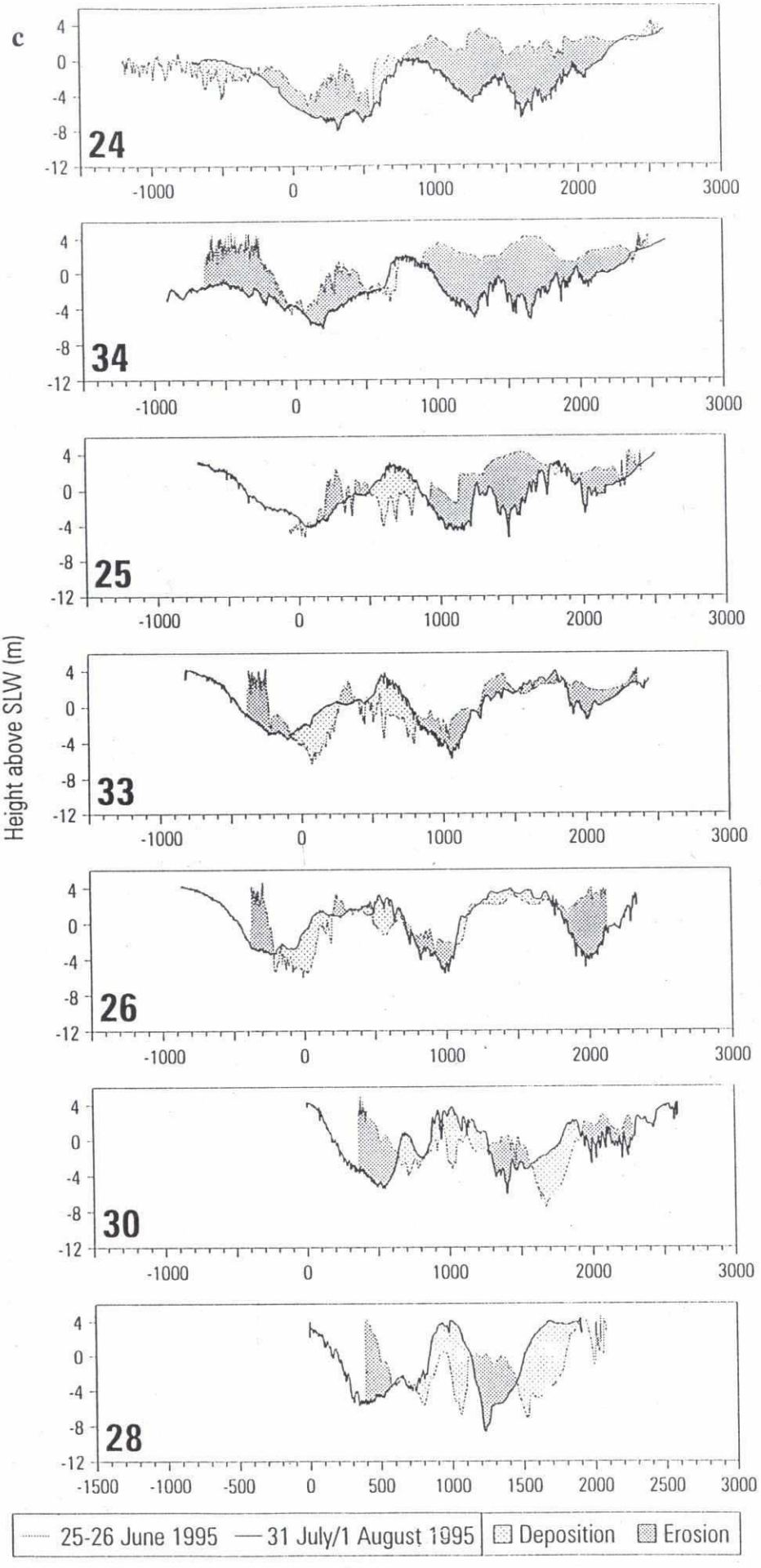

Figure 4.5: Superimposed cross-sections for the five bar transects (BT5X024, 34, 25, 33, and 26) and BT5X030 and 28, 750 and 1250 m downstream of BT5X026 respectively (see Figure 2.1b). The periods of special survey are (a) 10-14 August 1994→7-8, 13 March 1995, (b) 7-8, 13 March 1995→25-26 June 1995, (c) 25-26 June 1995→31 July/1 August 1995, (d) 31 July/1 August 1995→12-16 September 1995, and (e) 12-16 September 1995→24-26 February 1996. The area of each block of erosion and deposition is given in Table 4.2 later. Note that the February 1996 land survey is incomplete.

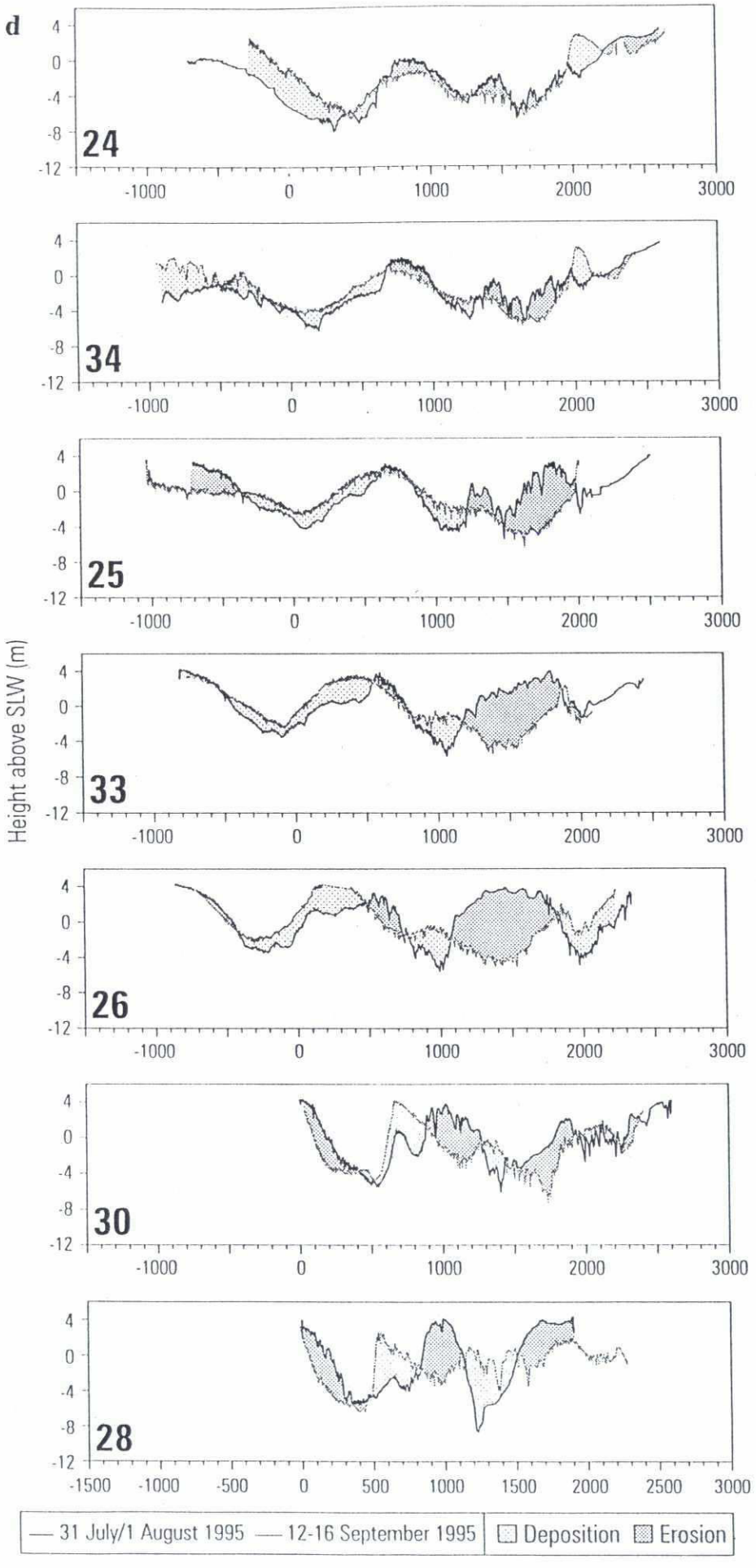

Figure 4.5: Superimposed cross-sections for the five bar transects (BT5X024, 34, 25, 33, and 26) and BT5X030 and 28, 750 and 1250 m downstream of BT5X026 respectively (see Figure 2.1b). The periods of special survey are (a) 10-14 August 1994→7-8, 13 March 1995, (b) 7-8, 13 March 1995→25-26 June 1995, (c) 25-26 June 1995→31 July/1 August 1995, (d) 31 July/1 August 1995→12-16 September 1995, and (e) 12-16 September 1995→24-26 February 1996. The area of each block of erosion and deposition is given in Table 4.2 later. Note that the February 1996 land survey is incomplete.

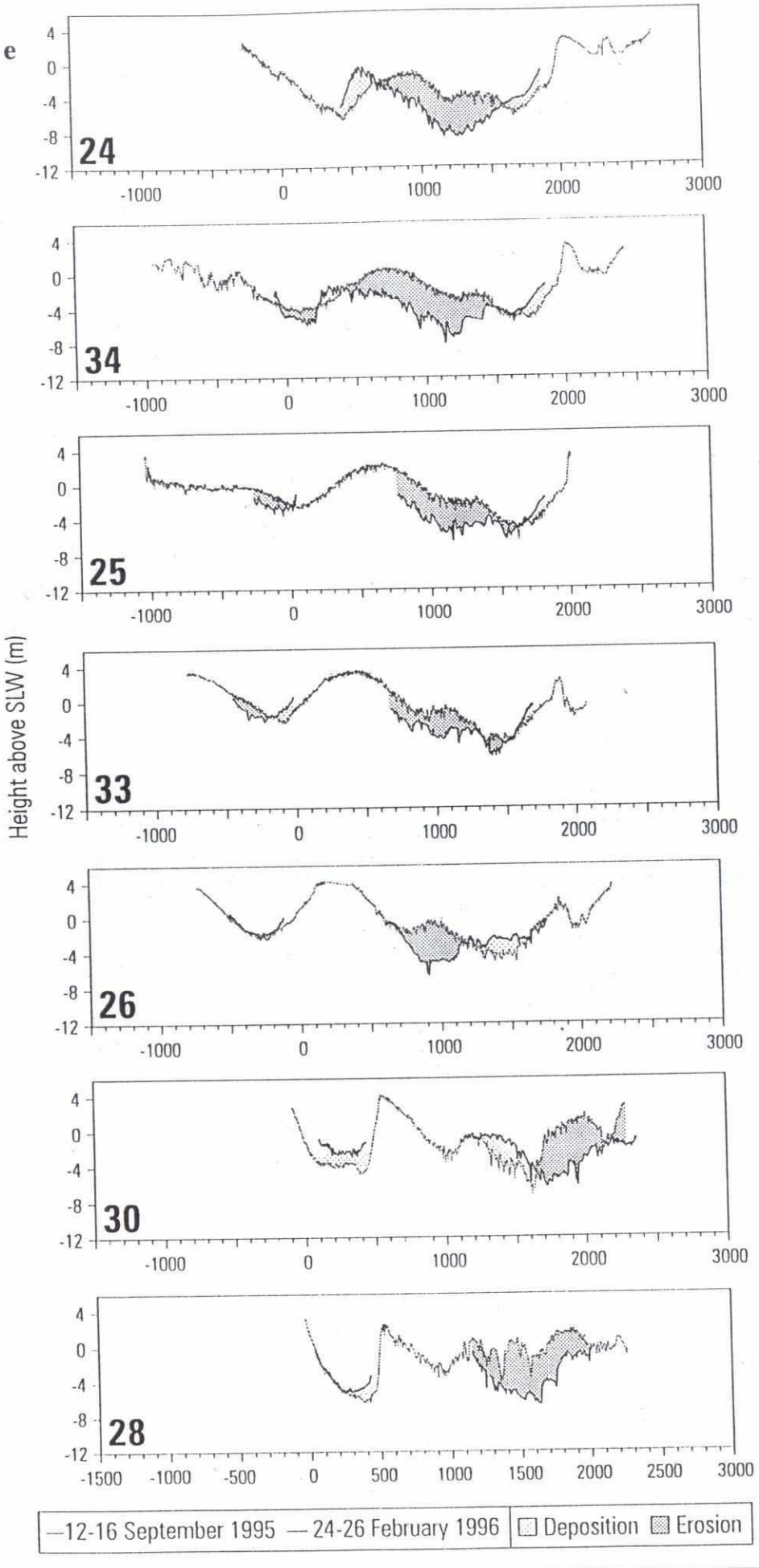

Figure 4.5: Superimposed cross-sections for the five bar transects (BT5X024, 34, 25, 33, and 26) and BT5X030 and 28, 750 and 1250 m downstream of BT5X026 respectively (see Figure 2.1b). The periods of special survey are (a) 10-14 August 1994→7-8, 13 March 1995, (b) 7-8, 13 March 1995→25-26 June 1995, (c) 25-26 June 1995→31 July/1 August 1995, (d) 31 July/1 August 1995→12-16 September 1995, and (e) 12-16 September 1995→24-26 February 1996. The area of each block of erosion and deposition is given in Table 4.2 later. Note that the February 1996 land survey is incomplete.

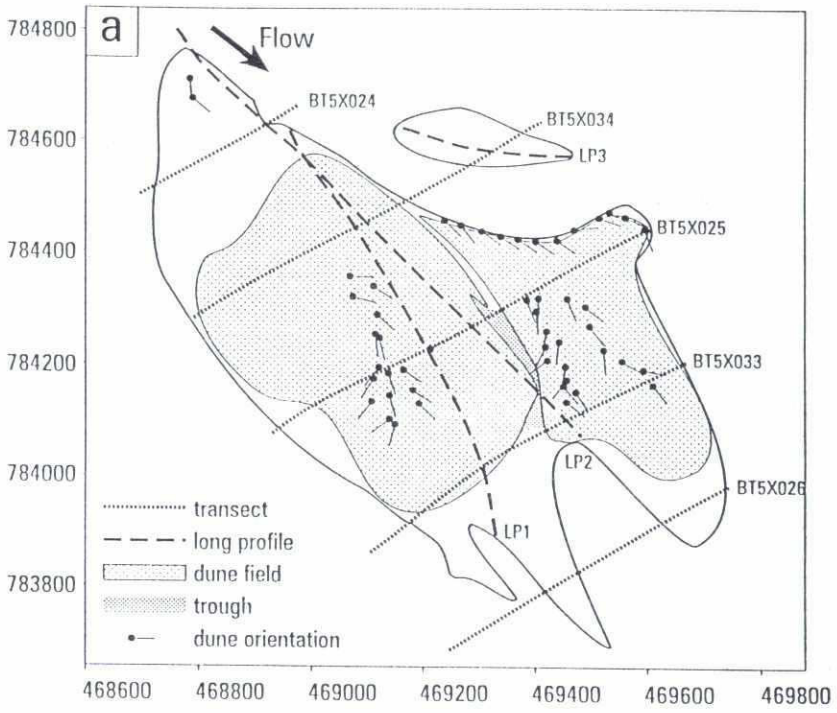

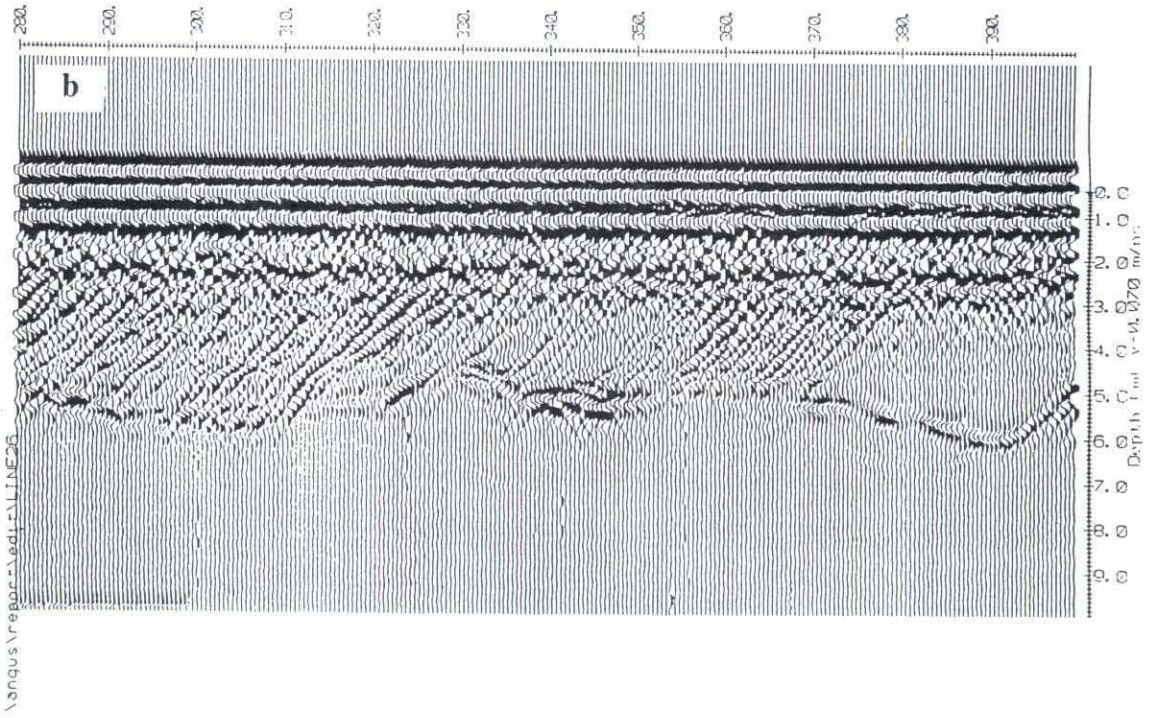

Figure 4.6: (a) Planform morphology of the emergent study bar as land surveyed in March 1995. The two dunes fields terminate in a 3 m high, steep, accretionary front (see text). Measurements of dune orientation indicate the flow was strongly divergent over the bartop. (b) 100MHz ground penetrating radar trace for transect BT5X026. The trace is west to east (left to right) with the lateral distance from the water edge shown on the top scale (280-400 m). The trace shows steeply dipping (note the vertical exaggeration), bar slip faces, prograding east to west, superimposed by a 1 m layer of low-amplitude dunes. An impermeable layer (strong radar reflectance) at 330 m cross-stream and 5-6 m depth, represents the 'old' bartail area where a substantial quantity of fine-grained sedimentation occurred (see text and Figure 4.6a).

A BT5X023

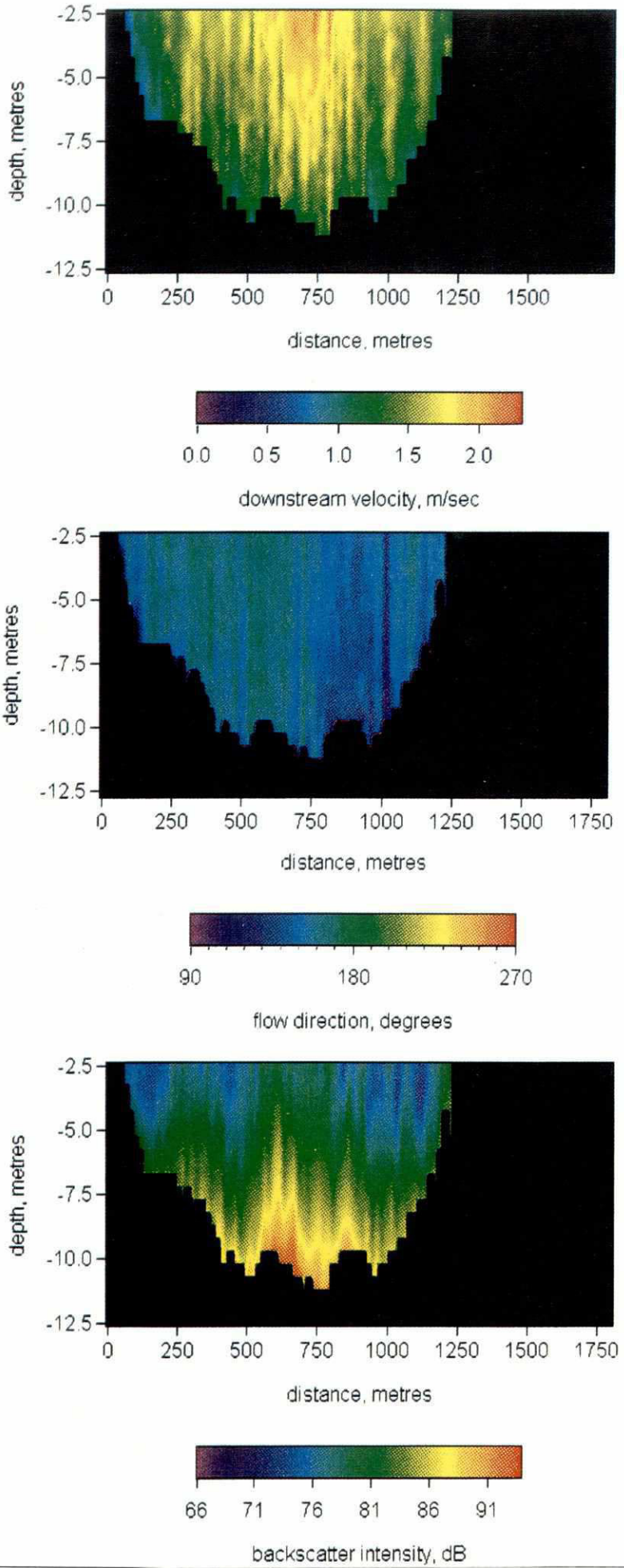

Figure 4.7: Spyglass® contoured ADCP records of the resolved (*U-W*) downstream velocity and direction and backscatter intensity for transects (a) BT5X023, (b) BT5X036, (c) BT5X021, (d) BT5X034 (see text and Figure 2.1b) taken on 11-12 August 1994. Flow directions must be considered relative to the bearing of the bar's long-axis which is 148°.

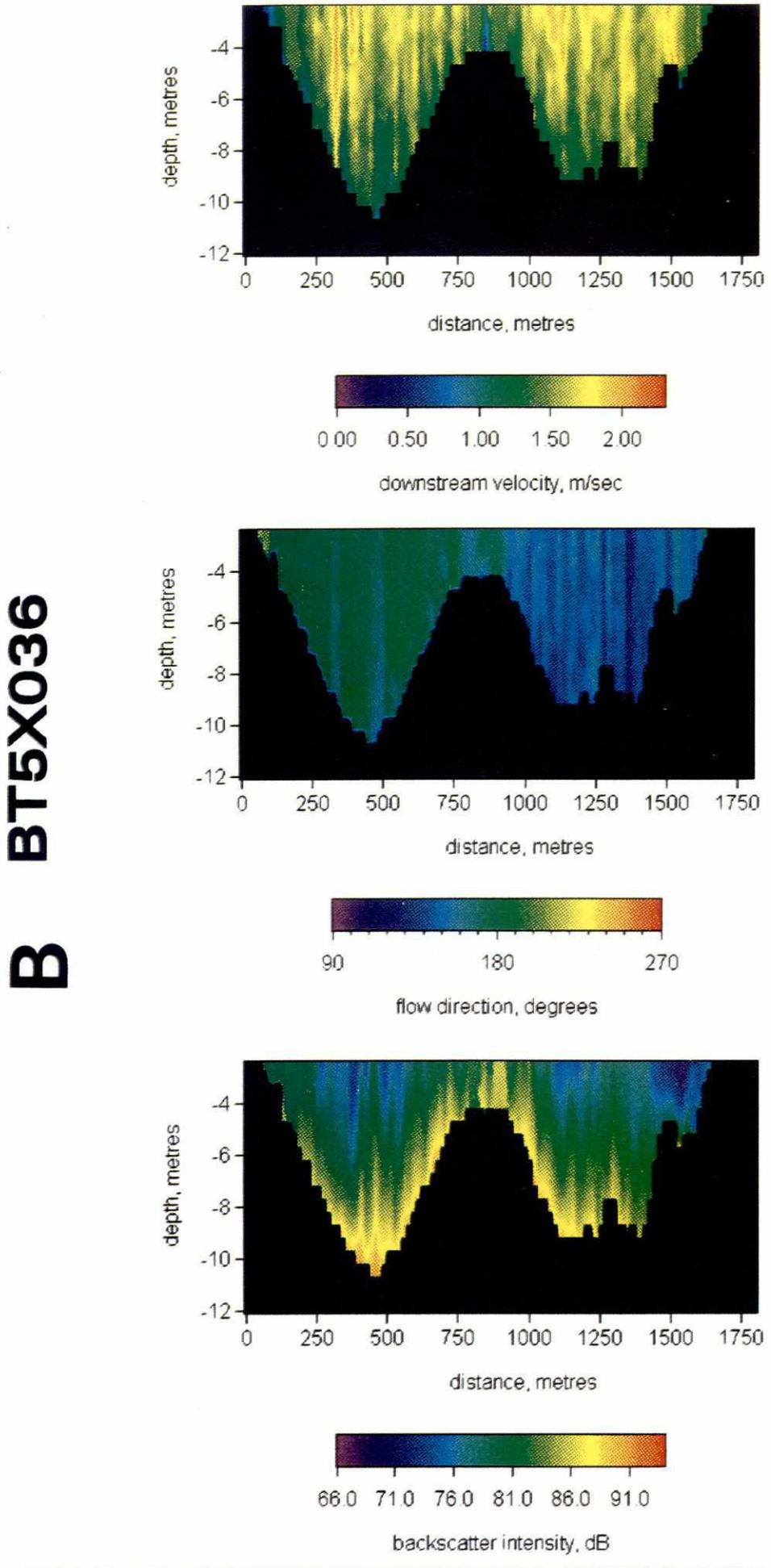

Figure 4.7: Spyglass® contoured ADCP records of the resolved (*U-W*) downstream velocity and direction and backscatter intensity for transects (a) BT5X023, (b) BT5X036, (c) BT5X021, (d) BT5X034 (see text and Figure 2.1b) taken on 11-12 August 1994. Flow directions must be considered relative to the bearing of the bar's long-axis which is 148°.

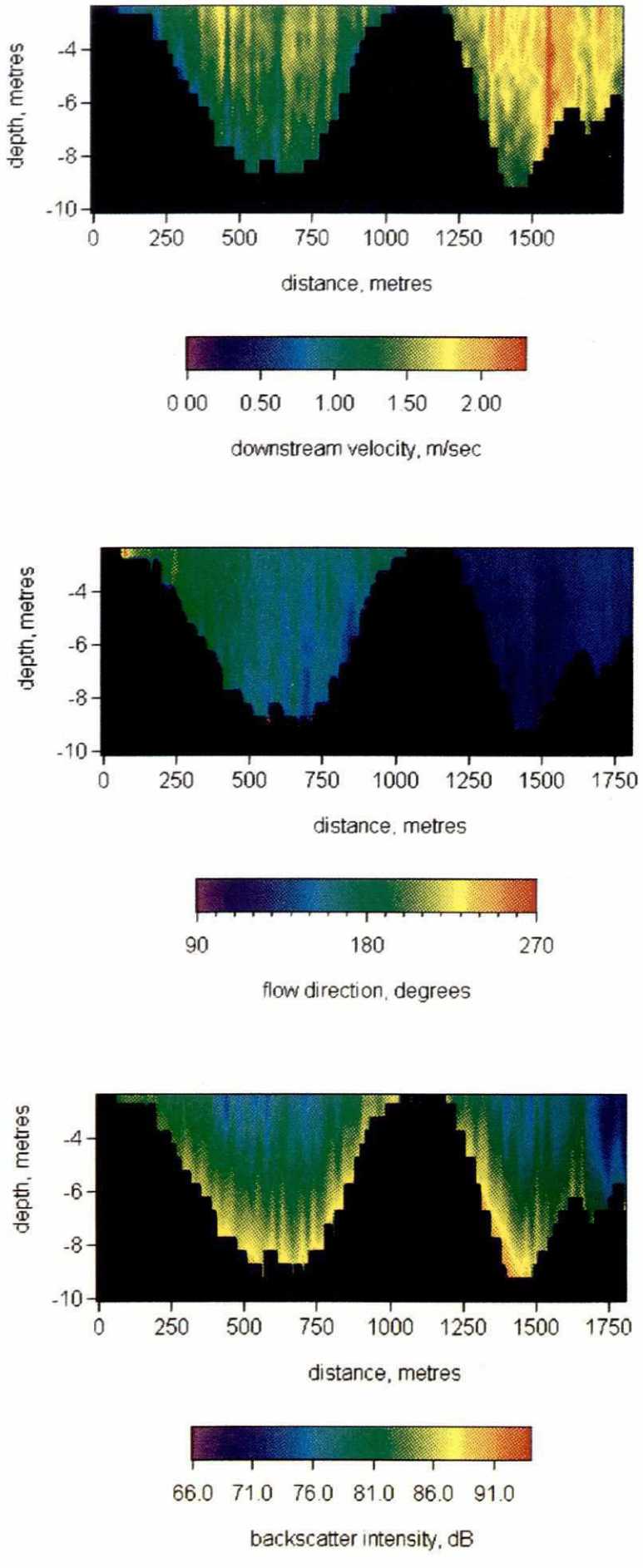

Figure 4.7: Spyglass® contoured ADCP records of the resolved (*U-W*) downstream velocity and direction and backscatter intensity for transects (a) BT5X023, (b) BT5X036, (c) BT5X021, (d) BT5X034 (see text and Figure 2.1b) taken on 11-12 August 1994. Flow directions must be considered relative to the bearing of the bar's long-axis which is 148°.

D BT5X034

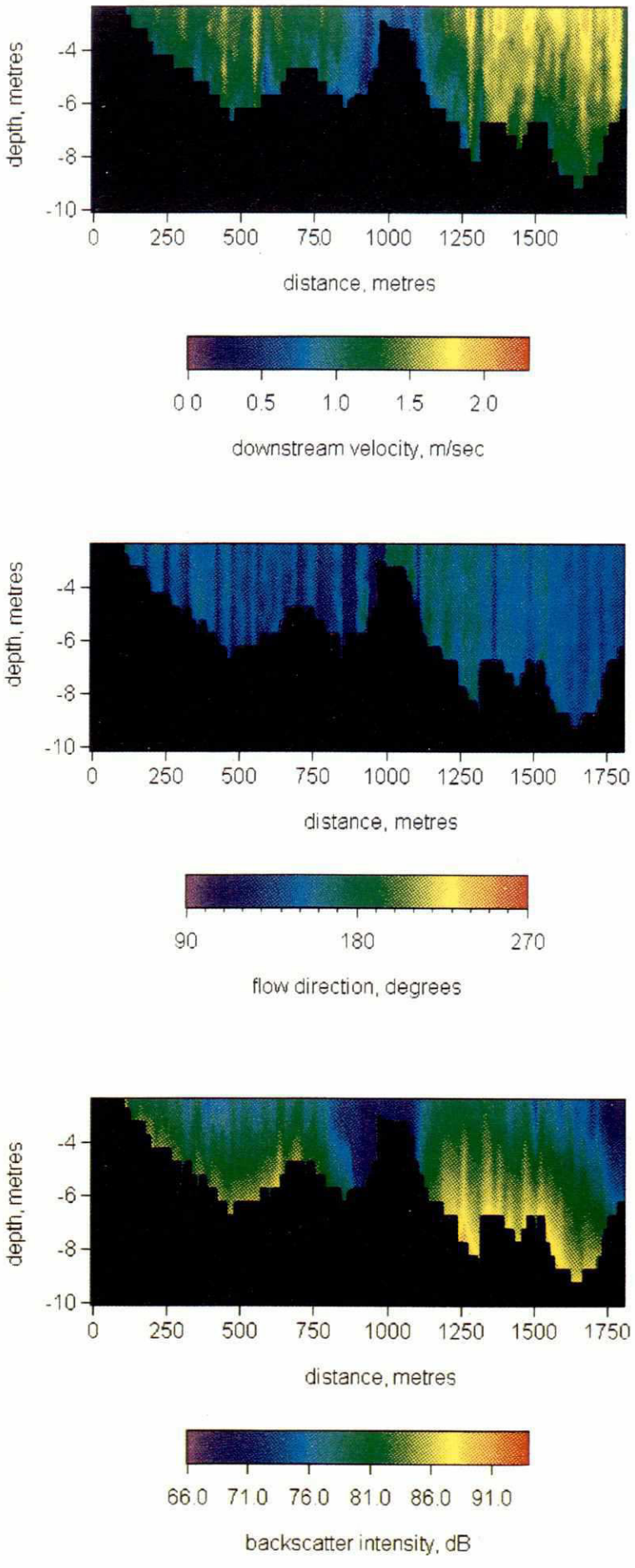

Figure 4.7: Spyglass® contoured ADCP records of the resolved (*U-W*) downstream velocity and direction and backscatter intensity for transects (a) BT5X023, (b) BT5X036, (c) BT5X021, (d) BT5X034 (see text and Figure 2.1b) taken on 11-12 August 1994. Flow directions must be considered relative to the bearing of the bar's long-axis which is 148°.

a

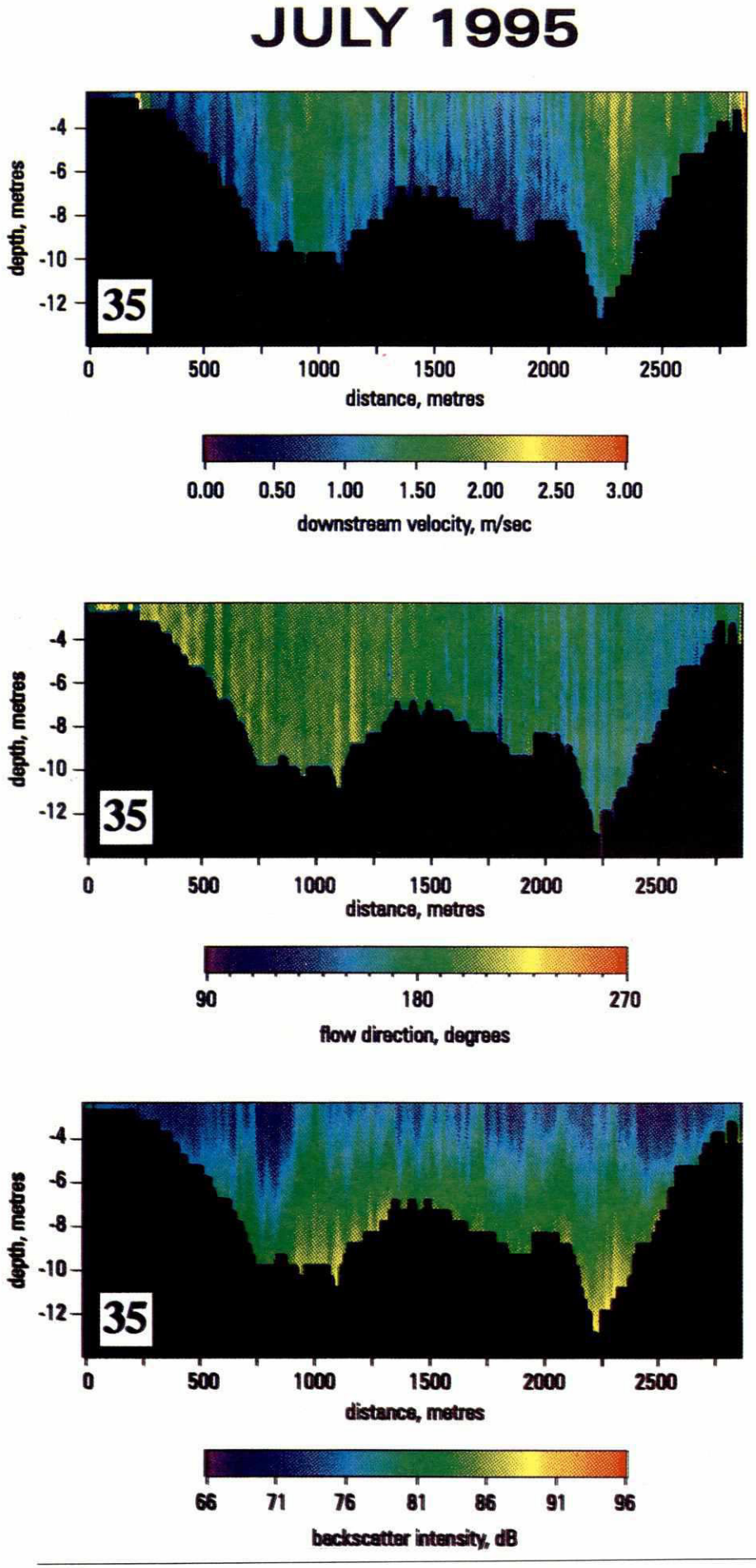

Figure 4.8: Spyglass® contoured ADCP records of the resolved (*U-W*) downstream velocity and direction and backscatter intensity for transects (a) BT5X035, (b) BT5X024, (c) BT5X034 (d) BT5X025, (e) BT5X033, and (f) BT5X026 (see Figure 2.1b) taken on 31 July 1995. The transects are 250 m apart with BT5X035 furthest upstream. Flow directions must be considered relative to the bearing of the bar's long-axis which is 148°.

b

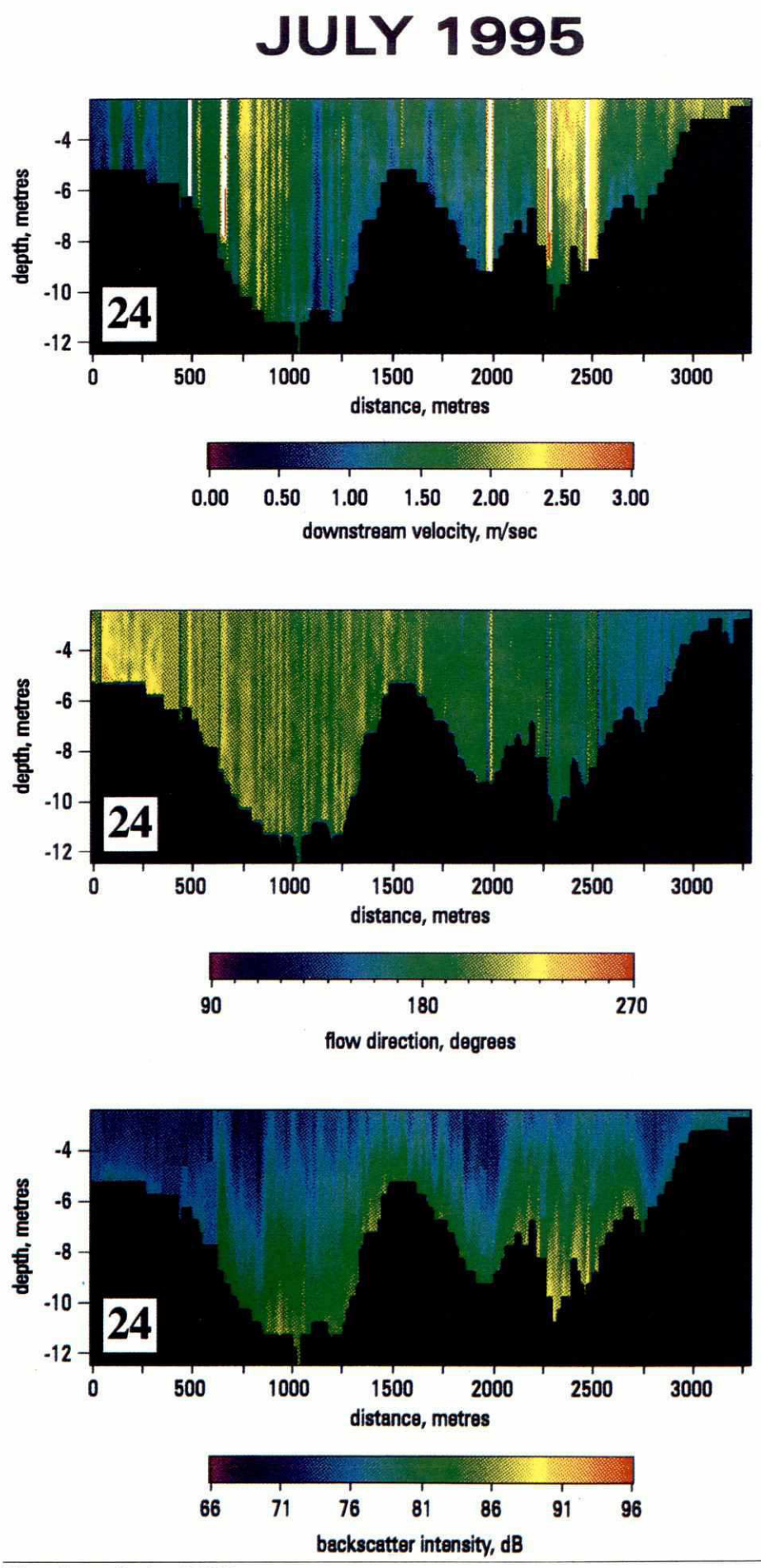

Figure 4.8: Spyglass® contoured ADCP records of the resolved (*U-W*) downstream velocity and direction and backscatter intensity for transects (a) BT5X035, (b) BT5X024, (c) BT5X034 (d) BT5X025, (e) BT5X033, and (f) BT5X026 (see Figure 2.1b) taken on 31 July 1995. The transects are 250 m apart with BT5X035 furthest upstream. Flow directions must be considered relative to the bearing of the bar's long-axis which is 148°.

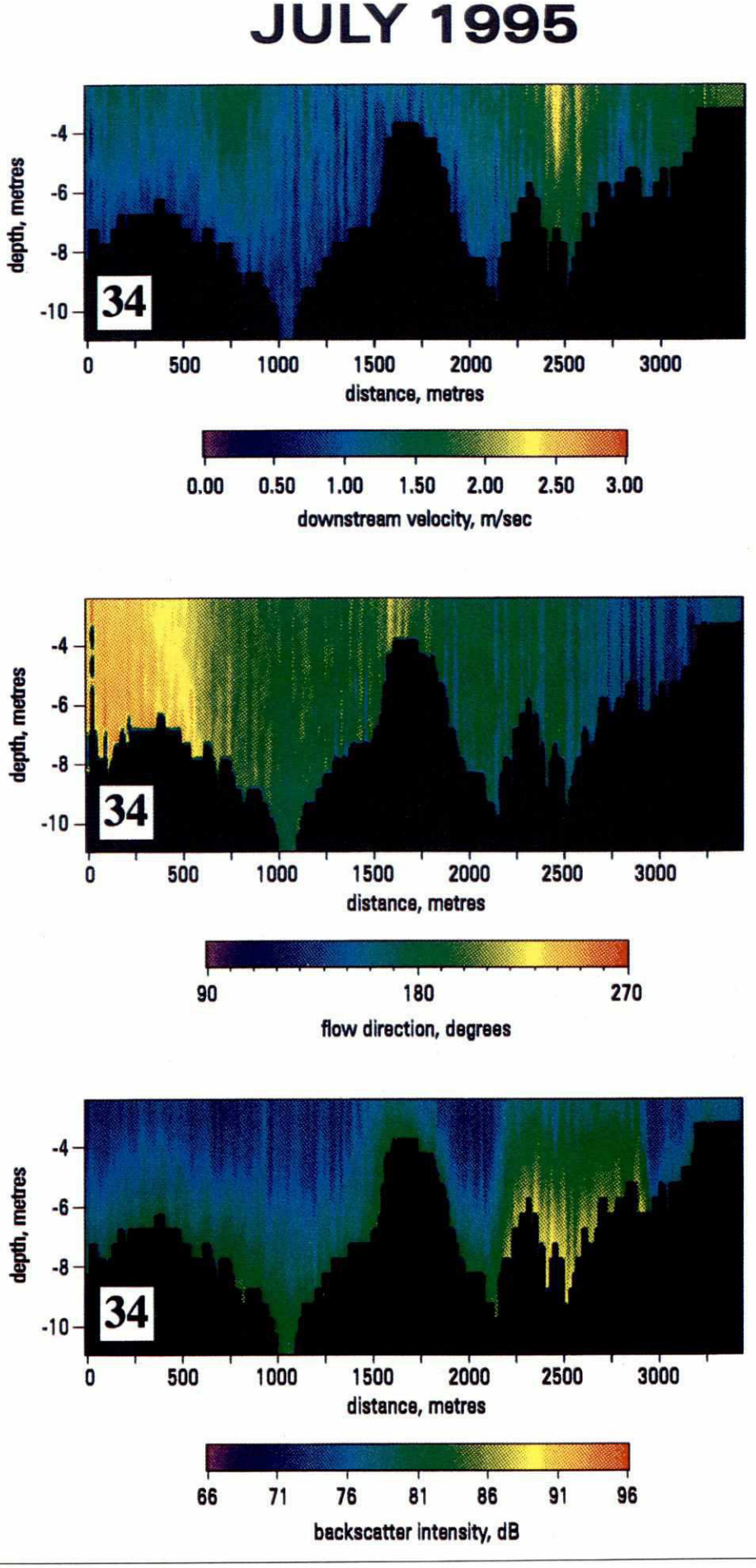

Figure 4.8: Spyglass® contoured ADCP records of the resolved (*U-W*) downstream velocity and direction and backscatter intensity for transects (a) BT5X035, (b) BT5X024, (c) BT5X034 (d) BT5X025, (e) BT5X033, and (f) BT5X026 (see Figure 2.1b) taken on 31 July 1995. The transects are 250 m apart with BT5X035 furthest upstream. Flow directions must be considered relative to the bearing of the bar's long-axis which is 148°.

d

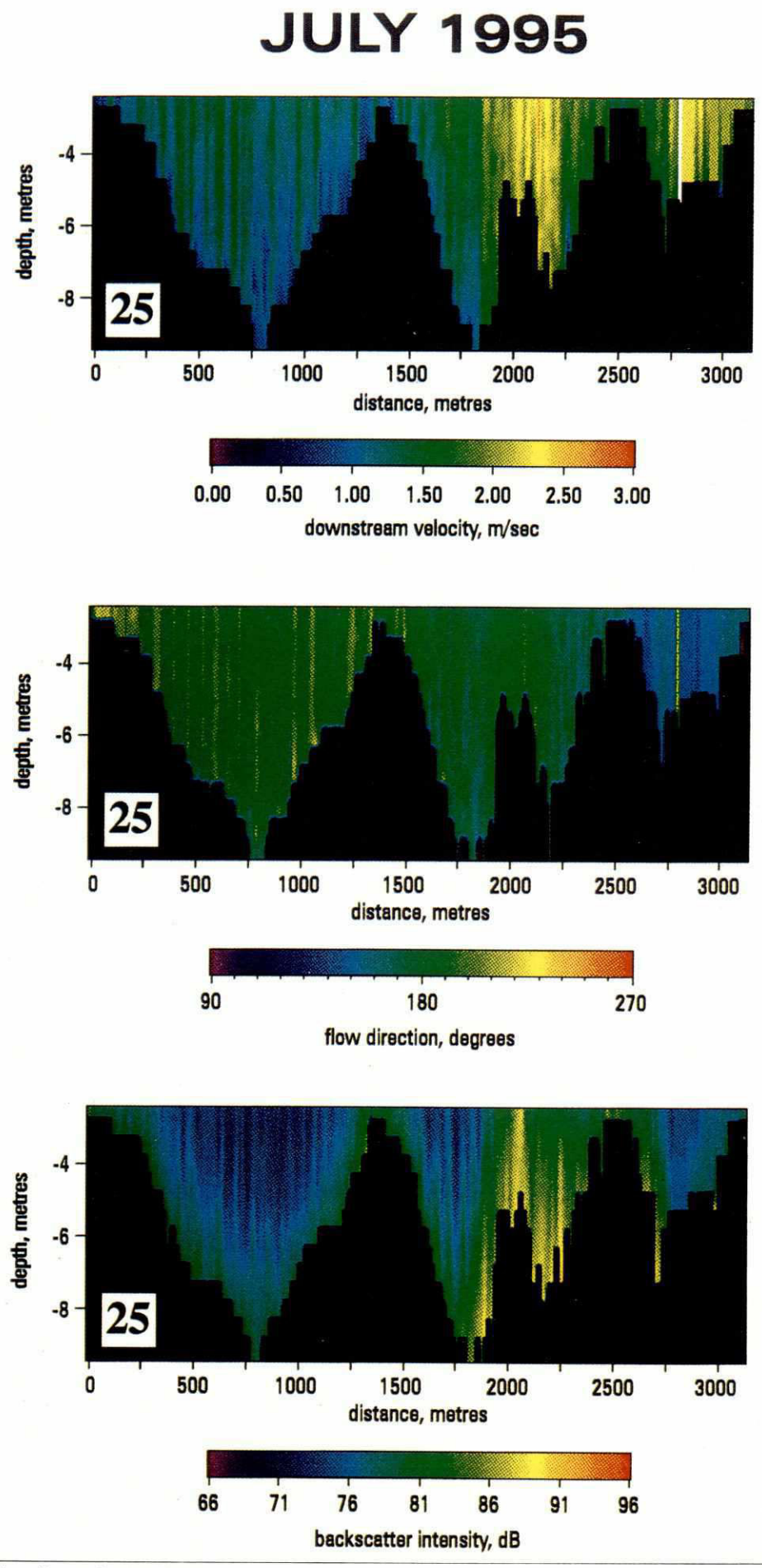

Figure 4.8: Spyglass® contoured ADCP records of the resolved (*U-W*) downstream velocity and direction and backscatter intensity for transects (a) BT5X035, (b) BT5X024, (c) BT5X034 (d) BT5X025, (e) BT5X033, and (f) BT5X026 (see Figure 2.1b) taken on 31 July 1995. The transects are 250 m apart with BT5X035 furthest upstream. Flow directions must be considered relative to the bearing of the bar's long-axis which is 148°.

e

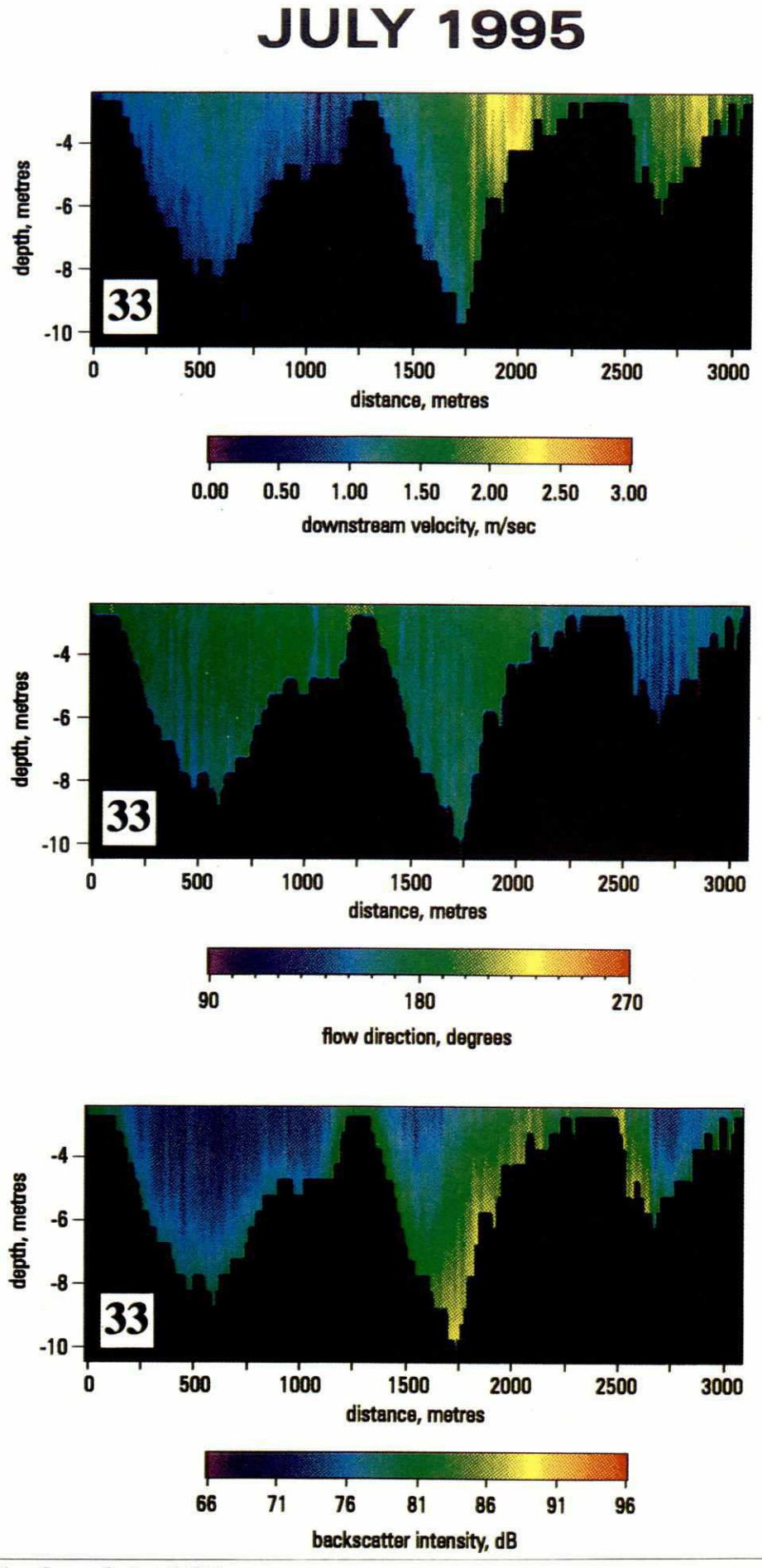

Figure 4.8: Spyglass® contoured ADCP records of the resolved (*U-W*) downstream velocity and direction and backscatter intensity for transects (a) BT5X035, (b) BT5X024, (c) BT5X034 (d) BT5X025, (e) BT5X033, and (f) BT5X026 (see Figure 2.1b) taken on 31 July 1995. The transects are 250 m apart with BT5X035 furthest upstream. Flow directions must be considered relative to the bearing of the bar's long-axis which is 148°.

f

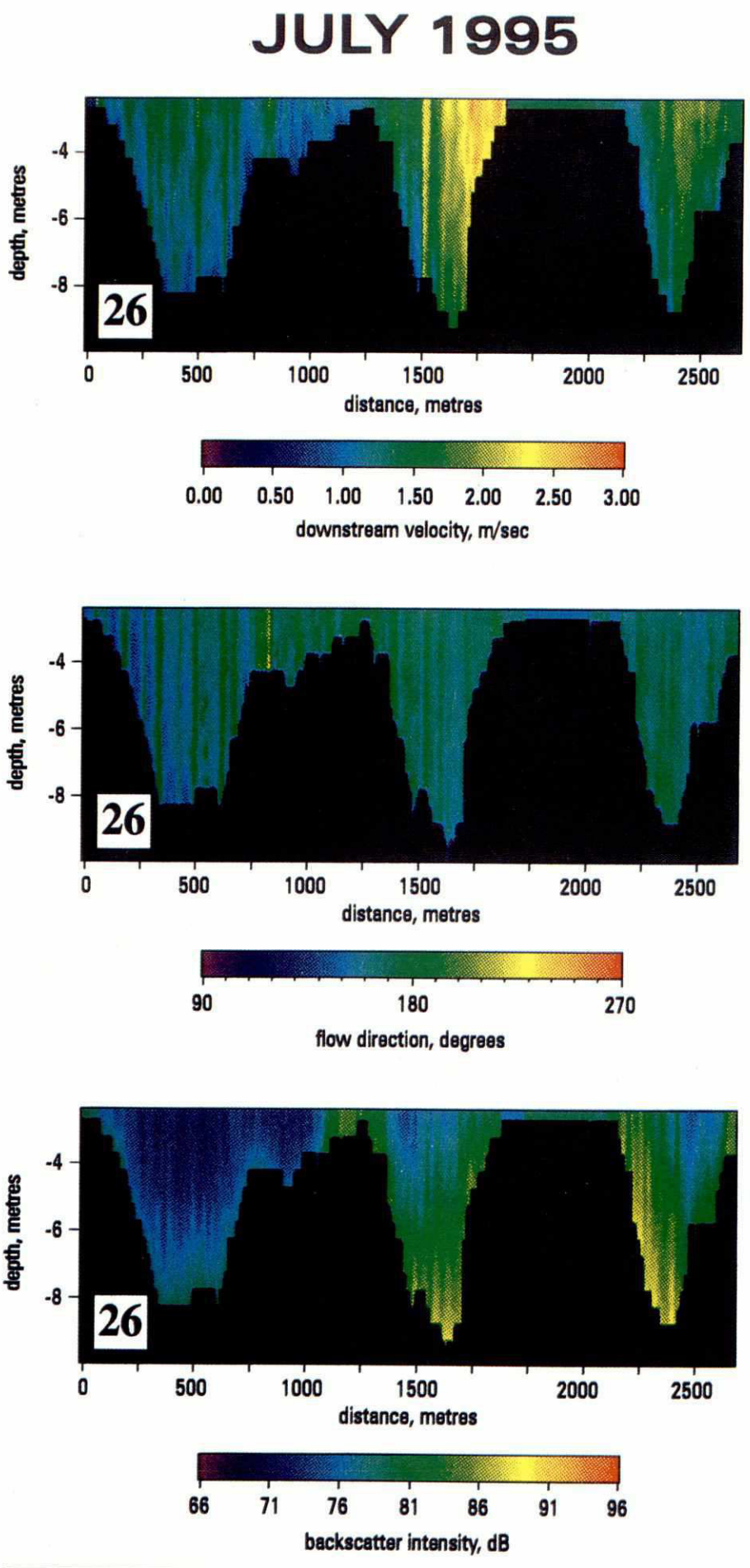

Figure 4.8: Spyglass® contoured ADCP records of the resolved (*U-W*) downstream velocity and direction and backscatter intensity for transects (a) BT5X035, (b) BT5X024, (c) BT5X034 (d) BT5X025, (e) BT5X033, and (f) BT5X026 (see Figure 2.1b) taken on 31 July 1995. The transects are 250 m apart with BT5X035 furthest upstream. Flow directions must be considered relative to the bearing of the bar's long-axis which is 148°.

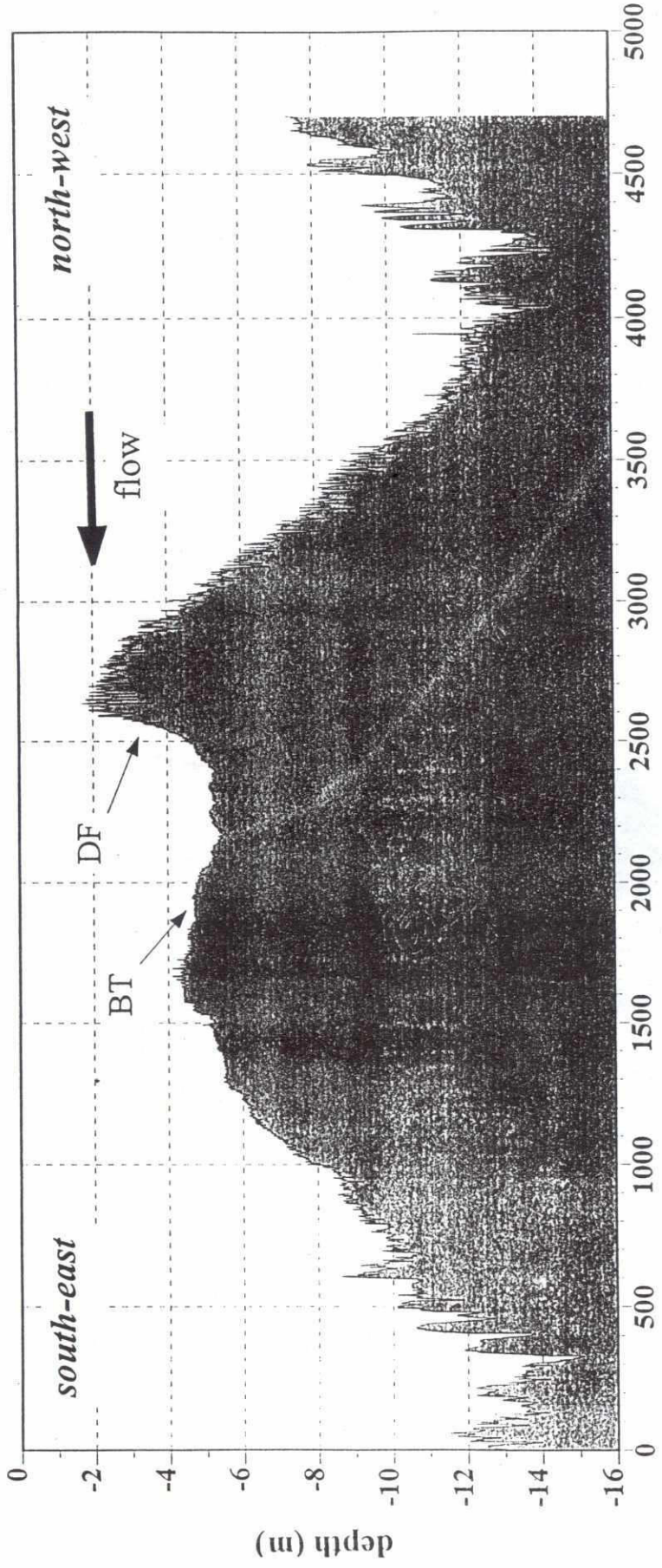

Figure 4.9: Downstream bed profile of the newly emergent bar in August 1994 (line BB1Y038). Note the accretionary dune front migrating onto the barhead (labelled DF) and the changing dune size over the bar with large dunes in the deeper flows around the bar flanks and progressively smaller dunes as flow shallows on the stoss side of the bar. The flat bartop area (labelled BT) has few dunes and is not characterised by upper-stage plane beds, thus it must be an area of lower sediment transport rates.

209

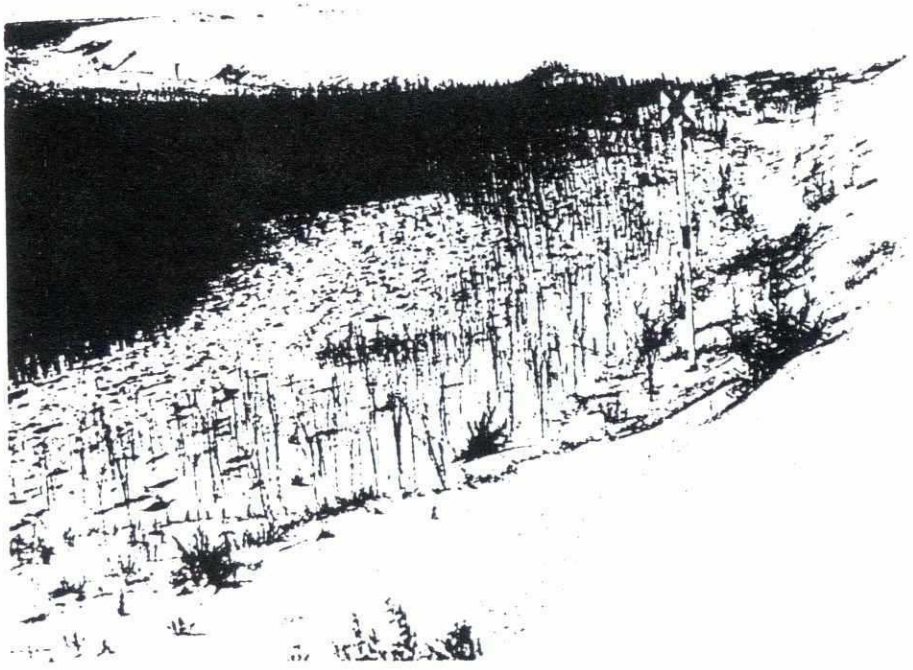

Figure 4.10: View of the accretionary dune fronts as exposed on the emergent study bartop in March 1995. The survey pogo is 1.8 m high and flow is right to left.

Figure 4.11: 100MHz ground penetrating radar trace for transect BT5X033 (250 m upstream of BT5X026 shown in Figure 4.6b). The trace is west to east (left to right) with the lateral distance from the water edge shown on the top scale (280-400 m). The trace shows bar slipface accretion, with several sharp erosion surfaces, superimposed by a 3m layer of stacked, low-amplitude, dunes. The dunes are typically 0.5 and 1 m high, with well defined crests and troughs.

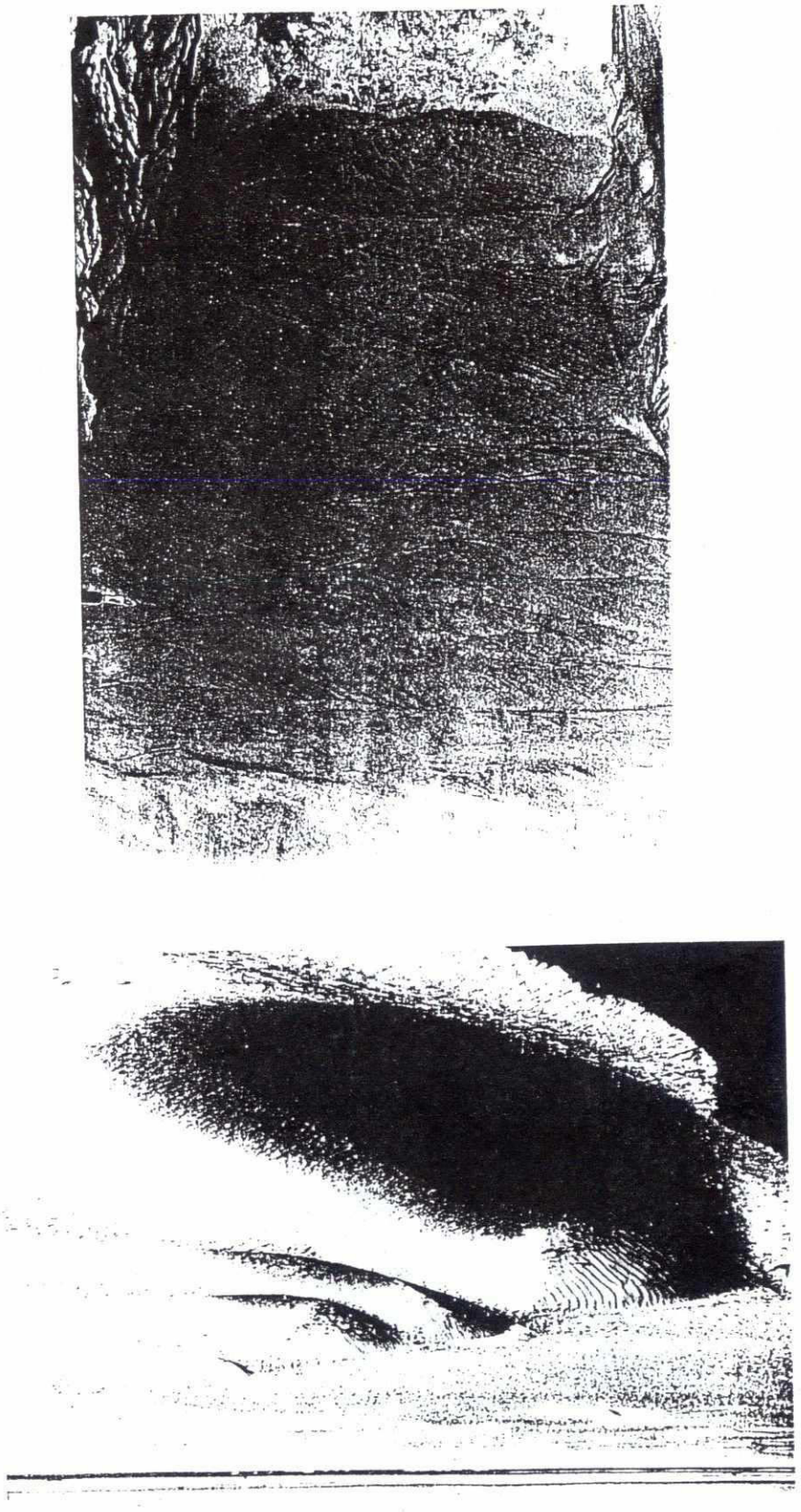

Figure 4.12: 2m trench section taken on GPR line BT5X026 showing the preservation of stacked, low-amplitude dunes with trough cross-stratification (note penknife for scale). Mean D_{50} grain size of the preserved dunes is 0.24 mm.